Spectral-Energy Efficiency Trade-Off of Relay-Aided Cellular Networks

by

Ivan Chui Choon Ku

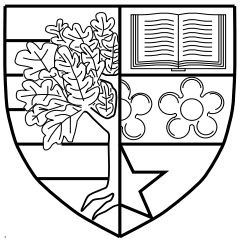

A thesis submitted in partial fulfilment for the degree of
Doctor of Philosophy

at

Heriot-Watt University
School of Engineering and Physical Sciences

July 2013

Abstract

Wireless communication networks are traditionally designed to operate at high spectral efficiency with less emphasis on power consumption as it is assumed that endless power supply is available through the power grid where the cells are connected to. As new generations of mobile networks exhibit decreasing gains in spectral efficiency, the mobile industry is forced to consider energy reform policies in order to sustain the economic growth of itself and other industries relying on it. Consequently, the energy efficiency of conventional direct transmission cellular networks is being examined while alternative green network architectures are also explored. The relay-aided cellular network is being considered as one of the potential network architecture for energy efficient transmission. However, relaying transmission incurs multiplexing loss due to its multi-hop protocol. This, in turn, reduces network spectral efficiency. Furthermore, interference is also expected to increase with the deployment of Relay Stations (RSs) in the network. This thesis examines the power consumption of the conventional direct transmission cellular network and contributes to the development of the relay-aided cellular network.

Firstly, the power consumption of the direct transmission cellular network is investigated. While most work considered transmitter side strategies, the impact of the receiver on the Base Station (BS) total power consumption is investigated here. Both the zero-forcing and minimum mean square error weight optimisation approaches are considered for both the conventional linear and successive interference cancellation receivers. The power consumption model which includes both the radio frequency transmit power and circuit power is described. The influence of the receiver interference cancellation techniques, the number of transceiver antennas, circuit power consumption and inter-cell interference on the BS total power consumption is investigated.

Secondly, the spectral-energy efficiency trade-off in the relay-aided cellular network is investigated. The signal forwarding and interference forwarding relaying paradigms are considered with the direct transmission cellular network taken as the baseline. This investigation serves to understand the dynamics in the performance trade-off. To select a suitable balance point in the trade-off, the economic efficiency metric is proposed whereby the spectral-energy efficiency pair which maximises the economic

profitability is found. Thus, the economic efficiency metric can be utilised as an alternative means to optimise the relay-aided cellular network while taking into account the inherent spectral-energy efficiency trade-off.

Finally, the method of mitigating interference in the relay-aided cellular network is demonstrated by means of the proposed relay cooperation scheme. In the proposed scheme, both joint RS decoding and independent RS decoding approaches are considered during the broadcast phase while joint relay transmission is employed in the relay phase. Two user selection schemes requiring global Channel State Information (CSI) are considered. The partial semi-orthogonal user selection method with reduced CSI requirement is then proposed. As the cooperative cost limits the practicality of cooperative schemes, the cost incurred at the cooperative links between the RSs is investigated for varying degrees of RS cooperation. The performance of the relay cooperation scheme with different relay frequency reuse patterns is considered as well.

In a nutshell, the research presented in this thesis reveals the impact of the receiver on the BS total power consumption in direct transmission cellular networks. The relay-aided cellular network is then presented as an alternative architecture for energy efficient transmission. The economic efficiency metric is proposed to maximise the economic profitability of the relay network while taking into account the existing spectral-energy efficiency trade-off. To mitigate the interference from the RSs, the relay cooperation scheme for advanced relay-aided cellular networks is proposed.

To my family & closest of friends

Acknowledgments

This dissertation could not have been completed without the help of my supervisors, colleagues, friends and family. I would like to take this opportunity to express my utmost gratitude to them.

My greatest appreciation goes to my supervisor, Prof. Cheng-Xiang Wang. I thank him for the guidance, encouragement and advice that he has provided throughout my PhD studies. I'm especially grateful to my second supervisor, Prof. John Thompson, who has tirelessly answered my queries with admirable wisdom and depth as well as providing me with assuring words. I owe to both my supervisors a big thank you.

The generous financial support of Mobile Virtual Center of Excellence (Mobile VCE) is also acknowledged and very much appreciated for without it, I would not have been able to commence and complete this work. I would also like to thank Prof. Peter Grant for his constructive views.

I am enormously delighted to have the privilege of knowing my colleagues of past and present, namely, Xuemin Hong, Xiang Cheng, Omar Salih, Zengmao Chen, Yi Yuan, Margaret Anyaegbu, Raul Hernandez, Ammar Ghazal, Yu Fu, Fourat Haider, Murtadha Al-Saedy, Mario Soflano and Isabel Liu. I thank you for all the wonderful moments and may our friendship lasts a lifetime. I wish to personally acknowledge Yufen Hao for being my trusted confidante and providing me with constant moral support. Thank you for being such a wonderful person.

My appreciation is also extended to the family members of the Chaplaincy. Specifically, my heartfelt gratitude goes to Rev. Dr. Alistair Donald who graciously allowed me to stay in the Chaplaincy as I was completing my PhD studies. I also wish to take this opportunity to give thanks to Tillie Boulogne for sincerely showing me her concern and care, to Fiona Johnson for the most memorable Chaplaincy trips, as well as to Janis Eglitis and Alfred Pozarickij for willing to put up with me.

My warmest regards goes to no other than Chantranut Khoosuwan. I could not be more blessed that my PhD journey has led me to someone as special as you.

Last but not least, my special gratitude goes to my parents and brother for their unconditional love and unwavering support.

Contents

List of Figures

List of Tables

Abbreviations

3G	Third Generation
3GPP	Third Generation Partnership Project
4G	Forth Generation
AF	Amplify-and-Forward
AR	Adaptive Relaying
AWGN	Additive White Gaussian Noise
BER	Bit Error Rate
BLER	BLock Error Rate
BS	Base Station
CAGR	Compound Annual Growth Rate
CAPEX	CAPital EXpenditure
CDF	Cumulative Distribution Function
CF	Compress-and-Forward
CMP	Cooperative Multi-Processing
CO_2	Carbon diOxide
CO_2e	Carbon diOxide equivalent
CoMP	Cooperative Multi-Point
CSI	Channel State Information

D-TR-STBC	Distributed Time-Reversal Space-Time Block Code
D2D	Device to Device
DF	Decode-and-Forward
DOSTBC	Distributed Orthogonal Space-Time Block Code
DTCN	Direct Transmission Cellular Network
ECR	Energy Consumption Ratio
FSUS	Full Semi-orthogonal User Selection
GBP	Great Britain Pounds
GHG	GreenHouse Gasses
GPRS	General Packet Radio Services
GSM	Global System for Mobile Communications
GSMA	Groupe Speciale Mobile Association
HSDPA	High-Speed Downlink Packet Access
i.i.d.	independent and identically distributed
IC	Interference Cancellation
ICT	Information and Communication Technology
IDEC	Independent RS DECoding
IF	Interference Free
IFR	Interference Forwarding Relay
IMT–A	International Mobile Telecommunications–Advanced
IRC	Interference Rejection Combining
ITU	International Telecommunication Union
JDEC	Joint RS DECoding
LoP	Localised Precoding

LTE	Long Term Evolution
LTE–A	Long Term Evolution–Advanced
m.u.	monetary unit
MIMO	Multiple Input Multiple Output
MISO	Multiple Input Single Output
MMSE	Minimum Mean Square Error
Mobile VCE	Mobile Virtual Center of Excellence
MRC	Maximum Ratio Combiner
MT	Maximum ratio Transmit
NUN	Norm-based User Negotiation
OFDM	Orthogonal Frequency Division Multiplexing
OPEX	OPerational EXpenditure
OUS	Optimum User Selection
PA	Power Amplifier
PAPR	Peak to Average Power Ratio
PSUS	Partial Semi-orthogonal User Selection
QoS	Quality of Service
RACN	Relay-Aided Cellular Network
RF	Radio Frequency
RFR	Relay Frequency Reuse
RHS	Right Hand Side
RS	Relay Station
SEET	Spectral-Energy Efficiency Trade-off
SER	Symbol Error Rate

SFBC	Space Frequency Block Code
SFR	Signal Forwarding Relay
SIC	Successive Interference Cancellation
SIMO	Single Input Multiple Output
SINR	Signal-to-Interference-plus-Noise Ratio
SIR	Signal-to-Interference Ratio
SMS	Short Message Service
SNR	Signal-to-Noise Ratio
SP	Signal Processing
SUS	Semi-orthogonal User Selection
SVD	Singular Value Decomposition
TDMA	Time Division Multiple Access
UE	User Equipment
UK	United Kingdom
UMTS	Universal Mobile Telecommunications System
USB	Universal Serial Bus
UWB	Ultra Wide-Band
V-BLAST	Vertical-Bell Laboratories Layered Space-Time
WIFI	wireless local area network
Ws	Watt-second
XOR	eXclusive OR
ZF	Zero Forcing

Symbols

$\mathbf{X}$	matrix notation
$\mathbf{x}$	vector notation
X or x	scalar notation
$\mathcal{S}$	set notation
$\mathbf{X}^{\dagger}$	pseudo-inverse of a matrix
$\mathbf{X}^{\mathrm{H}}$	Hermitian transpose of a matrix
$\mathbf{X}^{\mathrm{T}}$	transpose of a matrix
$\mathbf{X}^{-\mathbf{1}}$	inverse of a matrix
$\mathrm{diag}\,(\mathbf{X})$	diagonal of a matrix
$\|\mathbf{X}\|_{\mathrm{F}}^2$	squared Frobenius norm of a matrix
$\|\mathbf{x}\|$	Euclidean distance of a vector
$\|x\|$	absolute value of a scalar quantity
$x!$	factorial operator
$\oplus$	XOR operator
$\mathrm{diag}\,(x_1, \cdots, x_M)$	an $M \times M$ diagonal matrix with non-zero elements of $(x_1, \cdots, x_M)$
$\|\mathcal{S}\|$	the cardinal of a set
$\mathbf{I}_N$	identity matrix of size $N \times N$
$\det[\,\cdot\,]$	determinant operator
$\mathrm{tr}\,(\,\cdot\,)$	trace operator
$\lceil\,\cdot\,\rceil$	ceiling operator

$\mathbb{E}\{\cdot\}$	expectation operator
$(\cdot)^*$	conjugate operator
d_{RS}	RS distance from the BS
T	time duration of a transmission frame
t_D	fraction of T utilised for direct transmission
t_R	fraction of T utilised for relay transmission
τ_{bc}	broadcast phase fraction of a relay transmission time slot
τ_r	relay phase fraction of a relay transmission time slot
β_R	relay confidence
$\mathcal{G}_{Direct}$	the set of UEs for direct transmission
$\mathcal{G}_{Relay}$	the set of UEs for relay transmission
$b(i,j)$	the BS from the ith sector of the jth cell
$r(i,j,m)$	the mth RS from the ith sector of the jth cell
$u(i,j,k)$	the kth user from ith sector of the jth cell
$(1,1)$	index for the base sector of the base cell
$f_{b(i,j)}$	the BS transmit frequency at the jth sector of the ith cell
$f_{r(i,j,m)}$	the mth RS transmit frequency at the jth sector of the ith cell
$f_{u(i,j,k)}$	the kth UE receive frequency at the jth sector of the ith cell
$\mathcal{X}$	the set of interfering BSs in a particular sector of the base cell
$\mathcal{P}_{u(i,j,k)}$	the set of interfering RSs to the kth UE at the jth sector of the ith cell
$b(i_0,j_0)$	the strongest interfering BS to the kth UE at the jth sector of the base cell
$r(i_0,j_0,m_0)$	the designated RS to forward $b(i_0,j_0)$ interference to the kth UE at the jth sector of the base cell
η_b	frequency reuse factor of the BS
η_r	frequency reuse factor of the RS

P_{BS}	allocated RF transmit power for BS
P_b	effective RF transmit power for BS
P_{RS}	allocated RF transmit power for RS
P_r	effective RF transmit power for RS
P_{ref}	reference RF transmit power
$P_{c,ref}$	circuit power consumption at P_{ref}
$P_{c,b}$	BS circuit power consumption
$P_{c,r}$	RS circuit power consumption
P_{op}	operational power consumption
α_b	effective operation efficiency of the BS
α_r	effective operation efficiency of the RS
N_b	number of BS antennas per sector
N_r	number of RS antennas
N_u	number of UE antennas
d_{ISD}	inter-site distance
r_{cell}	cell radius
N_{Sec}	number of sectors per cell
B_{sys}	system bandwidth
B_{coop}	RS–RS cooperative link bandwidth
σ_s	shadowing standard deviation
$L_{X,Y}$	path loss between node X and node Y
$\rho(\theta)$	antenna pattern
N_0	noise power spectral density
r_{base}	data rate of the base service
κ_r	revenue per bit
κ_c	energy cost per Ws
T_{TTI}	transmit time interval
τ_{coop}	cooperative time fraction
θ	quantisation bits

Chapter 1

Introduction

1.1 Problem Statement

Since the first successful transatlantic wireless transmission was demonstrated by Marconi in 1901 [1], wireless communication has never ceased to evolve in scale and complexity as it continues to transform the lives of many across the globe. Today, wireless communication permeates in almost every aspect of modern technologies and lifestyles, spanning from complex infrastructures like the satellite and deep space communication systems to simple applications like the privately owned amateur radios and Bluetooth enabled devices. In wireless mobile cellular network, the appetite for high transmission rate grows rapidly from one generation of mobile network to the next in order to cater for the increasingly demanding wireless applications that progress from simple Short Message Service (SMS) to voice and multimedia content delivery. Unfortunately, bandwidth resources are becoming scarce as more applications are introduced to satisfy the demands for faster delivery of data which is increasingly rich in multimedia content. Thus, wireless cellular networks are usually designed to have high spectral efficiency.

However, mobile operators are now facing the fact that the incremental improvement in spectral efficiency of each new generation of mobile network is becoming less obvious. This is worrying as traffic is expected to grow exponentially when the complete

shift towards wireless internet services occurs. Besides that, the wireless infrastructure is now huge due to the widespread deployment of macro cells over the decades as coverage and capacity are of paramount importance. These traditional macro cells typically employ direct transmission schemes and may consume large amount of operational power. The energy problems of the mobile industry may be further aggravated as it is expected to be an enabler of sustainable growth to other industries as they begin incorporating wireless internet solutions into their business models to reduce their own carbon footprint. Thus, there is a real chance that the mobile industry will face an energy crisis in the foreseeable future [2]. In order for the mobile industry to sustain its growth, a new paradigm shift towards energy efficient network design is necessary.

Relaying transmission has been identified as one of the key technologies in future wireless communication networks [3]. While conventional Direct Transmission Cellular Networks (DTCNs) have large cell sizes, future networks will deploy progressively smaller cells with lower transmission power due to an emphasis on energy efficiency. This will create coverage holes where User Equipments (UEs) in those areas may experience bad signal reception, resulting in high call drop rates. In this case, low cost Relay Stations (RSs) are ideal infrastructures to guarantee that coverage is still maintained especially in the affected areas. In fact, relaying transmission has already been considered in the current Long Term Evolution–Advanced (LTE–A) standards.

Nevertheless, relaying transmission is not without its own issues. On one hand, the Relay-Aided Cellular Network (RACN) is seen as one of the possible solutions towards realising green communication architectures by assisting the transmission of Base Stations (BSs) so that the latter can operate at reduced transmit power, thus saving energy. On the other hand, the introduction of RSs into the network may potentially increase the overall interference level. This is more profound in the urban and suburban areas where cell sites are more densely deployed and RSs are expected to be in greater number for each cell. Furthermore, the very nature of relay transmission introduces multiplexing loss which could affect the network spectral efficiency if not properly managed.

1.2 Motivation

While much research is on the spectral efficiency of direct transmission schemes, there is a growing interest in the energy efficiency of such schemes in light of the increasing awareness of the potential energy crisis faced by the mobile industry. However, most work focus on transmitter side strategies and less attention is given towards investigating the impact of receivers on the power consumption of direct transmission schemes. A more holistic power consumption model which includes not only the Radio Frequency (RF) transmission power of the Power Amplifier (PA) module but also the circuit power of the Signal Processing (SP) module should be employed to reflect the energy efficiency values more accurately.

There is also a growing interest towards incorporating relaying transmission into cellular networks which conventionally employ only direct transmission schemes in order to improve energy efficiency. However, multiplexing loss is inherent in relaying transmission due to its multi-hop requirement. This affects negatively on the spectral efficiency of the network as a whole. Consequently, there is a trade-off between spectral efficiency and energy efficiency in a relay-aided cellular network. This Spectral-Energy Efficiency Trade-off (SEET) warrants a careful study as it will impact on the operational feasibility of the network. Thus, a balance operating point along the SEET is essential. As economic profitability is one of the key performance indicator in the operation of the mobile network, the economic efficiency metric is introduced to decide on the suitable operating point along the SEET that will maximise profitability.

Furthermore, the inevitable increase in interference due to the introduction of RSs in RACNs must be mitigated in order to improve the network performance. This is especially so if the RSs are to be deployed in urban and suburban areas where the network performance is already interference limited. Therefore, advanced relay transmission techniques should be devised to mitigate interference and to improve the SEET in RACNs.

1.3 Contributions

The key contributions of the thesis are summarised as follows:

- **Investigating the power consumption of direct transmission cellular networks:**

  The impact of the receiver on the BS total power consumption for downlink Multiple Input Multiple Output (MIMO) DTCNs is investigated. The conventional linear and Successive Interference Cancellation (SIC) receivers are investigated, with both Zero Forcing (ZF) and Minimum Mean Square Error (MMSE) weight optimisation approaches being considered for each of them. Besides the PA module whose power consumption is determined by the required RF transmit power, the circuit power consumption in the SP module is also considered when characterising the total power consumption of the BS. Note that this power consumption model is utilised throughout the thesis when calculating energy efficiency. The influence of the SP module and inter-cell interference on the BS total power consumption is also investigated.

- **Analysing the SEET in RACNs:**

  The performance of the RACN is investigated by comparing both the signal forwarding and interference forwarding relaying paradigms. Each relaying paradigm employs the adaptive MIMO relaying scheme that switches between Decode-and-Forward (DF) and Amplify-and-Forward (AF) relaying. The spectral and energy efficiency values are utilised as performance measures with the MIMO direct transmission scheme taken as the baseline. It is demonstrated that there is a trade-off between spectral and energy efficiency. The economic efficiency metric is then proposed to find a balance in the trade-off to maximise the profitability of the scheme. From that, it is demonstrated that operating at optimum energy efficiency might not necessarily be economically profitable. The performance of different frequency reuse schemes for both the BS and RS is also examined.

- **Mitigating interference via relay cooperation in relay-aided cellular networks:**

  A relay cooperation scheme for advanced RACNs is proposed with the intention to mitigate interference at the individual sectors of the cells. Both the Joint RS DECoding (JDEC) and Independent RS DECoding (IDEC) approaches are considered during the broadcast phase of the relaying transmission. While, joint relay transmission incorporating the proposed Partial Semi-orthogonal User Selection (PSUS) method which requires partial Channel State Information (CSI) knowledge is implemented during the relay phase of the relaying transmission. Other user selection methods requiring global CSI knowledge are also being compared. The spectral, energy and economic efficiency values of the relay cooperation scheme are then evaluated. Furthermore, the cost incurred at the cooperative link between the collaborating RSs is analysed for different relay cooperation configurations. The performance of the proposed relay cooperation scheme is also examined under different Relay Frequency Reuse (RFR) patterns.

The work presented in this thesis has led to the following publications:

Journals

1. **I. Ku**, C. -X. Wang, and J. S. Thompson, "Spectral-energy efficiency tradeoff in relay-aided cellular networks," *IEEE Trans. Wireless Commun.*, submitted for publication.

2. **I. Ku**, C. -X. Wang, and J. S. Thompson, "The spectral, energy and economic efficiency of relay-aided cellular networks," *IET Commun.*, accepted for publication.

3. C. Han, T. Harrold, S. Armour, I. Krikidis, S. Videv, P. M. Grant, H. Haas, J. S. Thompson, **I. Ku**, C. -X. Wang, T. A. Le, M. R. Nakhai, J. Zhang, and L. Hanzo, "Green radio: Radio techniques to enable energy efficient wireless networks," *IEEE Commun. Mag.*, vol. 49, no. 6, pp. 46–54, Jun. 2011.

Conferences

1. **I. Ku**, C. -X. Wang, and J. S. Thompson, "Spectral-energy efficiency tradeoff in multicell cellular networks with adaptive relay cooperation," in *Proc. IEEE GLOBECOM'12*, California, USA, Dec. 2012, pp. 4585–4590.

2. **I. Ku**, C. -X. Wang, J. S. Thompson, and P. M. Grant, "Impact of receiver interference cancellation techniques on the base station power consumption in MIMO systems with inter-cell interference," in *Proc. IEEE PIMRC'11*, Toronto, Canada, Sep. 2011, pp. 1798–1802.

3. **I. Ku**, C. -X. Wang, J. S. Thompson, and P. M. Grant, "Transmission energy consumption in MIMO systems under inter-cell interference," in *Proc. IEEE WiAd'11*, London, UK, Jun. 2011, pp. 263–267.

Technical Reports

1. **I. Ku**, C. -X. Wang, and J. S. Thompson, "Spectral-energy efficiency tradeoff in multicell cellular networks with adaptive relay cooperation," Mobile VCE Tech. Rep. TR-GR-0110, Feb. 2012.

2. **I. Ku**, C. -X. Wang, and J. S. Thompson, "Spectral-energy efficiency tradeoff in relay-based cooperative communication systems with inter-cell interference," Mobile VCE Tech. Rep. TR-GR-0066, Feb. 2011.

3. **I. Ku**, C. -X. Wang, and J. S. Thompson, "A study on the influence of receiver interference cancellation techniques on base station transmission energy in MIMO systems," Mobile VCE Tech. Rep. TR-GR-0026, Jan. 2010.

1.4 Thesis Organisation

The remainder of this thesis is organised as follows:

Chapter 2 begins by providing some historical background on the climate change issue and the importance of reducing the carbon footprint of the industries. The challenges of the mobile industry as an enabler of sustainable economic growth are described next. Following that, the Mobile Virtual Center of Excellence (Mobile VCE) Green Radio research program is introduced. Next, the spectral and energy efficiency metrics utilised in this thesis are described. This is followed by an overview of the relaying transmission use scenarios and its classification.

Chapter 3 investigates the impact of the receiver on the BS total power consumption. It begins with the description of the DTCN. Next, both the conventional linear and SIC receivers with the ZF and MMSE weight optimisation approaches are presented together with their respective spectral efficiency and RF transmit power expressions. The power consumption model which considers both the RF transmit power and circuit power is then introduced to quantify the total power consumption. Analysis on the power consumption for Single Input Multiple Output (SIMO) transmission and for a large number of receive antennas are also given.

Chapter 4 focuses on the RACN where two relaying paradigms, namely, the signal forwarding and interference forwarding relaying, are considered. The DTCN is taken as a comparison. Firstly, the system model is presented whereby the employed network setup and transmission protocol are explained. The power consumption model and an analysis on the network interference are also given here. The Signal Forwarding Relay (SFR) and Interference Forwarding Relay (IFR) are then described while the formulation for energy efficiency optimisation is described next. Following that, the proposed economic efficiency metric together with its optimisation formulation which takes into consideration the SEET condition in the RACN are then presented.

Chapter 5 presents the method of mitigating interference in the RACN. Similarly, it begins by introducing the employed system model where the transmission protocol and power consumption model are given. Analysis on the network interference and the

impact of various RFR patterns on the interference level is then presented. Both the JDEC and IDEC techniques utilised during the broadcast phase are then discussed. The proposed Cooperative Multi-Processing (CMP) relaying employed during the relay phase is presented next. Other relaying strategies, for example, the Interference Free (IF), Maximum ratio Transmit (MT) and Localised Precoding (LoP) relaying, are also compared. Various user selection methods are then presented, with the PSUS user selection method being the one proposed. The cooperative cost of the relay cooperation scheme, which is associated with the exchange of cooperative information through the cooperation link between the RSs, is also examined. Taking the cooperative cost into consideration, the formulation for both energy efficiency and economic efficiency optimisation is then described.

Finally, Chapter 6 concludes the thesis and gives some suggestions for future research topics.

Chapter 2

Background

2.1 Climate Change: The Price of Economic Development

The introduction of the improved steam engine in 1769 by James Watt ushered in an unprecedented growth in trade and commerce during the Industrial Revolution period (1750 - 1850). The substitution of manual labour with steam powered machinery was prevalent in new generation factories of the day and this, in turn, revolutionised the production of many industries like textile, metallurgy and mining. Transportation also greatly benefited from the invention of the steam engine as steam turbine-powered ships and steam locomotives quickly replaced conventional transportation systems that required the muscle power of both man and beast. The Industrial Revolution which began in the United Kingdom (UK) quickly caught on in Europe, North America, Japan and subsequently permeated throughout the known world. As a result, the social, cultural and economic conditions of the world population progressed in one way or the other till the present time.

The rapid progress of industrialisation which started two centuries ago has left us oblivious of our responsibilities to the environment. This is clearly illustrated in Fig. 2.1 [4] which shows the CO_2 concentration in the earth atmosphere for the past

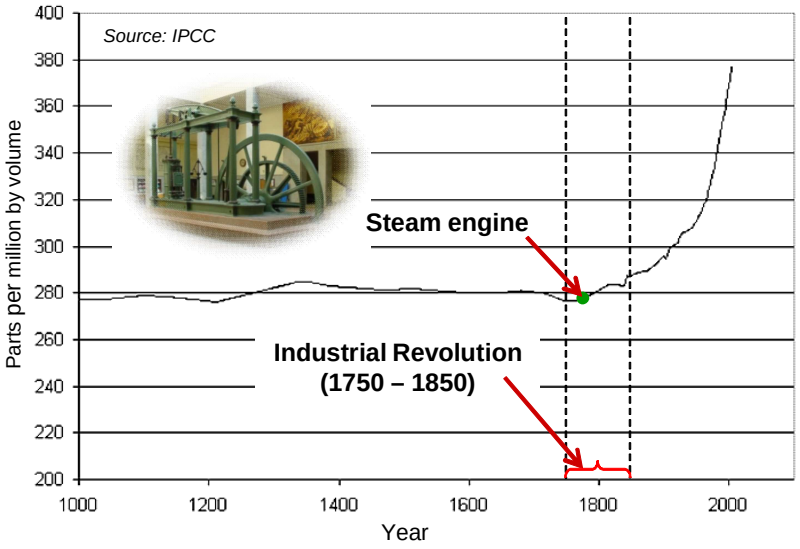

FIGURE 2.1: The atmospheric concentration of CO_2 from year 1000 to 2004 [4].

1000 years. It is observed that a sharp increase in CO_2 concentration occurred after the start of the Industrial Revolution. The production of GreenHouse Gasses (GHG), mainly CO_2, from decades of fossil fuel burning to power the steam engines and later the modern petrol engines let to the global warming threat whose magnitude we are just coming to comprehend in the last decade [5]. Today, governments around the world, not to mention the general public, begin to acknowledge the realities of global warming and the devastating damage that it brings not only to the environment but also to our very existence. The melting of the polar ice caps, mega storms, irregular animal migration patterns, changing global temperatures and failing agricultural crops causing widespread famine are just a few examples among the many physical evidences of climate change due to global warming that can no longer be ignored.

Since the last decade, we have improved our understanding on the negative effects of CO_2 on global temperatures with studies by climatologists showing a necessity for industrialised countries to decrease GHG emissions by as much as 80% from 1990 levels by 2050. Heeding this, the UK became the first country in the world to establish legally binding domestic commitments [6] to achieve the GHG reduction target.

In response to the environmental law that formally encapsulates our legal obligations, strategies to facilitate a major reduction in CO_2 production are urgently needed.

Putting our economic development to a complete standstill is not an option as continuous economic growth is an integral part of the growing world population. Instead, a sustainable growth which is characterised by an economy that is progressively less dependent on fossil fuels must be sort after for energy security reasons and to reduce the risk of an irreversible environmental disaster. One way to reduce our dependency on fossil fuels is to seek out alternate green and renewable energy resources like solar energy, geothermal energy, wind energy, wave energy and also the more controversial nuclear fission energy. Since this precludes the necessity of inventing and perfecting new technologies, the idea of efficiently harvesting and utilising these green energy resources at large scales is a long term goal though much inroads have been made.

Closer to the present time, we observe that major industries across the world begin to integrate into their cooperate mission a sense of corporate responsibility towards the environment by adopting company policies, good practices and new business models that are environmentally friendly. For example, employees are encouraged to minimise their travelling whenever possible during the course of discharging their duties. Instead, teleconferencing and emails are recommended to reduce their carbon footprint. For utility companies, smart metering systems are beginning to be the norm. These systems periodically record energy consumption at target sites which is then reported back daily to the central system through wireless communication. Remote monitoring is also possible with these systems. Besides that, smart grid systems are also seen as a potential solution to curb the rising energy crisis. A smart grid system, which smart metering can be a component of, refers more to an intelligent network of power grid that is able to automatically gather data ranging from fault locations to behaviour of customers and suppliers to facilitate reliable and economical electricity generation and distribution. From these examples, it is clear that the technological solutions have one important common characteristic. To reduce carbon footprint, these technologies provide a more efficient means of gathering and manipulating information flow in a network, be it administrative or technical in nature, through Information and Communication Technology (ICT).

2.2 Mobile Communication: Enabler of Sustainable Economic Growth

While wireless communication of old was expensive and less functional, thus, was only predominantly accessible to the military and major corporations, the debut of the Global System for Mobile Communications (GSM) system in the early 1990s started a global proliferation of mobile usage to the wider population due to cheaper services to customers and low cost roll-outs. The role of the mobile industry of today is very different from what it used to be a few decades ago.

Because of the widespread adoption at present time, the mobile industry is now a force that could enable transformation of business models in other industries. This vital role as an enabler of economic development was documented by International Telecommunication Union (ITU) and World Bank studies since the 1980s and was formally acknowledged by governments at the World Summit on the Information Society in 2003 through a set of development targets to be achieved by 2015 [7]. The articles in [8] further strengthened this perception by successfully documenting the impact of mobile telephony on the economic landscape in Africa during late 2009 and its future role as the country experienced a shift from voice and text services to wireless internet. This trend is also mirrored in other parts of the world where migration from traditional wired lines to wireless means, mostly via mobile devices, is fast taking place. This comes from the fact that the continuous development in international businesses and the changing habits of private internet usage, like the frequent updates of Facebook accounts wherever the user happens to be, necessitate the global availability of the internet which can only be practically realised by wireless technology.

By having a global economic presence, the mobile industry is well positioned to contribute to the paradigm shift towards global economic sustainability which is happening now. Once seen as an enabler of economic development, the mobile industry is also now seen as an enabler of sustainable economic growth. This is because as other industries increasingly rely on the ICT sector to implement their energy efficient and

environmentally friendly policies and business models to reduce their carbon footprints, the mobile industry, which is a major player in the ICT sector, has the crucial role of ascertaining that its communication infrastructures are well placed to support the realisation of the commendable policies of these industries. The ability of wireless technology to enable fast and reliable delivery of information any time and anywhere helps other industries to coordinate transactions across different time zones at varied geographical areas. Because business transactions can be executed efficiently without the unnecessary need for travelling (thus, reducing carbon footprint), economy growth which is sustainable can potentially be realised.

2.3 Challenges of the Mobile Industry

Being an enabler of sustainable economic growth for other industries is a double-edged sword for the mobile industry. On the one hand, the mobile industry stands to prosper as the number of industries that rely on it increases in the coming decades. On the other hand, the growth of the mobile industry may be under threat if sustainability from within its own domain is not ensured.

The inevitable transition from simple voice telephony to wireless internet means that data circulation in a mobile network will increase significantly. Coupled with the fact that a rapidly growing subscriber base is almost certain, the mobile network faces an unprecedented surge in traffic not seen a couple of decades back as aptly illustrated in Fig. 2.2 [9]. This huge strain to its infrastructure has to be mitigated well in order for it to feasibly support the expected increase in demand for wireless access while ensuring its own growth is sustainable. Generally, the two most important challenges that will be encountered are the energy cost and carbon footprint of the mobile industry itself as the demand for its services by other industries increases sharply in the near future.

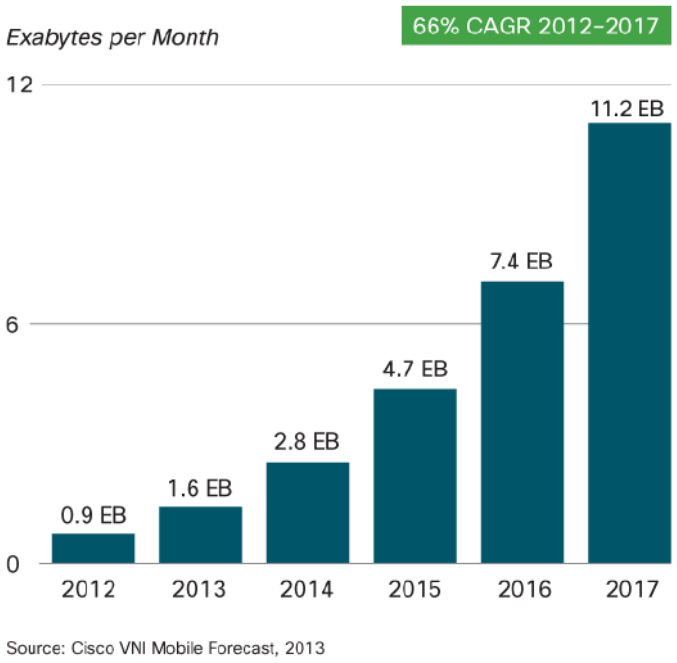

FIGURE 2.2: Mobile data traffic growth from 2012 to 2017 [9].

2.3.1 Energy Cost of the Mobile Industry

The rapid adoption of wireless internet is evident, for example, when Hutchison's High-Speed Downlink Packet Access (HSDPA) Universal Serial Bus (USB) dongles were introduced to the mass market. Within a year, it was found that data traffic exceeded voice traffic by a ratio of 47:3 in their UK networks [10]. Similar trends had also been reported in [11] and [12].

Mobile operators can cope with the rise in traffic demand by increasing the capacity of the network in several ways. Additional BSs can be deployed in areas that require more traffic. Besides that, more carriers can be utilised to transmit data over the channel, thus, requiring extra bandwidth. Last but not least, the spectral efficiency of existing bandwidths can be improved to accommodate higher data rate per Hertz. Seeing that the installation cost of each BS is high (0.15 million Great Britain Pounds (GBP) per site [13]) and the procurement of additional bandwidth is also very costly (22 billion GBP in the UK for Third Generation (3G) licensed spectrum [14]), increasing spectral efficiency of the existing bandwidth is the most viable option for almost all mobile operators. However, increasing spectral efficiency usually comes at a cost

of decreasing energy efficiency. While this trade-off is often overlooked in the past as spectral efficiency is pushed to its limits, the same design mindset may not be applicable today for several reasons.

Firstly, the surge in traffic due to the fast-paced transition to wireless internet will undoubtedly cause the energy consumption of the network to quickly surpass that of its present time rate where a network operator in the UK typically consumes around 40 - 50 MW of power [15], notwithstanding the power consumed at the mobile handsets. As far as the network operator is concern, energy consumption has a positive correlation to its OPerational EXpenditure (OPEX). An increase in energy consumption increases its OPEX which, in turn, increases its perceived cost per bit to operate the network. Therefore, if the traffic forecast in Fig. 2.2 is accurate, the cost per bit incurred by the network operator due to energy consumption will escalate exponentially as wireless internet penetrates to a greater extend into other parts of the developing world where internet mobility is just about to make its impact felt. Thus, with the rising energy cost of today, sacrificing energy efficiency while pursuing higher and higher spectral efficiency is no longer economically attractive.

Secondly, statistics showed that the data revenue received by the network operator is growing at a rate which lags behind the speed at which traffic is growing [16]. In fact, it only grows linearly as traffic flow increases exponentially. This is a direct consequence of the conventional billing scheme commonly employed by network operators. Unlimited internet access packages for flat payment rates are offered by the network operators as each of them hopes to attract as many users as possible to adopt its mobile broadband service. This generates a perception among mobile users to expect excellent quality of service at the lowest price possible from their network providers. As a result, network operators of today are struggling to keep up with both the high traffic demands of mobile users and increasing energy cost against a backdrop of an almost stagnant growth in revenue. It is thus paramount that energy consumption is decreased to restore the cost-revenue imbalance by increasing the energy efficiency of the network.

It is also worth noting that spectral efficiency improvement is diminishing as one generation of mobile network migrates to another. As illustrated in Fig. 2.3 [17], out of the 35% Compound Annual Growth Rate (CAGR) spectral efficiency gains registered as the network migrates from General Packet Radio Services (GPRS) to Long Term Evolution (LTE) 2×2 MIMO, only 12% CAGR is due to the so called next generation mobile networks while the rest of the larger gains being contributed by the Third Generation Partnership Project (3GPP) generation networks. As we progress further to Forth Generation (4G) mobile networks and beyond, even tighter gains in spectral efficiency are expected.

Thus, for a low priced wireless internet service to remain profitable, mobile operators will have to improve the energy efficiency of their networks through advanced transmission techniques and network architectures in order to deliver significant reduction in the associated cost per bit. As profitability is one of the major concerns of mobile operators, this motivates the design of the proposed economic efficiency metric in Chapter 4 to measure the economic fitness of the transmission scheme under consideration. The economic efficiency metric serves to complement the more conventional

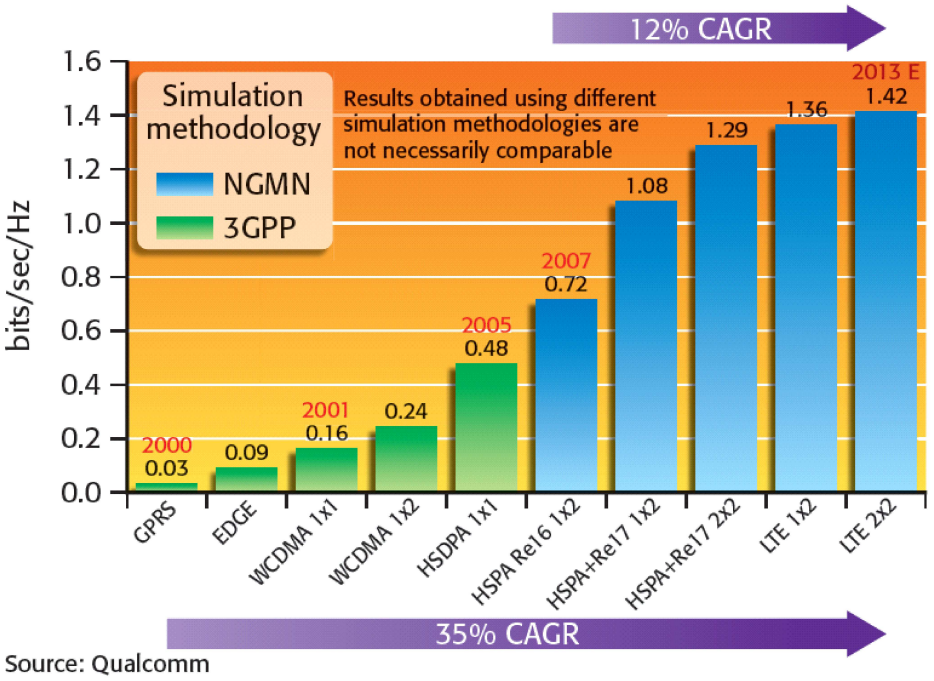

FIGURE 2.3: The spectral efficiency improvement in various generation of mobile networks [17].

spectral and energy efficiency metrics which are also used to evaluate the performance of the scheme under consideration.

2.3.2 Carbon Footprint of the Mobile Industry

At 34 billion tonnes of global CO_2 emissions in 2011 [18], it was stated in [19] that the ICT sector contributes around 2% of that total, of which 0.7% is due to the mobile industry [20]. Although the percentage contributed by the mobile industry seems unconcernedly small at present, this may not be the same reality in the near future when traffic volume is expected to rise considerably.

In the mobile industry, it is widely accepted that the source of carbon emission is largely due to either embodied energy or operation energy. Embodied energy relates to the energy consumption during the production of the product or service. This includes activities like raw material extraction, transportation, manufacture, assembly and installation. At the end of its life cycle, embodied energy also includes the energy spent during disposal activities like disassembling, deconstructing and finally decomposing or recycling of the product or service. As such, embodied energy forms part of the CAPital EXpenditure (CAPEX) of the mobile operators. On the other hand, operation energy relates to the energy spent during the operational lifetime of the product or service. It is the energy consumed by the various physical components of the devices that make up the product or service while performing the designated communication tasks. The operation energy contributes to the OPEX of the mobile operators.

In Fig. 2.4 [11], the CO_2 emissions per subscriber per year for both the BS and mobile handset is shown. About 75% of the total 10.7 kg of CO_2 emissions produced by the mobile handset is due to embodied energy, making it the dominant source of its carbon footprint. This is because these handsets are usually expected to have a short product lifetime of around 1.5 to 2 years as product turnover rate is high. Moreover, new generation batteries are very energy efficient and thus, drives the operation energy of the mobile handset even lower.

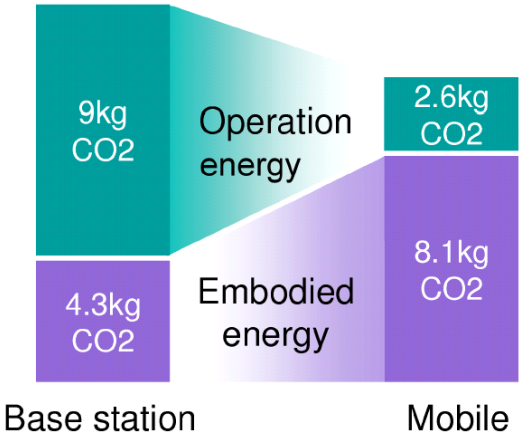

FIGURE 2.4: Comparison of CO_2 emissions per subscriber per year between a BS and a mobile handset in terms of embodied and operation energy [11].

On the other hand, a total of 13.3 kg of CO_2 emissions per subscriber per year is produced by the BS. While this total is greater than that of the mobile handset, about 65% of it is due to the operation energy of the BS, making it the dominant source of its carbon footprint. This is because of the long product lifetime of the BS which is typically around 10 to 15 years. A BS in a 3G mobile network typically consumes around 4.5 MWh of energy annually [21]. With around 12,000 BSs (200,000 BSs in developing markets like China) in a 3G network, this amounts to an energy consumption of over 50 GWh per annum [22]. Consequently, the BS is identified as the most energy consuming network component in a 3G mobile network [23] and thus, having the largest carbon footprint. Since a large amount of CO_2 emission resulting from this energy consumption is due to the operation energy, it is imperative that methods to increase the energy efficiency of the BS must be introduced.

Early Initiatives from the Mobile Industry

The mutual coupling between CO_2 emissions and OPEX in wireless networks was quickly realised by the mobile industry [24]. As a result, many mobile operators are committed to deliver significant reduction in energy consumption and CO_2 emissions

as part of their business operation targets. Among the very first to declare their intentions were Orange and Vodafone as stated in their year 2007 corporate responsibility reports in [25] and [26], respectively.

As a simple first step to fulfil their declared commitments, mobile operators have started purchasing energy from renewable resources in an effort to reduce their carbon footprint from the very top of their operation hierarchy. Although commendable, reducing carbon footprint through this method does not necessarily translate to a reduction in OPEX which relates more to the operational aspects of the network. In a bid to reduce the OPEX of the wireless network which are expected to rise exponentially in the near future as seen in Section 2.3.1, we witness the reintroduction of the metropolitan wireless local area network (WIFI) as part of the access network. Furthermore, the novel concept of femto-cell deployment has also recently garnered strong support from the mobile industry though many technical challenges have yet to be resolved. These technologies are popular choices as they reduce the OPEX of the wireless network by offloading parts of the data traffic to the wired network. Energy consumption of the BSs in the wireless network can thus be reduced and this, in turn, contributes to the reduction of CO_2 emissions.

Perhaps the most important development which highlighted the early initiatives from the mobile industry is the announcement of the 'Green Manifesto' in November 2009, together with the Climate Group, during the Groupe Speciale Mobile Association (GSMA) conference in Asia. The manifesto publicly declared the commitment of the mobile industry as a whole towards reducing GHG emissions. This included recommending policies for governments and the United Nations Climate Change Conference in Copenhagen. The effectiveness of the 2009 'Green Manifesto' in reducing the carbon footprint in wireless networks is closely monitored and positive results have been documented in the recent report in [23].

2.4 Mobile VCE: Green Radio

The importance in reducing OPEX and thus, carbon emissions, in wireless networks to achieve sustainable growth in the mobile industry is now evident. In the UK, this realisation has come to the attention of a group of mobile operators that had earlier coalesced in a non-profitable organisation called Mobile VCE (www.mobilevce.com). The primary goal of Mobile VCE is to address strategic research that can deliver significant growth opportunities to its members. Since its inception during the late 1990s, it has contributed positively to various innovative changes in the telecommunication industry through its Core Programs.

In early 2007, discussions were held among the Mobile VCE members to identify key drivers for its new research program that would strategically address the energy crisis of the mobile industry. The term Green Radio was first coined within the Mobile VCE community during these discussions, which prior to that only existed in reference to the color of the military radios and the name given to a radio station that broadcast environmental issues. The Mobile VCE Green Radio program, which forms a part of its Core 5 Program, was formally launch in October 2008. Being a pioneer in the field, the term Green Radio was quickly adopted by the rest of the mobile industry and academics alike. It also inspired the establishment of other like minded research initiatives around the world like EARTH (www.ict-earth.eu), GreenTouch (www.greentouch.org), YorkZhejiangLab for Cognitive Radio and Green Communications (www.yzlab.org), as well as GREEN (network.ee.tsinghua.edu.cn/green973). Today, research in green communications has become a vibrant and important field in its own, attracting many industrialists and academics.

2.4.1 Vision

The aspiration of the Mobile VCE Green Radio program is to design future wireless networks that achieve an ambitious 100 fold energy consumption reduction over the current networks. This target is to be reached without significantly compromising the existing network Quality of Service (QoS). More importantly, a holistic view of

energy consumption should be considered while the endeavour is undertaken. Thus, not only the RF transmit power but other costs relating to the deployment, operation and decommissioning of the wireless network should also be considered whenever it is appropriate.

2.4.2 Research Methodology

The goal of reducing energy consumption in future wireless networks has been addressed by studying energy issues in the architecture and technique aspects of Green Radio. While the research outcomes of Green Radio can be found in [27], some of the research topics are highlighted next.

2.4.2.1 Architecture of Green Radio

The purpose of the architectural investigation is to propose alternative approaches to the existing network topology that offer good trade-off between energy and spectral efficiency. Promising architectures that have been considered include protocols that enable delayed transmission (30% energy reduction) and BS sleep modes (90% energy reduction for no load cases) in conventional cellular networks.

Besides that, future cell size is expected to decrease as the RF transmit power is reduced in order to be more energy efficient. To maintain coverage, architectures involving the deployment of femto-cells (38% to 52% energy reduction) and the use of multi-hop relaying (58% energy reduction) have been considered. These two architectures enable the access network to be brought closer to the users. However, one must be aware of the back-haul cost that is required to provide the additional control signalling and connectivity to the core network as well as the increased interference level resulting from a denser network topology. A few of these architectures have been selected for further study by considering the wide area network, enterprise network and home network deployment scenarios.

2.4.2.2 Techniques Across the Protocol Stack

The proposed techniques which span across the protocol stack involve modification to the physical and network layers as well as the redesigning of hardware components in order to deliver improved energy efficiency.

Effective signal processing at the physical layer and radio resource management at the network layer can reduce the RF transmit power while maintaining the required QoS. At the physical layer, MIMO transmission techniques have been demonstrated to achieve 72% energy reduction by incorporating Space Frequency Block Code (SFBC) diversity techniques while novel radio resource management and scheduling techniques at the network layer have shown to deliver 44% to 50% energy reduction. Besides that, novel network coding techniques that also operate at the network layer have been investigated and have shown to provide 16% to 25% energy reduction.

Besides that, modification to the hardware components that alter the functionality of the transmission system can increase energy efficiency by reducing the total energy consumption relative to the RF transmit power. For example, the proposed Class-J Ultra Wide-Band (UWB) PA design has been shown to demonstrate a 70% drain efficiency over a frequency range of 0.5 GHz to 1.8 GHz. While, investigation into antenna design revealed that the minimisation of dielectric loss holds the key to improve energy efficiency whereby a 95% energy saving has been demonstrated for an air gap dielectric antenna operating at 2.1 GHz over a 300 MHz transmission bandwidth.

2.5 Performance Metrics

In this section, two performance metrics namely, the spectral and energy efficiency, are described. These metrics are utilised to evaluate the performance of the transmission schemes that will be described later in the work.

2.5.1 Spectral Efficiency

Let us consider a point-to-point MIMO transmission as shown in Fig. 2.5 with node X having N_b transmit antennas and node Y having N_u receive antennas. The channel between them is described by a $N_u \times N_b$ complex channel matrix $\mathbf{H}_{X,Y} \in \mathbb{C}^{N_u \times N_b}$. Also, let B_{sys} be the available bandwidth for transmission and P_{RF} be the RF transmit power of node X. The noise experienced by node Y is Gaussian distributed with zero mean and power spectral density N_0. Assuming error free transmission, the spectral efficiency of the transmission link is defined as [28]

$$C_{X,Y} = \max_{\mathrm{tr}(\mathbf{R}_X)=N_b} \log_2 \det \left[\mathbf{I}_{N_u} + \frac{P_{RF}}{N_b N_0 B_{sys}} \mathbf{H}_{X,Y} \mathbf{R}_X \mathbf{H}_{X,Y}^{\mathrm{H}} \right] \tag{2.1}$$

where $\mathbf{R}_X$ is the $N_b \times N_b$ signal covariance matrix. The spectral efficiency in (2.1) has unit of bits/s/Hz.

If the channel is unknown to the transmitter, in this case, node X, the best transmit strategy is to allocate equal power to all the N_b transmit antennas. Therefore, the signal covariance matrix is an identity matrix given by

$$\mathbf{R}_X = \mathbf{I}_{N_b}. \tag{2.2}$$

On the other hand, if the CSI is known to node X, optimisation of $\mathbf{R}_X$ can be done to further maximise the link spectral efficiency of (2.1). By using the Singular Value Decomposition (SVD) method [29], the channel matrix $\mathbf{H}_{X,Y}$ can be decomposed into

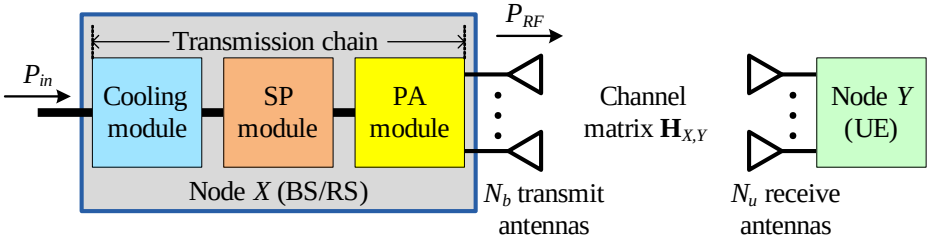

FIGURE 2.5: MIMO transmission between node X and node Y.

three components given by

$$\mathbf{H}_{X,Y} = \mathbf{U}\boldsymbol{\Gamma}\mathbf{V}^{\mathrm{H}} \tag{2.3}$$

where $\mathbf{U}$ and $\mathbf{V}$ are the $N_u \times r$ left singular and $N_b \times r$ right singular unitary matrices, respectively, with r being the rank of $\mathbf{H}_{X,Y}$. Besides that, $\boldsymbol{\Gamma} = \mathrm{diag}\left\{\gamma_i \,|i = 1, \cdots, r\right\}$ where the scalar γ_i is the ith singular value of $\mathbf{H}_{X,Y}$. The signal covariance matrix that maximises (2.1) thus takes the form of

$$\mathbf{R}_X = \mathbf{V}\boldsymbol{\Pi}\mathbf{V}^{\mathrm{H}} \tag{2.4}$$

where $\boldsymbol{\Pi}$ is the diagonal power loading matrix whose non-zero elements are the result of applying the water filling algorithm on the channel gains of $\mathbf{H}_{X,Y}$ which are given by the diagonal elements of $\boldsymbol{\Gamma}^2$. Furthermore, the values of $\boldsymbol{\Pi}$ must not violate the power constraint given by $\mathrm{tr}\left(\mathbf{R}_X\right) \leqslant N_b$. Typically, the spectral efficiency with channel knowledge present at the transmitter is higher than the case where the channel is unknown.

2.5.2 Energy Efficiency

2.5.2.1 Power Consumption Model

Again, let us consider the transmission setup as shown in Fig. 2.5. In the downlink transmission of a RACN which the work here primarily focuses on, node X can be the BS or RS while node Y is the UE. We will thus consider the operational power consumption at node X only because the BS (as discussed in Section 2.3.1 and Section 2.3.2) and, somewhat to a lesser extend, the RS consume the majority of the power in such a network.

In Fig. 2.5, the transmission chain of node X includes the antennas, PA module, SP module, cooling module and cables. The RF transmit power P_{RF} is the sum power radiated from the antennas of node X in order for it to transmit information to node Y. The power consumption of the whole transmission chain of node X is considered while

calculating the total operational power consumption $P_{op,total}$ which incidentally, is also the input power P_{in}. The linear power consumption model is utilised to encapsulate the power consumption of the transmission chain and provide a linear relationship between the input power P_{in} and the radiated RF power P_{RF} [30]. Thus, we have the total operational power defined as

$$P_{op,total} = P_{in} = \alpha P_{RF} + P_c \tag{2.5}$$

where α is the aggregate effect of the cable losses and the antenna/amplifier efficiency while P_c is the circuit power consumption of the SP module. Similar to [31], [32] and [33], the circuit power consumption is modelled as being proportional to the maximum RF transmit power. This is to represent future green BS (and RS) architecture where the constant power should ideally be zero when no transmission is occurring. Assuming P_{RF} is the maximum RF power that node X can radiate, the circuit power consumption is given as

$$P_c = \frac{P_{c,ref}}{P_{ref}} P_{RF} \tag{2.6}$$

where $P_{c,ref}$ is the circuit power consumption measured at the reference RF transmit power P_{ref}. In our work, we assume $P_{c,ref} = 577$ W at $P_{ref} = 40$ W. This conforms to the typical values found in the literature, for example, in [34] and [35].

2.5.2.2 Energy Consumption Ratio

In Green Radio, the energy efficiency of a system is measured by the Energy Consumption Ratio (ECR) metric which is defined as the energy consumed per delivered information bit [30]. Let $E_{op,total}$ be the total energy consumed at node X while transmitting M_{bits} information bits for a duration of time T. The ECR is thus

$$\begin{aligned} \text{ECR} &= \frac{E_{op,total}}{M_{bits}} \\ &= \frac{P_{op,total}}{B_{sys} C_{X,Y}} \end{aligned} \tag{2.7}$$

where the second expression of (2.7) is obtained by substituting the expression before it with $E_{op,total} = P_{op,total}T$ and $M_{bits} = B_{sys}C_{X,Y}T$, while having $C_{X,Y}$ and $P_{op,total}$ as defined in (2.1) and (2.5), respectively. The ECR metric has unit of J/bit.

2.5.3 User Location and Average Performance Calculation

Unless otherwise specified, a number of users are uniformly dropped across the sector during each numerical simulation. The users are served using either direct transmission or relay transmission, depending on which transmission scheme provides them with higher spectral efficiency given their current locations. The average sector performance is then calculated by summing the spectral and energy efficiency values associated with the users and averaging it across many randomised user drops.

2.6 Relaying Transmission

Relaying transmission has been considered as one of the promising technical solutions towards realising the vision of green communication networks in the future. In fact, it is already considered in the LTE standard to enable network operating at lower power consumption and it is also expected to be included in the International Mobile Telecommunications–Advanced (IMT–A) and LTE–A standards [3].

2.6.1 Use Scenarios of Relaying Transmission

The purpose of utilising RSs in wireless networks very much depends on the deployment scenarios. We will now consider a few scenarios where relaying transmission technology can be potentially beneficial to mobile operators [36].

2.6.1.1 Rural Area

In this scenario, it is expected that the penetration of wireless mobile services in rural areas is low (although this may change in the near future). Due to the low uptake of mobile services, the user density in the rural area is characteristically low and uniformly distributed. Deployment cost becomes an issue to mobile operators as it is not economical to install many macro BSs just to provide services to the thin distribution of users. As rural areas are usually wide, extensive coverage needs to be provided by a small number of macro BSs. One conventional method to meet this requirement is to increase the transmit power of the macro BSs. As the inter-site distance is large, interference among cells may not be critical, although, this approach may not be energy efficient.

Relaying transmission can fulfil the requirement of providing wide coverage at low transmit power in rural areas as illustrated in Fig. 2.6. By using RSs to extend the coverage area beyond that possible with a single macro BS transmitting at low power, ubiquitous user coverage is attainable at an improved energy efficiency. Deployment cost can be reduced too as it is cheaper and easier to deploy relays together with a few macro BSs than to install many expensive macro BSs. However, to continue servicing the users without having to deploy too many RSs, the coverage of each RS can be extended to several kilometres by allowing it to transmit at relatively higher power. The increase in interference as a result of this is tolerated as coverage is more crucial than capacity gains in rural areas with low traffic. Site planning becomes important as well since RSs transmitting at higher power tend to be deployed at fixed locations.

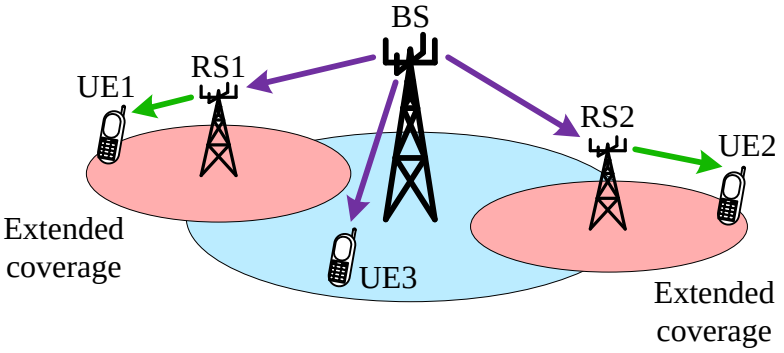

FIGURE 2.6: Relaying transmission in rural area.

2.6.1.2 Urban and Suburban Areas

Unlike rural areas, the user distribution in urban and suburban areas tend to be non-homogeneous. Instead, users are distributed in clusters called hot spots. The user density is also found to be higher than the rural area due to the higher penetration of mobile services in these areas which are economically more developed. Due to the densely deployed BS cell sites which are common in these areas, the RS coverage need not be as wide as the rural area. Therefore, RSs with low transmit power are used.

As capacity is crucial in this scenario, multiple fixed location or nomadic RSs are deployed within each BS coverage area to serve specific hot spots as shown in Fig. 2.7. At hot spot A, the RS functions as an in-between for the BS and the UEs. Traffic flow is reduced as the BS does not need to communicate with every UE at the hot spot. Instead, the BS transmits all the data only once to the RS which will then communication with the respective UEs. At hot spot B, traffic is offloaded seamlessly to another cell site having idle resources via an RS that manages the handover signalling overhead. In these two cases, the RS helps by decreasing the load of the busy BS so that the remaining UEs can be served at a higher capacity.

Due to the dense deployment of both BS and RS sites, interference becomes a major issue and has to be mitigated if any capacity gains from relaying transmission are to be made. Thus, employing RSs with low transmit power is favoured as this helps in

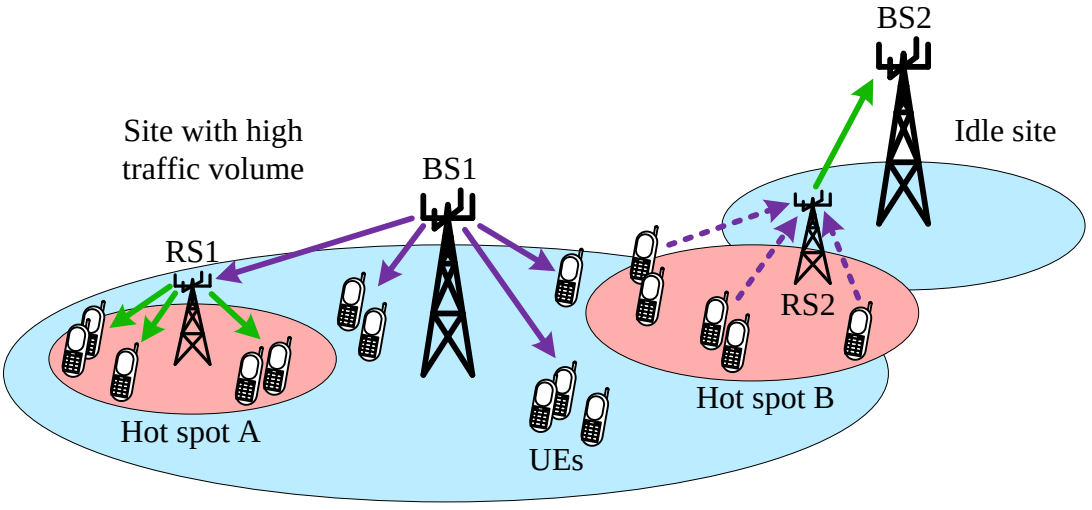

FIGURE 2.7: Relaying transmission in urban and suburban areas.

reducing the aggregate interference to adjacent cells as well as being more energy and cost efficient to deploy due to their compact size.

2.6.1.3 Blind Spots

As site planning is never easy especially on a terrain with many irregularities in forms, it is common to find a BS having its transmit antennas being blocked by surrounding objects like high-rise buildings and hills which are higher than the BS height. This causes a blind spot to form behind the obstructing objects. The UEs in the blind spot area would experience bad signal quality, often resulting in call dropping or no reception at all. It is not feasible to relocate the BS in order to eradicate blind spots. However, due to its compact size and flexibility, an RS can be easily deployed to a suitable location where its role is to relay information from the BS to the UE which is in the blind spot. This is illustrated in Fig. 2.8.

Blind spots can also happen indoors where coverage is poor due to both reflection and refraction of the signals coming from the BS as they past through the walls and into the interior hallways of the building. The affected indoor users may experience prolonged deep fading, especially if they are at the end of a large building far away from the BS. In this situation, throughput can again be improved by means of an indoor RS as shown in Fig. 2.9. However, care must be taken when configuring the indoor RS to ensure that the performance gain by using relaying transmission is no less than that could be achieved through the outdoor-to-indoor BS–UE direct

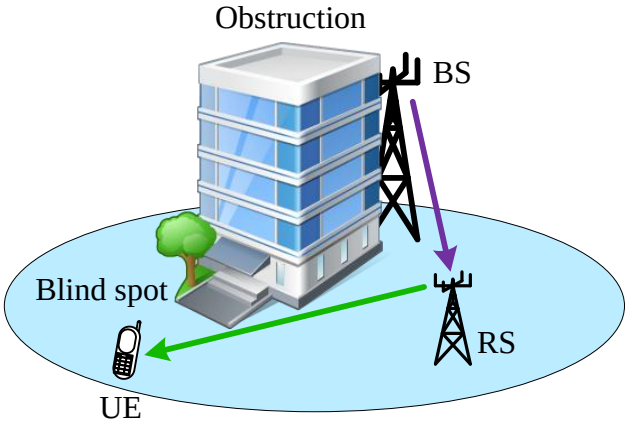

FIGURE 2.8: Relaying transmission for outdoor blind spots.

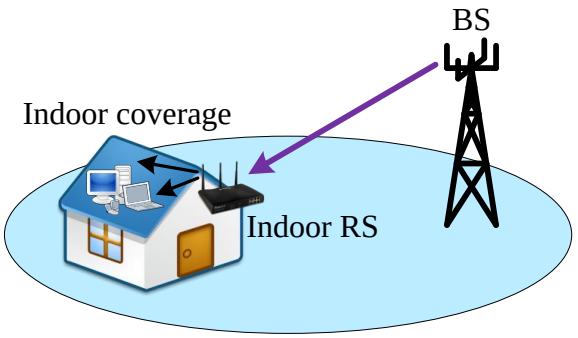

FIGURE 2.9: Relaying transmission for indoor blind spots.

transmission. In order to avoid excessive penetration loss at the BS–RS back-haul link, thus, compromising on performance, one RS may be placed preferably near an opening of the building, for example, a window or on the roof. Another RS may be deployed somewhere inside the building to provide the needed indoor coverage. The two RSs can then communicate by using a separate bandwidth from the underlying cellular system. One of the disadvantage is that site optimisation to improve the performance of the back-haul link can be a challenge if the indoor RSs are installed by the individual users rather than being planned by the mobile operators.

2.6.1.4 Emergency Ad-Hoc Network

During a state of emergency like the occurrence of natural disasters such as flooding and earthquake or in the advent of a terrorist attack, there might not be a communication infrastructure in place at the disaster sites to coordinate humanitarian aid or other crucial activities. In these cases, a temporary ad-hoc network must be quickly rolled out to the affected areas in order to at least establish the basic fulfilment of a functional communication system. This temporary network must also be easy to tear down once its purpose is accomplished.

Relaying transmission can be one of the solutions to this scenario. As illustrated in Fig. 2.10, one or a number of RSs can be quickly deployed in and around the disaster areas to provide a communication link to the affected individuals, humanitarian workers and military. The natural back-haul of the RS means that it can connect to

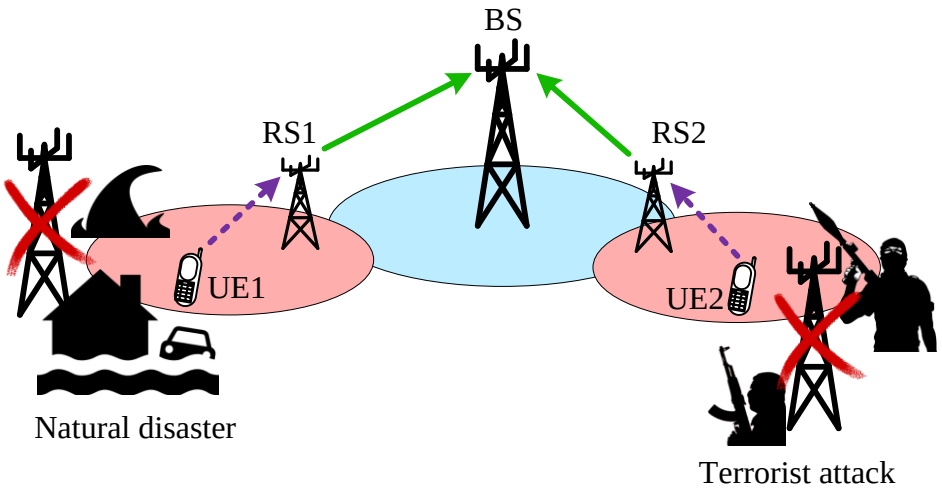

FIGURE 2.10: Relaying transmission supporting emergency ad-hoc network setup.

the nearest functional cell site to relay information to a fully functional network that will be utilised to process the main communication tasks.

2.6.1.5 Wireless Back-haul Assistance

When it is not economical or geographically difficult to install a wired back-haul, for instance, between two BSs, the more flexible and cost effective wireless back-haul [37] can be provided by the RS as shown in Fig. 2.11. In this case, the RS does not communicate with any UEs as its sole purpose is to provide a reliable link between the two BSs.

In order to achieve a high performance wireless link, the conventional point-to-point microwave link may not be suitable as it succumbs easily to signal attenuation due to its dependence on weather condition. This is unlike the cellular network spectrum utilised by mobile operators which is generally more resilient to unfavourable weather conditions. However, there must be idle resources available in the cellular network for the RS to utilise. Because of that, the partial use of the cellular network spectrum by the RSs for reliable wireless back-haul purposes is only suitable in places with very low traffic flow, for example, in the rural areas where the spectrum is underutilised most of the time. In this case, it may also be favourable for the RS to transmit at

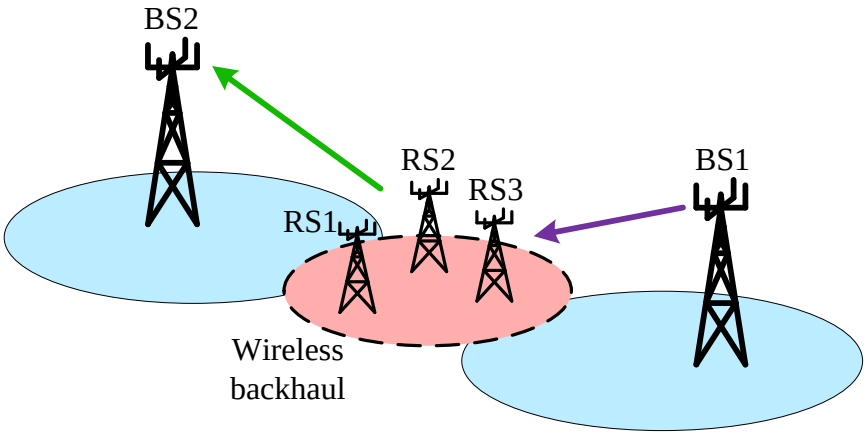

FIGURE 2.11: Relaying transmission providing wireless back-haul assistance.

higher power to further guarantee a high capacity wireless link as interference in rural areas is not a major concern.

2.6.1.6 Group Mobility

Group mobility poses new communication challenges to the wireless network. Mobile users on-board modern high-speed public transport often have low quality of service. Data rates drop significantly and the lifespan of batteries is shortened. Furthermore, voice calls are often harsh and discordant. These problems are due to several factors. Firstly, the signal strength is decreased due to penetration loss as it passes through the walls of the vehicles. Besides that, frequent transmission of control signals for measurement and handover is needed by the group of on-board UEs as the high-speed vehicle passes through quickly from one cell site to another. Additional power is thus needed to overcome both the penetration loss and the frequent signalling. This causes the batteries of the UEs to drain quickly. Furthermore, signal congestion often happens as group mobility induces a large amount of concurrent handover signalling from all the on-board UEs each time the vehicle passes through different cell sites. The congestion ultimately forces connection to be broken, resulting in calls being frequently dropped.

As depicted in Fig. 2.12, relaying transmission might again help to partially alleviate the problem by installing a RS on top of the public transport. Handover signalling

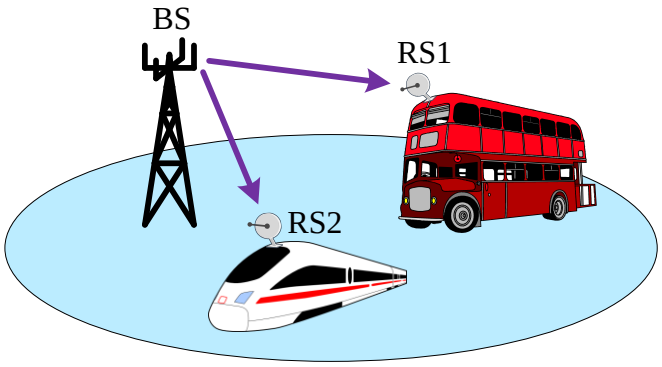

FIGURE 2.12: Relaying transmission for group mobility.

is now managed by the RS instead of the many individual UEs on-board the public transport. This reduces traffic congestion at the cell site. Besides that, the RS–UE access link is usually good as the distances between the on-board UEs and the RS are small. Its high quality link is also due to the fact that the UEs appear to be stationary with respect to the RS. Therefore, the batteries on the UEs will last longer as lower power is now needed for the transceivers. Nevertheless, the reliability of the BS–RS back-haul link must be guaranteed to ensure an improved overall performance. This is challenging as the back-haul link is exposed to fast fading environment due to the high-speed vehicles.

2.6.1.7 Device to Device Communication

In a dense urban environment, BSs are deployed at locations that will maximise the coverage of outdoor users. Consequently, indoor coverage can be poor, especially in the centre of large buildings. Outdoor blind spots are also commonly occurring in urban environment due to high-rise buildings. These coverage problems can be solved with additional small cell deployments or with fixed relays as seen in Section 2.6.1.3. However, this can be costly and sometimes impractical.

In the absence of fixed relay infrastructures, Device to Device (D2D) communication provides an alternative approach to solving poor coverage conditions. As illustrated in Fig. 2.13 for D2D communication, users with a strong signal would help nearby users with a weak signal by relaying the desired information to the latter. This greatly reduces coverage holes and restores service to users with a weak direct link

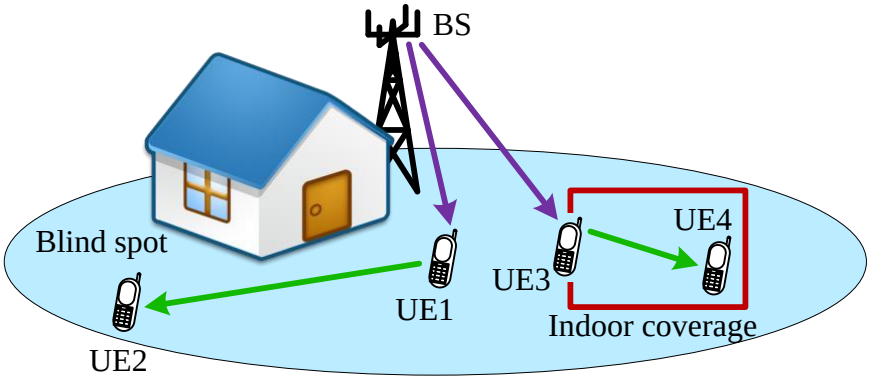

FIGURE 2.13: Device to device communication.

signal. Besides improving the performance of the devices, D2D communication also helps in offloading traffic from cellular networks, thus, improving energy efficiency. However, D2D communication has its own set of technical challenges. Firstly, service identification is important to determine which devices are suitable to participate in the transmission. Methods for dynamic resource sharing between the cellular network and D2D communication must also be designed.

2.6.2 Classification of Relaying Transmission

Since introduced by Meulen [38], relaying transmission has been widely researched over the past decades, resulting in a rich body of work in the literature. This section attempts to provide an overview of the many genres of relaying transmission by classifying them into several mutually exclusive categories as shown in Fig. 2.14. Thus, existing relay transmission schemes can be identified by relating them to at least an attribute in each category. In relaying transmission, at least two basic transmission channels are involved in forming an information pipeline from the source to the destination. The spectral efficiency of different relaying transmission schemes is derived by combining or comparing scaled versions of these basic transmission channels. As there are many ways of doing this, a general spectral efficiency expression that consolidates all relaying transmission schemes is impossible by far. However, each basic transmission channel is typically a direct transmission channel having spectral efficiency similar to (2.1).

2.6.2.1 Relaying Transmission Mechanisms

In this section, four main types of relaying transmission mechanisms are described. They are the DF, AF, Compress-and-Forward (CF) and hybrid relaying mechanisms.

Decode-and-Forward Relaying

In DF relaying, the RS will attempt to decode the received signal before forwarding it to the UE. To guarantee successful decoding, the BS transmission rate must not exceed the BS–RS link capacity. Additionally, it must not exceed the RS–UE link capacity as well in order for the UE to be able to decode the relayed signal. The duration of both the broadcast phase and relay phase can be further optimised, for example, in [39]–[41], to improve performance.

Because the RS decodes the received signal before relaying it to the UE, there will be no background noise present in the relayed signal itself. However, the disadvantage is that the BS–RS link must always be reliable in order for the RS to constantly perform successful decoding on the received signal. This is a challenging criteria to meet especially when the RS is deployed in a fast fading environment. The RS also must have prior knowledge regarding some of the system parameters, for example,

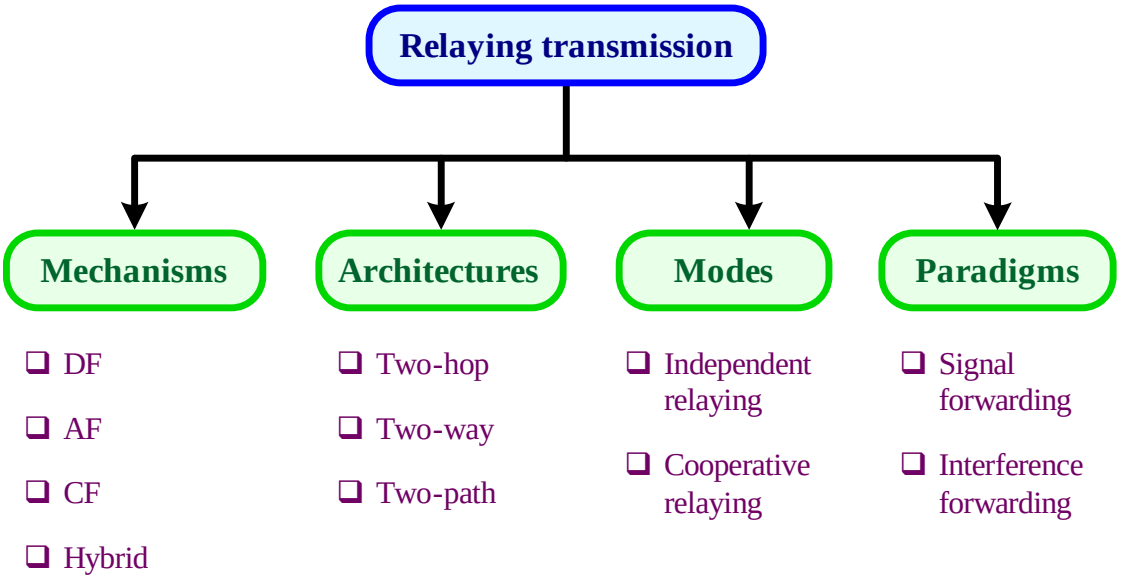

FIGURE 2.14: Classification of relaying transmission.

the modulation scheme and the transmission frame structure, to perform its decoding tasks. Therefore, it is non-transparent to the underlying cellular network where it is deployed.

Amplify-and-Forward Relaying

Unlike DF relaying, the RS adopting the AF mechanism does not attempt to decode the received signal. Instead, it simply amplifies the received signal before relaying it to the UE. If the RS amplifies the received signal with a scalar value, it is known as a repeater. Repeaters are suitable in an environment where the noise present at the RS is low or the RS–UE link quality is high. This is to ensure that some form of Signal-to-Noise Ratio (SNR) gain is achieved at the UE when the amplified signal plus noise is being relayed.

A more advanced version of AF relaying can be implemented if the RS has both the broadcast phase and relay phase channel knowledge. In this case, an amplification matrix can be designed in such a way as to completely decompose the end-to-end channel which is between the BS and UE into several independent sub-channels, each supporting one data stream. This results in an improved multiplexing gain. Examples of this can be found in [42]. Since AF relaying does not require decoding of the received signal, it is easier to implement as it does not need to know the operational parameters of the underlying cellular network, that is, it can be deployed transparently.

Compress-and-Forward Relaying

The CF relaying mechanism is suitable if there is a BS–UE direct link and the RS is closer to the UE than it is to the BS. In this case, the RS will relay to the UE an observation of the signal it received during the broadcast phase. It does so by quantising the received signal into a series of samples. Because of that, it is also known in the literature as quantise-and-forward relaying. The samples are then compressed into a string of discrete bits using source coding such as Wyner-Ziv coding [43], [44] and Voronoi coding [45] to exploit the correlation between the received signals at

both the RS and UE. Next, the compressed signal is relayed to the UE which then will combine both observations it received from the RS and BS in order to reconstruct the signal for data extraction.

In CF relaying, the noise amplification at the RS is not as severe as AF relaying. Provided that the RS–UE link capacity is high enough, the duration of the relay phase can be made relatively short, depending on the desired accuracy or the tolerated distortion of the received observation samples at the UE.

Hybrid Relaying

In hybrid relaying, a combination/modification of the above relaying mechanisms can be employed by the RS. For example, the conventional DF relaying is demanding as it requires the RS to decode the whole coded message sent by the BS during the broadcast phase before relaying the decoded message to the UE. If decoding error is encountered, the RS may request for the entire message to be resent or remain silent during the relay phase. Hybrid DF schemes are proposed to relax this stringent requirement. In dynamic DF relaying [46], [47], the RS may start decoding the message before the BS finishes transmitting it. The time it can start decoding depends on the BS-RS link quality as it has to wait until the accumulated mutual information over the BS–RS link is comparable to the BS transmission rate. Whereas in partial DF relaying [48], [49], the RS is allowed to partially decode the message if it is unable to perform full decoding of the entire message. This reduces noise amplification as compared to AF relaying while not having the stringent requirement to decode the entire message as compared to the conventional DF relaying.

Besides that, DF and CF relaying can be combined to achieve better performance as investigated in [50] whereby the RS firstly decodes the message before compressing and relaying it to the UE. In [51], [52], a scheme with two RSs was presented with one RS employing DF relaying while the other CF relaying. While, the RS in [53] is able to switch between DF relaying and AF relaying, depending on which providing better throughput.

2.6.2.2 Relaying Transmission Architectures

Relaying transmission can also be categorised according to its architecture which also determines its signalling protocol. Three main types are presented here, namely, the two-hop, two-way and two-path relaying architectures.

Two-Hop Relaying

In Fig. 2.15(a), the two-hop relaying architecture [54] is illustrated together with its signalling protocol in Fig. 2.15(b). The RS usually operates in half-duplex mode, that is, it cannot transmit and receive simultaneously on the same time and frequency. During the broadcast phase, the BS occupies a certain duration of time to transmit its signal while the RS listens. During the relay phase, the RS processes the received signal from the BS according to one of the mechanisms in Section 2.6.2.1 and utilises the remaining time duration to transmit the processed signal to the UE.

The two-hop relaying architecture incurs a certain amount of multiplexing loss as two hops are needed for each information packet to reach the UE. As the number of hops increases, for example, in a multi-hop relaying, both multiplexing loss and complexity would increase. For that reason, the two-hop relaying provides the best trade-off

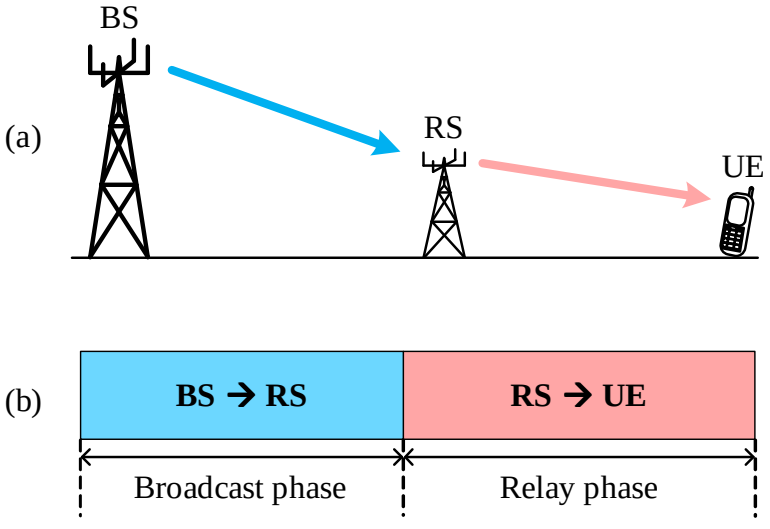

FIGURE 2.15: (a) The two-hop relaying architecture for downlink transmission and (b) its corresponding signalling protocol.

between complexity and performance. In this relaying architecture, either uplink or downlink transmission occurs at any given instance.

Two-Way Relaying

Unlike two-hop relaying, the two-way relaying architecture improves spectrum utilisation by allowing both uplink and downlink to occur simultaneously via the RS. This is illustrated in Fig. 2.16(a) with its corresponding signalling protocol in Fig. 2.15(b). During the first duration known as the access phase, both the BS and UE transmit their signals to the RS. The combined signals are processed at the RS before it transmits its version of the processed signals to both the BS and UE. At the destinations, both the BS and UE recover the desired signals by utilising both the relayed signal and the knowledge of their own transmitted signals during the access phase.

Many strategies can be employed for two-way relaying. In [55], the DF mechanism is utilised at the RS to process the aggregated signals it received from the BS and UE. While in [56], [57], the AF mechanism is employed instead. In the recent years, network coding [58] and its physical layer counterpart known as physical network coding [59], are being considered in the two-way relaying architecture. Other examples that investigated hybrid solutions can be found in [60]–[63].

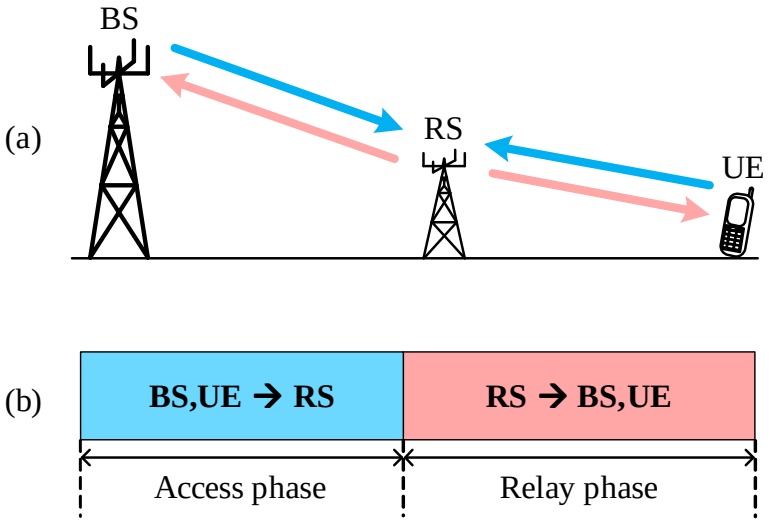

FIGURE 2.16: (a) The two-way relaying architecture and (b) its corresponding signalling protocol.

Two-Path Relaying

As shown in Fig. 2.17(a), two RSs are required in the two-path relaying architecture. Unlike the previous architectures where there is a dedicated relay slot for the relay phase, the RSs in two-path relaying alternately transmit in every time slot as illustrated in Fig. 2.17(b). Specifically, RS1 will listen during the first time slot while both the BS and RS2 transmit. During the second time slot, it is the turn for RS2 to listen while both the BS and RS1 transmit. The UE will alternately listen to each RS as they relay their signals during their respective time slots.

Multiplexing loss is recovered in two-path relaying as information packets are transmitted by the BS during each time slot. Given the nature of the timing protocol, an additional time slot is needed for the UE to completely receive all the transmitted information packets. This is not a huge penalty as the number of information packets is usually large. Some examples of two-path relaying are given in [64]–[67].

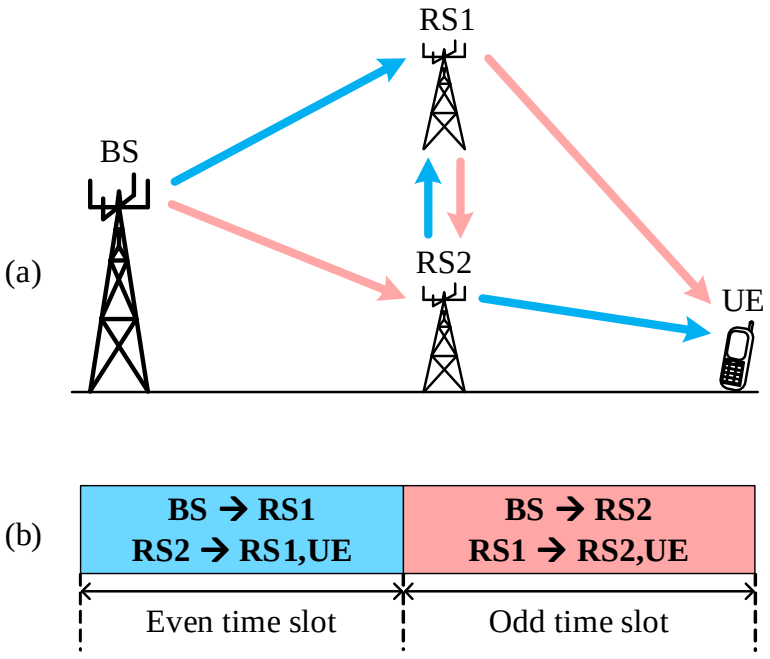

FIGURE 2.17: (a) The two-path relaying architecture and (b) its corresponding signalling protocol.

2.6.2.3 Relaying Transmission Modes

In this section, two possible relaying transmission modes are described. They are the independent and cooperative relaying modes.

Independent Relaying

Independent relaying is the simplest mode of relaying whereby the RSs transmit their signals in an uncoordinated manner as shown in Fig. 2.18(a). As a result, the received signal at the UE is contaminated with interference from the undesired RSs which are being allocated with the same network resource for relaying. This could be a major problem especially for cellular networks operating in urban areas where RSs are more densely deployed, thus, having overlapping coverage.

Employing frequency reuse planning schemes can mitigate potential interference of nearby RSs [68]–[71]. This, however, may result in inefficient utilisation of valuable bandwidth resources. Other interference mitigation methods include cognitive relaying [72], managing number of active RSs [73], interference neutralisation [74], interference aware resource allocation [75], decode/amplify-and-cancel [76], as well as rate splitting [77].

Cooperative Relaying

Cooperative relaying incorporates the principles of cooperative communication into its relaying and, thus, enjoys the benefit of throughput enhancement. In cooperative relaying, the RSs collaborate to perform joint transmission during the relay phase as illustrated in Fig. 2.18(b). In other words, the RSs perform Cooperative Multi-Point (CoMP) relaying towards the assigned UE group. Cross interference is mitigated as the signals from the RSs are coherently transmitted to the UEs. With the absence of interference from the cooperative RSs, the SNRs and, consequently, the throughput of the UEs improve. Transmit power may also be reduced to achieve the targeted QoS, leading to improved energy efficiency.

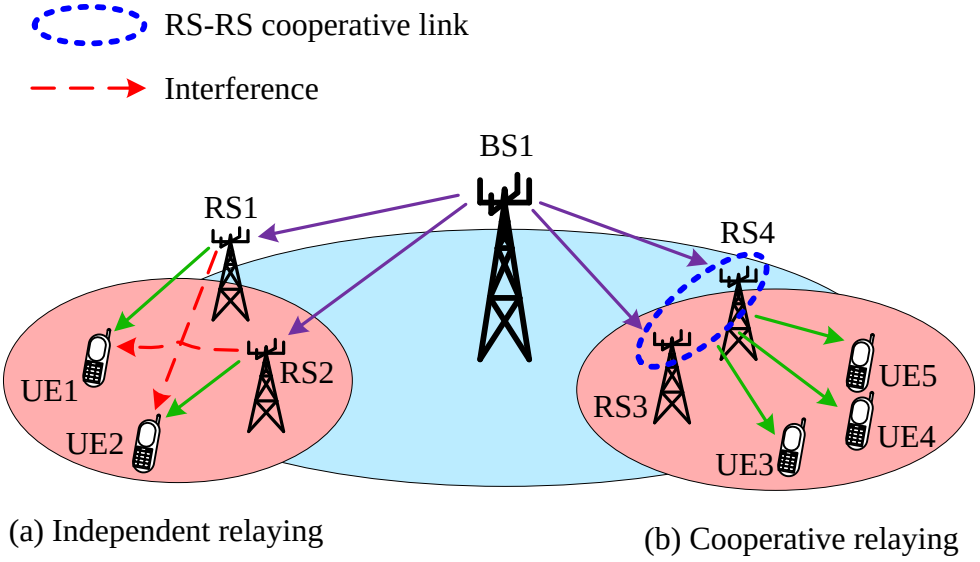

FIGURE 2.18: Relaying transmission modes: (a) Independent relaying and (b) cooperative relaying.

However, the cost of cooperative relaying lies in the amount of cooperative information that is required to facilitate joint transmission. Cooperative information may consist of both the CSI and data. In order for the RSs the share cooperative information, cooperative links are established between them. These links may borrow resources from the underlying cellular network but since cooperative relaying is more likely to be deployed in resource-constrained environment to enhance throughput, the more practical alternative is for the cooperative links to utilise separate bandwidth found in, for example, the microwave or UWB channels. Furthermore, cooperative relaying schemes that require reasonable amount of cooperative information should be designed and the frequency of access to this information should be kept low. Otherwise, the cost of installing cooperative links that demand prohibitively high data rate and power consumption would far outweigh the increase in performance that cooperative relaying may bring to the cellular network.

2.6.2.4 Relaying Transmission Paradigms

Relaying transmission may also be broadly categorised into different paradigms according to the purpose of the relayed signal. Two relaying transmission paradigms can be found in the literature. They are either the SFR or IFR paradigms.

Signal Forwarding Relaying

The idea behind SFR is to increase the received signal quality at the UE by relaying a copy of the desired signal to it as shown in Fig. 2.19(a). The overall throughput may be improved especially when the signal from the BS–UE direct link is weak. The UE can have the option of optimally combining the received signal obtained during both the broadcast and relay phases by using, for example, the Maximum Ratio Combiner (MRC) method [78] to realise the diversity gain.

Interference Forwarding Relaying

On the other hand, a copy of the dominant (strongest) interference is relayed to the UE in the IFR scheme [79]–[81]. This is illustrated in Fig. 2.19(b). The aim here is to further increase the strength of the dominant interference so that the UE can reliably detect and decode it. Upon successful decoding, the UE then subtracts it from its direct link received signal. This improves the quality of the received signal. Alternative, the UE can utilise the Interference Rejection Combining (IRC) method [82] to detect the desired signal. The performance of the IRC method can be increased if implemented together with IFR as the interference statistics can be estimated more

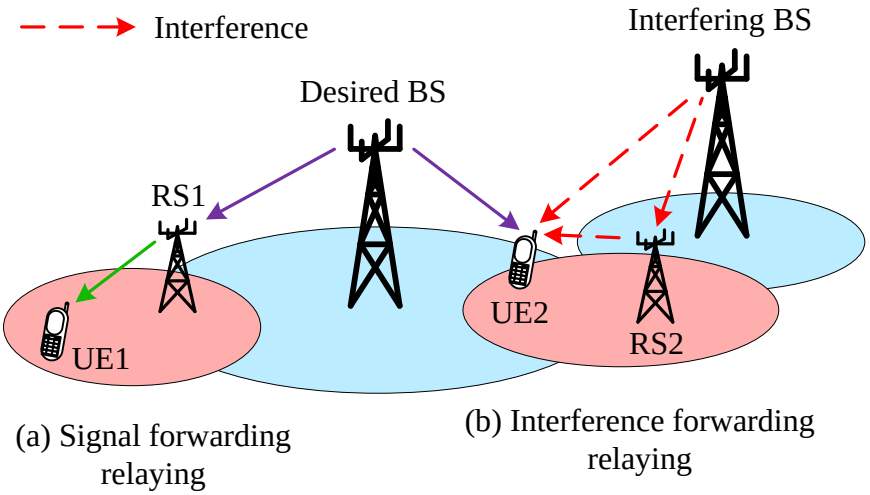

FIGURE 2.19: Relaying transmission paradigms: (a) Signal forwarding relaying and (b) interference forwarding relaying.

accurately as a result of having two copies of the same interference source at the UE. Therefore, the SNR at the UE is improved in the absence of the dominant interference.

2.7 Conclusions

In this chapter, some background knowledge on climate change is provided. It is argued that a change in the traditional ways of business is necessary to provide a sustainable economic growth in the future. To achieve this, many regard the ICT sector, and more specifically the mobile industry, as a viable catalyst in initiating the paradigm shift towards a greener economy by reducing the carbon footprint of other industries. This increases the strain on the mobile networks and unless energy efficient countermeasures are taken early, mobile operators are expecting to face an imminent energy crisis as traffic load is anticipated to grow exponentially. Relaying transmission has been presented as a promising technology to reduce the energy consumption of a network by facilitating the reduction in transmission power. Some possible use scenarios are given to illustrate the usefulness of relaying transmission while a classification approach is also provided to systematically categorise the many types of relaying transmission found in the literature. Based on this classification, the work in this thesis will mainly focus on the DF and AF relaying mechanisms having the two-hop relaying architecture with both the independent and cooperative relaying modes and both the signal forwarding and interference forwarding relaying paradigms.

Chapter 3

Power Consumption of Direct Transmission Cellular Networks

3.1 Introduction

It was reported in [23] that BSs consume the most operational power, typically around 60% of the total power in the mobile network infrastructure. Therefore, the reduction of BS power consumption is key in reducing the overall carbon footprint of the mobile industry in an effort to reduce the global carbon footprint which stands at 245 Mt Carbon diOxide equivalent (CO_2e) in 2009, a rise of 155 Mt CO_2e since 2002.

MIMO communication system is being considered in emerging wireless communication standards such as the LTE–A to reduce BS power consumption during signal transmission besides promising high data rates without increasing bandwidth utilisation [83]. However, MIMO suffers from complex signal processing, making practical implementation a challenge. The development of the Vertical-Bell Laboratories Layered Space-Time (V-BLAST) receiver structure [84] provides a good trade-off between performance and complexity. Since then, with the move to LTE–A, research has been predominantly focused on further improving the receiver interference cancellation and signal detection capabilities to better balance data rate and complexity [85]–[87].

Efforts in reducing BS transmission energy are usually focused on transmission side techniques. Examples here include power allocation [88]–[91], beamforming [92]–[96], rate allocation [97]–[101] and antenna selection [102]–[105]. In [106], the authors proposed a transmission mode switching scheme that switches between SIMO and MIMO modes to save energy. In [107], a channel estimation scheme was proposed to minimise both the transmitter and receiver energy consumption. While in [108], the energy efficiency of the Multiple Input Single Output (MISO) Orthogonal Frequency Division Multiplexing (OFDM) transmission scheme with power and capacity constraints was investigated. In [109], the energy efficiency of random network coding for LTE–A networks was examined while in [110], energy efficiency improvement in both the PA and SP modules was demonstrated through appropriate use of constellation modulation techniques. The authors in [111] achieved transmit power reduction in OFDM systems through a Peak to Average Power Ratio (PAPR) reduction scheme. In [112], energy efficiency analysis was carried out on a point-to-point transmission system without considering any receiver Interference Cancellation (IC) techniques. On the other hand, several receiver IC techniques were considered in [113]–[116] to reduce the complexity, and thus, energy consumption, at the receiver.

Little work has been presented to investigate the impact of receiver IC techniques on the BS total power consumption that includes the energy consumption of both the PA and SP modules. The authors in [117] attempted to address this but the energy efficiency was limited to only the RF transmit power. Examples of BS power consumption model can be found in [34] and [35].

The following list describes our contributions in order to address some of the shortcomings of the previous work.

1. We investigate the BS power consumption for the downlink of DTCNs.

2. We analyse the BS power consumption for both the conventional and SIC receivers. For each receiver, both the ZF and MMSE weight optimisation approaches are considered.

3. We consider the circuit power consumption of the SP module when evaluating the BS power consumption as it is well known that MIMO circuits require a substantial amount of power to operate.

4. We demonstrate that depending on the number of transmit/receive antennas and the type of receiver IC technique, different transmission power is needed to achieve a targeted Signal-to-Interference-plus-Noise Ratio (SINR) value at the receiver output.

5. We show that treating inter-cell interference from adjacent BSs as background noise when detecting the desired signal is not an energy efficient approach.

The rest of the chapter is organised as follows. In Section 3.2, the system model of the direct transmission scheme is described. Next, the receiver IC techniques are presented in Section 3.3 while the power consumption model is given in Section 3.4. The SIMO energy consumption and analysis for a large number of receive antennas are given in Section 3.5 and Section 3.6, respectively. This is followed by some simulation results and discussions in Section 3.7. Finally, the chapter concludes in Section 3.8.

3.2 System Model

Let us consider a MIMO communication system consisting of a BS with N_b transmit antennas communicating to a receiver with N_u receive antennas. We label this BS as BS^A to differentiate it from other BSs. All the N_b transmit antennas are assumed to transmit at an equal power. Furthermore, let us assume there are I adjacent BSs as shown in Fig. 3.1 and the receiver is within their transmission range. Let BS^i be the ith adjacent BS having L_i transmit antennas. Therefore, assuming a full spatial multiplexing system, the complex signal vector received by the N_u receive antennas at a particular time under the uncorrelated Rayleigh flat fading channel condition is

$$\mathbf{y} = \sum_{m=1}^{N_b} \mathbf{h}_m^A s_m + \sum_{i=1}^{I} \sum_{l=1}^{L_i} \mathbf{h}_l^i x_l^i + \mathbf{z}. \tag{3.1}$$

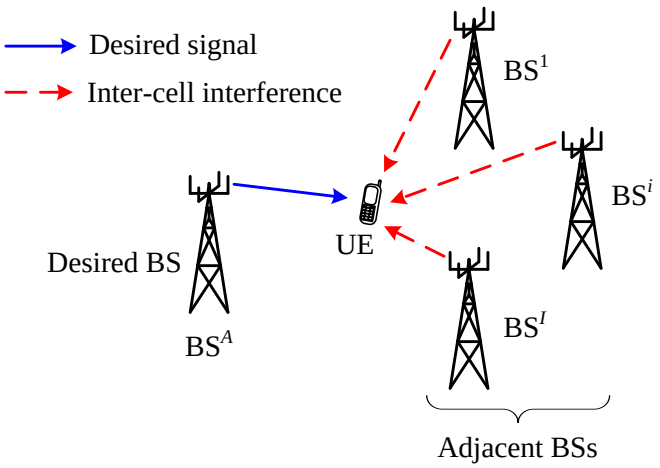

FIGURE 3.1: Multicell MIMO cellular network topology.

Here, $\mathbf{h}_m^A = \left(h_{1,m}^A, \cdots, h_{N_u,m}^A\right)^{\mathrm{T}}$ is the channel vector from the mth ($m = 1, \cdots, N_b$) transmit antenna of BS^A to the receiver. The complex coefficient $h_{n,m}^A$ in $\mathbf{h}_m^A$ is a complex random variable, the absolute value of which follows a Rayleigh distribution, and represents the complex channel coefficient from the mth transmit antenna of BS^A to the nth ($n = 1, \cdots, N_u$) receive antenna. The complex symbols to be transmitted at time t from BS^A and BS^i are denoted by s_m and x_l, respectively. The second term in (3.1) is the additive interference contributed by the I adjacent BSs with $\mathbf{h}_l^i = \left(h_{1,l}^i, \cdots, h_{N_u,l}^i\right)^{\mathrm{T}}$ being the channel vector from the lth transmit antenna of BS^i to the receiver. Furthermore, the vector $\mathbf{z} = (z_1, \cdots, z_{N_u})^{\mathrm{T}}$ represents the noise present at the receiver with its elements being independent and identically distributed (i.i.d.) complex Additive White Gaussian Noise (AWGN) random variables having zero mean and variance σ^2. The average power of the mth transmitted symbol of BS^A is given by $\mathbb{E}\{s_m s_m^*\} = p_m^A$.

3.3 Receiver Interference Cancellation Techniques

3.3.1 The Conventional Linear Receiver

In the conventional linear receiver structure, the estimated symbol from the mth transmit antenna of BS^A is given by $\hat{s}_m = \mathbf{w}_m^{\mathrm{H}}\mathbf{y}$, where $\mathbf{w}_m = (w_{1,m}, \cdots, w_{N_u,m})^{\mathrm{T}}$ is the complex weight vector for the mth symbol. Substituting (3.1) for $\mathbf{y}$, we have the

following expression

$$\hat{s}_m = \underbrace{\mathbf{w}_m^{\mathrm{H}}\mathbf{h}_m^A s_m}_{\text{desired signal}} + \underbrace{\sum_{j\neq m}^{M}\mathbf{w}_m^{\mathrm{H}}\mathbf{h}_j^A s_j}_{\text{intra - cell interference}} + \underbrace{\sum_{i=1}^{I}\sum_{l=1}^{L_i}\mathbf{w}_m^{\mathrm{H}}\mathbf{h}_l^i x_l^i}_{\text{inter - cell interference}} + \underbrace{\mathbf{w}_m^{\mathrm{H}}\mathbf{z}}_{\text{noise}}. \tag{3.2}$$

The intra-cell interference refers only to the interference from different antennas of BS^A, the desired BS. While, the inter-cell interference is the interference from the I adjacent BSs. The SINR at the output of the receiver for the mth symbol can be expressed as

$$\mathrm{SINR}_m = \frac{\left|\mathbf{w}_m^{\mathrm{H}}\mathbf{h}_m^A\right|^2 p_m^A}{\sum\limits_{j\neq m}^{M}\left|\mathbf{w}_m^{\mathrm{H}}\mathbf{h}_j^A\right|^2 p_j^A + \sum\limits_{i=1}^{I}\sum\limits_{l=1}^{L_i}\left|\mathbf{w}_m^{\mathrm{H}}\mathbf{h}_l^i\right|^2 p_l^i + \sigma^2\|\mathbf{w}_m\|^2} \tag{3.3}$$

where p_j^A $(j = 1, \cdots, N_b)$ and p_l^i $(l = 1, \cdots, L_i)$ are the symbol power transmitted from the jth and lth antennas of BS^A and BS^i, respectively. Since there is no CSI available at the transmit side, equal power allocation is assumed at all transmit antennas of the BSs, i.e., $p_1^A = \cdots = p_{N_b}^A = p_{\mathrm{Conv}}^A$ and $p_1^i = \cdots = p_{L_i}^i = p^i$. Thus, p_{Conv}^A represents the RF power per antenna allocated to each symbol transmitted from BS^A for the conventional linear receiver. Furthermore, we consider two weight optimisation approaches [115] to calculate $\mathbf{w}_m$ at the receiver. Let $\mathbf{H} = \mathbf{H}^A = \left(\mathbf{h}_1^A, \cdots, \mathbf{h}_{N_b}^A\right)$. In the ZF weight optimisation approach, the weights are

$$\mathbf{W}_{\mathrm{ZF}} = (\mathbf{w}_1, \cdots, \mathbf{w}_{N_b}) = \left(\mathbf{H}\mathbf{H}^{\mathrm{H}}\right)^{-1}\mathbf{H} \tag{3.4}$$

while in the MMSE weight optimisation approach, the weights are given as

$$\mathbf{W}_{\mathrm{MMSE}} = (\mathbf{w}_1, \cdots, \mathbf{w}_{N_b}) = \left(\mathbf{H}\mathbf{H}^{\mathrm{H}} + \sigma^2\mathbf{I}_N\right)^{-1}\mathbf{H}. \tag{3.5}$$

We can further rewrite (3.3) into a more compact matrix form given by

$$\left[\mathbf{D}^A - \mathbf{Q}\left(\mathbf{R}^A - \mathbf{D}^A\right)\right]\mathbf{p}^A = \left[\mathbf{Q}\sum_{i=1}^{I}\mathbf{R}^i\mathbf{p}^i + \sigma^2\mathbf{Q}\mathbf{u}\right], \ m\forall N_b. \tag{3.6}$$

The matrix $\mathbf{R}^A = \left\{ \left|\mathbf{w}_m^{\mathrm{H}}\mathbf{h}_j^A\right|^2 : 1 \leq m,\, j \leq N_b \right\} = \left|\mathbf{W}^{\mathrm{H}}\mathbf{H}^A\right|^2$, where $\mathbf{W}$ can be either (3.4) or (3.5). Likewise, we define $\mathbf{R}^i = \left\{ \left|\mathbf{w}_m^{\mathrm{H}}\mathbf{h}_l^i\right|^2 : 1 \leq m \leq N_b,\ 1 \leq l \leq L_i \right\} = \left|\mathbf{W}^{\mathrm{H}}\mathbf{H}^i\right|^2$, where $\mathbf{H}^i = \left(\mathbf{h}_1^i, \cdots, \mathbf{h}_{L_i}^i\right)$. The matrix $\mathbf{D}^A$ is a $N_b \times N_b$ diagonal matrix with its non-zero elements taken from the diagonal elements of $\mathbf{R}^A$. Furthermore, we define $\mathbf{Q} = \mathrm{diag}\left(\mathrm{SINR}_1, \cdots, \mathrm{SINR}_{N_b}\right)$, $\mathbf{u} = \left(\mu_1, \cdots, \mu_{N_b}\right)^{\mathrm{T}}$, $\mathbf{p}^A = \left(p_1^A, \cdots, p_{N_b}^A\right)^{\mathrm{T}}$ and $\mathbf{p}^i = \left(p_1^i, \cdots, p_{L_i}^i\right)^{\mathrm{T}}$. Since equal power allocation for all transmit antennas within the same BS is assumed, we have $\mathbf{p}^A = \mathbf{c}^A p_{\mathrm{Conv}}^A$ and $\mathbf{p^i} = \mathbf{c}^i p^i$, where $\mathbf{c}^A$ and $\mathbf{c}^i$ are $N_b \times 1$ and $L_i \times 1$ unit column vectors, respectively. After some algebraic manipulation to isolate p_{Conv}^A, the expression in (3.6) can thus be rewritten as

$$p_{\mathrm{Conv}}^A = \left[\mathbf{D}^A\mathbf{c}^A - \mathbf{Q}\left(\mathbf{R}^A - \mathbf{D}^A\right)\mathbf{c}^A\right]^{-1}\left[\mathbf{Q}\sum_{i=1}^{I}\mathbf{R}^i\mathbf{c}^i p^i + \sigma^2\mathbf{Q}\mathbf{u}\right]. \tag{3.7}$$

Depending on the weight optimisation approach, the ZF-Conv and the MMSE-Conv receivers are considered. Correspondingly, p_{Conv}^A can be further classified to $p_{\mathrm{ZF-Conv}}^A$ and $p_{\mathrm{MMSE-Conv}}^A$ depending on whether the ZF-Conv or MMSE-Conv receiver is being considered. The $p_{\mathrm{ZF-Conv}}^A$ and $p_{\mathrm{MMSE-Conv}}^A$ values are calculated by averaging them over a large number of channel realisations for a specified SINR and interference power p^i. Their values will then be used to calculate the power consumption of the PA in the later section of this chapter.

From (3.2), we observe that N_u multiplications and N_u additions followed by one decision operation are required to estimate each symbol in the conventional linear receiver. Therefore, the processing complexity and hardware requirements at the receiver scale with N_u.

3.3.2 The Successive Interference Cancellation Receiver

In a SIC receiver, which is utilised in V-BLAST, the intra-cell interference is reconstructed from previous detected symbols transmitted from BS^A and subtracted from the received signal vector to improve detection of the current symbol. We assume a SIC receiver without optimal sorting for simplicity, i.e., the symbols are detected in

the same order as they were transmitted. Therefore, the SINR for the mth symbol can be written as

$$\mathrm{SINR}_m = \frac{\left|\mathbf{w}_m^{\mathrm{H}}\mathbf{h}_m^A\right|^2 p_m^A}{\sum_{j=1}^{m-1}\left|\mathbf{w}_m^{\mathrm{H}}\mathbf{h}_j^A\right|^2 p_j^A e_j^A + \sum_{j=m+1}^{M}\left|\mathbf{w}_m^{\mathrm{H}}\mathbf{h}_j^A\right|^2 p_j^A + \sum_{i=1}^{I}\sum_{l=1}^{L_i}|\mathbf{w}_m^{\mathrm{H}}\mathbf{h}_l^i|^2 p_l^i + \sigma^2\|\mathbf{w}_m\|^2} \tag{3.8}$$

where $e_j^A = \beta_j \mathrm{E}\left\{|s_j - \tilde{s}_j|^2\right\}$ and β_j is the detection error probability of the jth symbol. Likewise, equal power allocation is assumed at all transmit antennas of the BSs, i.e., $p_1^A = \cdots = p_{N_b}^A = p_{\mathrm{SIC}}^A$ and $p_1^i = \cdots = p_{L_i}^i = p^i$.

Since an equal power allocation scheme is assumed, we can rewrite (3.8) into a form similar to (3.7) for p_{SIC}^A, the transmitted symbol power per antenna from BS^A for the SIC receiver. Thus, we have

$$p_{\mathrm{SIC}}^A = \left[\mathbf{D}^A\mathbf{c}^A - \mathbf{Q}\left(\mathbf{R}_{\mathrm{SLT}}^A\mathbf{G} + \mathbf{R}_{\mathrm{SUT}}^A\right)\mathbf{c}^A\right]^{-1}\left[\mathbf{Q}\sum_{i=1}^{I}\mathbf{R}^i\mathbf{c}^i p^i + \sigma^2\mathbf{Q}\mathbf{u}\right] \tag{3.9}$$

where $\mathbf{G} = \mathrm{diag}\left(0, e_1^A, \cdots, e_{M-1}^A\right)$, while $\mathbf{R}_{\mathrm{SLT}}^A$ and $\mathbf{R}_{\mathrm{SUT}}^A$ are $N_b \times N_b$ strictly lower triangular and strictly upper triangular matrices, respectively, with their non-zero elements taken from the corresponding elements in $\mathbf{R}^A$.

The ZF and MMSE weight optimisation approaches are also considered here. Therefore, depending on the weight optimisation approach, we have the ZF-SIC and MMSE-SIC receivers. Correspondingly, p_{SIC}^A can be further classified to $p_{\mathrm{ZF-SIC}}^A$ and $p_{\mathrm{MMSE-SIC}}^A$ depending on whether the ZF-SIC or MMSE-SIC receiver is being considered. Similarly, the $p_{\mathrm{ZF-SIC}}^A$ and $p_{\mathrm{MMSE-SIC}}^A$ values are calculated by averaging them over a large number of channel realisations for a specified SINR and interference power p^i and will be used to calculate the power consumption of the PA in the later section of this chapter.

Similar to the conventional linear receiver, N_u multiplications and N_u additions followed by one decision operation are required to estimate each symbol. However, the SIC receiver further requires the reconstruction of the received signal due to the estimated symbol and subtracting it from the original composite received signal in (3.1).

This additional step requires another N_u multiplication followed by N_u subtractions. Therefore, the processing complexity of the SIC receiver is roughly twice that of the linear conventional receiver. Both the processing complexity and hardware requirements of the SIC receiver also scale with N_u.

3.4 Power Consumption Model

In this work, we focus only on the BS power consumption as it was shown in [118] that the CO_2 emission due to operational energy consumption of the BS components is at 68% of its total CO_2 emission while the mobile handset stood at 24%. Furthermore, the typical size of the mobile handset will put an upper limit on the number of receive antennas N_u that can be practically installed. Since the receiver processing complexity and hardware requirements scale with N_u, the power consumption of the mobile handset will also be limited by the number of receive antennas that can be practically installed.

We are interested in the impact of different receiver IC techniques on the BS total power consumption at different power consumption ratios between the SP and PA modules. The SP module consists of circuits for the digital to analogue converter, mixer, baseband digital signal processor, and so on. Each transmit antenna is assumed to be attached to a SP module and a PA module. Let the power consumption per antenna of the PA module be given as

$$P_{\text{amp}} = \frac{P_{\text{RF}}}{\vartheta} \tag{3.10}$$

where P_{RF} is the required RF transmit power per antenna corresponding to a particular receiver IC technique in order to obtain a targeted receiver output SINR. For example, we have $P_{\text{RF}} = p^{A}_{\text{MMSE-SIC}}$ if a SIC receiver with MMSE weight optimisation approach is considered. The efficiency of the PA is ϑ, where $0 \leq \vartheta \leq 1$. Thus, the total power consumption of the PA module for N_b transmit antennas is given by

$$P^{\text{Total}}_{\text{amp}} = N_b P_{\text{amp}}. \tag{3.11}$$

On the other hand, the circuit power consumption of the SP module is modelled as a proportion ϖ of the power consumed in the PA module of a reference system employing a particular receiver IC technique. We choose the 4×4 MIMO configuration as the reference system. Therefore, we have

$$P_{\mathrm{c}} = \varpi \frac{P_{\mathrm{RF}}^{4\times4}}{\vartheta} \tag{3.12}$$

where P_{c} and $P_{\mathrm{RF}}^{4\times4}$ are the circuit power consumption per antenna of the SP module and the RF transmit power per antenna of the 4×4 MIMO reference system, respectively. Thus, the total circuit power consumption of the SP module for N_b transmit antennas is given as

$$P_{\mathrm{c}}^{\mathrm{Total}} = N_b P_{\mathrm{c}}. \tag{3.13}$$

By summing the expressions (3.11) and (3.13), the BS total power consumption is given as

$$\begin{aligned} P_{\mathrm{Total}} &= P_{\mathrm{amp}}^{\mathrm{Total}} + P_{\mathrm{c}}^{\mathrm{Total}} \\ &= \frac{N_b}{\vartheta}\left(P_{\mathrm{RF}} + \varpi P_{\mathrm{RF}}^{4\times4}\right). \end{aligned} \tag{3.14}$$

The BS total power consumption model derived in (3.14) is similar to the existing models, e.g. [34] and [35]. In these models, the total power consumption is usually represented by the summation of two terms. The first term is related to the RF power being transmitted and it scales with a certain quantity of interest. In our case, it scales with the number of transmit antennas and is represented by $P_{\mathrm{amp}}^{\mathrm{Total}}$ in (3.14). The second term of these existing models is related to the constant power being consumed by the BS. This is represented by $P_{\mathrm{c}}^{\mathrm{Total}}$ in (3.14). In [34], the authors defined $P_{\mathrm{c}}^{\mathrm{Total}} = 412\mathrm{W}$ for a macro site with $P_{\mathrm{amp}}^{\mathrm{Total}}$ taking values of 226W, 452W and 904W. In [35], examples were given for a GSM macro site with $P_{\mathrm{c}}^{\mathrm{Total}} = 54.8\mathrm{W}$ and $P_{\mathrm{amp}}^{\mathrm{Total}} = 114\mathrm{W}$ and for a Universal Mobile Telecommunications System (UMTS) macro site with $P_{\mathrm{c}}^{\mathrm{Total}} = 73.5\mathrm{W}$ and $P_{\mathrm{amp}}^{\mathrm{Total}} = 267\mathrm{W}$.

Energy Consumption Ratio

The ECR metric is utilised to measure the energy efficiency of a transmission scheme. Here, it is defined as the ratio of the BS total power consumption to the transmission rate of the direct transmission scheme under consideration. By feeding back each SINR_m of s_m to BS^A so that the transmission rate of s_m is always at most $\log_2(1+\text{SINR}_m)$, we assume all N_b symbols can be detected. Under this assumption, the transmission sum rate is given as

$$R_{\text{sum}} = B_{sys} \sum_{m=1}^{N_b} \log_2(1+\text{SINR}_m) \tag{3.15}$$

where B_{sys} is the bandwidth of the system and SINR_m is defined in (3.3) and (3.8). Therefore, the ECR is given as

$$\text{ECR} = \frac{P_{\text{Total}}}{R_{\text{sum}}} \tag{3.16}$$

where P_{Total} is defined in (3.14). The ECR has a unit of Joules per bit (J/bit).

3.5 Single Input Multiple Output Power Consumption

In the SIMO case, there is no intra-cell interference as only one transmit antenna is used at BS^A. Thus, the transmit power per antenna of (3.7) and (3.9) becomes

$$p^A_{\text{Conv/SIC,SIMO}} = q\left(\sum_{i=1}^{I}\left|\left(\mathbf{h}_1^{\text{H}}\mathbf{h}_1\right)^{-1}\mathbf{h}_1^{\text{H}}\mathbf{H}^i\right|^2\mathbf{c}^i p^i + \sigma^2\left\|\left(\mathbf{h}_1^{\text{H}}\mathbf{h}_1\right)^{-1}\mathbf{h}_1^{\text{H}}\right\|^2\right) \tag{3.17}$$

where q is a scalar representing the receiver output SINR for the one and only transmit symbol. From (3.17), it is observed that in a SIMO system the same amount of transmission power is consumed for both the conventional linear and SIC receivers, regardless of the type of weight optimisation approach used. This is confirmed through simulation when $N_b = 1$.

3.6 Analysis for a Large Number of Receive Antennas

To facilitate the analysis for a large number of receive antennas, we utilise the Lemma presented in [106] which provides the following statement.

Lemma 3.1. *Given a channel matrix* $\mathbf{H}$ *with variance* γ*, we have* $\mathbf{H}^{\mathrm{H}}\mathbf{H} = N_u\gamma\mathbf{I}_{N_b}$ *as* N_u *becomes large.*

By applying Lemma 3.1 to the ZF parameters of the conventional receiver, we have

$$\begin{aligned}\mathbf{W}_{\mathrm{ZF}}^{\mathrm{H}} &= \left(\mathbf{H}^{\mathrm{H}}\mathbf{H}\right)^{-1}\mathbf{H}^{\mathrm{H}} \\ &= \frac{\mathbf{H}^{\mathrm{H}}}{N_u\gamma}\end{aligned} \tag{3.18}$$

$$\begin{aligned}\mathbf{R}^A &= \left|\mathbf{W}_{\mathrm{ZF}}^{\mathrm{H}}\mathbf{H}\right|^2 \\ &= \left|\frac{\mathbf{H}^{\mathrm{H}}\mathbf{H}}{N_u\gamma}\right|^2 \\ &= \mathbf{I}_{N_b}\end{aligned} \tag{3.19}$$

$$\mathbf{u} = \frac{\mathbf{c}}{N_u\gamma}. \tag{3.20}$$

Substituting (3.18), (3.19) and (3.20) into (3.7) and letting the receiver output SINR for all N_b symbols be q, we have

$$p_{\mathrm{ZF-Conv}}^A\big|_{N_u\to\infty} = \left(\mathbf{c}^A\right)^{-1}\left[q\sum_{i=1}^{I}\mathbf{R}^i\mathbf{c}^i p^i + \frac{\sigma^2 q}{N_u\gamma}\mathbf{c}^A\right]. \tag{3.21}$$

Similarly, by applying Lemma 3.1 to the following MMSE parameters of the conventional receiver, we have

$$\mathbf{W}_{\mathrm{MMSE}}^{\mathrm{H}} = \left(\mathbf{H}^{\mathrm{H}}\mathbf{H} + \sigma^2\mathbf{I}_{N_b}\right)^{-1}\mathbf{H}^{\mathrm{H}}$$

$$= \frac{\mathbf{H}^{\mathrm{H}}}{N_u\gamma + \sigma^2} \tag{3.22}$$

$$\begin{aligned}\mathbf{R}^A &= \left|\mathbf{W}^{\mathrm{H}}_{\mathrm{MMSE}}\mathbf{H}\right|^2 \\ &= \left|\frac{\mathbf{H}^{\mathrm{H}}\mathbf{H}}{N_u\gamma + \sigma^2}\right|^2 \\ &= \left(\frac{N_u\gamma}{N_u\gamma + \sigma^2}\right)^2 \mathbf{I}_{N_b}\end{aligned} \tag{3.23}$$

$$\mathbf{u} = \frac{N_u\gamma\mathbf{c}}{\left(N_u\gamma + \sigma^2\right)^2}. \tag{3.24}$$

Likewise, substituting (3.22), (3.23) and (3.24) into (3.7) and letting the receiver output SINR for all N_b symbols be q, we have

$$p^A_{\mathrm{MMSE-Conv}}\big|_{N_u\to\infty} = \left(\mathbf{c}^A\right)^{-1}\left[q\sum_{i=1}^{I}\mathbf{R}^i\mathbf{c}^i p^i + \frac{\sigma^2 q}{N_u\gamma}\mathbf{c}^A\right]. \tag{3.25}$$

We find that for large N_u, (3.21) is identical to (3.25), i.e., the required RF transmit power per antenna is identical when both the ZF and MMSE weight optimisation approaches are used for the conventional receiver. We do not analyse the case for the SIC receiver as its non-linear receiver structure does not permit mathematical tractability. However, we confirm through simulation that the SIC receiver mirrors the conventional receiver analytic results for both ZF and MMSE weight optimisation approaches.

By applying (3.16) to either (3.21) or (3.25), we can derive the minimum ECR that all the receivers described here converges to when N_u is large. The minimum ECR is given as

$$\mathrm{ECR}_{\min} = \frac{N_b\left(\left(\mathbf{c}^A\right)^{-1}\left[q\sum_{i=1}^{I}\mathbf{R}^i\mathbf{c}^i p^i + \frac{\sigma^2 q}{N_u\gamma}\mathbf{c}^A\right] + \varpi P^{4\times4}_{\mathrm{RF}}\right)}{\vartheta B_{sys}\log_2\left(1+q\right)}. \tag{3.26}$$

Therefore, for a given number of adjacent BSs I at a particular receiver output SINR q, the energy consumption for all four types of receivers described here converges to

$\text{ECR}_{\min}$ of (3.26) as the number of receive antennas N_u becomes large. This convergence limit will be confirmed through simulation in Section 3.7.

3.7 Simulation Results and Discussions

During simulations, it is assumed that all the BSs are located equidistant d from the targeted UE, that is, the cell edge performance of the UE is evaluated. The elements of the BS–UE channel matrix are made up of coefficients which take into account the effects of Rayleigh fast fading with unit variance, log-normal shadowing with standard deviation of 10 dB and path loss given by $131.1 + 42.8\log_{10}(d)$ dB with $d = 2000$ m. These expressions are taken from pp. 61–64 of [3]. Monte Carlo simulations were carried out and the average results of 50,000 runs were used to calculate the required transmission power of BS^A. The receiver knows only the CSI between BS^A and itself. This CSI is utilised to compute the ZF and MMSE weight vectors in order to detect the desired signal. Furthermore, perfect symbol detection is assumed for the SIC based receivers, i.e., $e_j^A = 0$. Practically, the probability of correct detection can be increased with the help of channel coding. In the following figures, adj-BS denotes an adjacent BS transmitting at RF power of 0.1W per antenna, thus, acting as an inter-cell interference source to the receiver. We assume the noise variance $\sigma^2 = 1$, system bandwidth $B_{sys} = 1$ MHz and the receiver output SINR is fixed at 6 dB for each symbol.

The influence of different receiver IC techniques on the required amount of transmission energy for a system with $N_u = 4$ receive antennas is illustrated in Fig. 3.2 for different number of transmit antennas N_b. For a given number of adjacent BSs, it is observed that ZF based receivers require higher ECR values than MMSE based receivers when $N_b \geq 2$. In the SIMO case ($N_b = 1$), it is observed that all receivers require the same ECR as shown by (3.17). Thus, compared to a MIMO system, a SIMO system requires less transmission energy but it does not offer any multiplexing gain. As the number of transmit antennas increases (MIMO case), it is observed that the the ECR begin to increase when ZF based receivers are considered while it

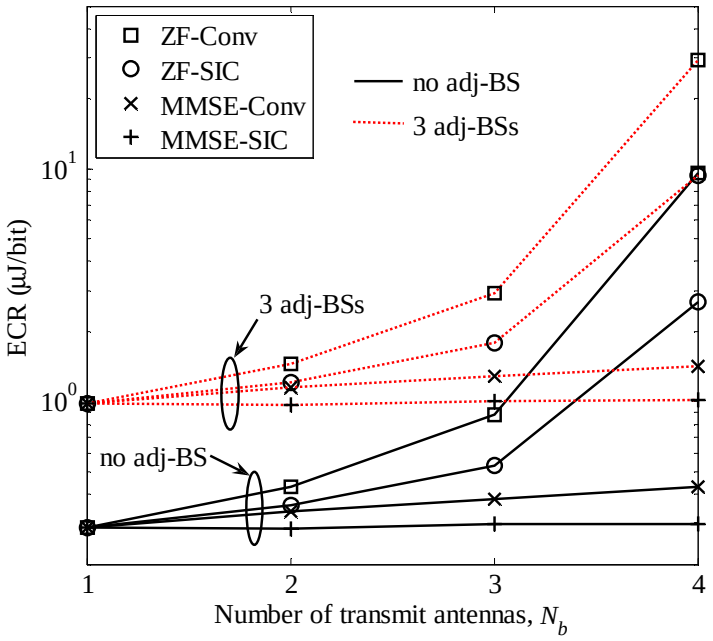

FIGURE 3.2: The ECR values of the desired BS (BS^A) with different receiver IC techniques v.s. the number of transmit antennas ($N_u = 4$).

remains fairly constant when the MMSE based receivers are considered. This could be attributed to how the weights of the receivers are designed. In the ZF case, the weights are designed in such a way that it will completely null out all interfering intra-cell components, leaving only the desired signal to be detected. This, however, will greatly amplify the AWGN noise and the inter-cell interference. As the number of transmit antennas increases, so will the amplification of other undesired components in the receive signal vector by the very same ZF weights used to suppress the intra-cell interference. Therefore, the transmission energy from the desired BS has to be increased in order to maintain the same level of SINR at the receiver output. On the other hand, the MMSE receiver has its weights designed in such a way that it tries to minimise the effect of both intra-cell interference and noise, effectively contributing to a less severe amplification of the undesired components in the receive signal vector. Consequently, MMSE receivers require much less transmission energy to maintain the same receiver output SINR as the number of transmit antennas increases.

If the number of adjacent BS increases in Fig. 3.2, we observe that all receivers require more transmission energy. This is due to the fact that the adjacent BSs increase interference additively by a given factor and thus, the transmission energy

level has to be increased by a factor proportional to it in order to maintain the same receiver output SINR. On the whole, SIC receivers require less transmission energy than the conventional linear receiver, with the MMSE-SIC receiver providing the best performance in terms of energy savings at the BS.

In Fig. 3.3, the ideal ECR values with different receiver IC techniques are shown for various number of receive antennas. The ECR values are ideal because we do not consider the influence of circuit power consumption as we would like to clearly illustrate the impact that the receiver IC techniques have on the BS transmission energy alone. The inclusion of circuit power consumption will be considered in later part of this section. From Fig. 3.3, it is observed that the ECR decreases as the number of receive antennas N_u is steadily increased for a fixed number of transmit antennas ($N_b = 4$). When $N_u > N_b$, it is observed that the ECR for all four types of receiver decreases. This could be due to the increase in receive diversity gain. As the number of available receive antennas increases, better signal quality can be derived as the desired transmitted symbol energy arriving at the receiver can be optimally summed and detected over a larger set of receive antennas. Therefore, less transmission energy is required to maintain the same receiver output SINR. As the number of receive

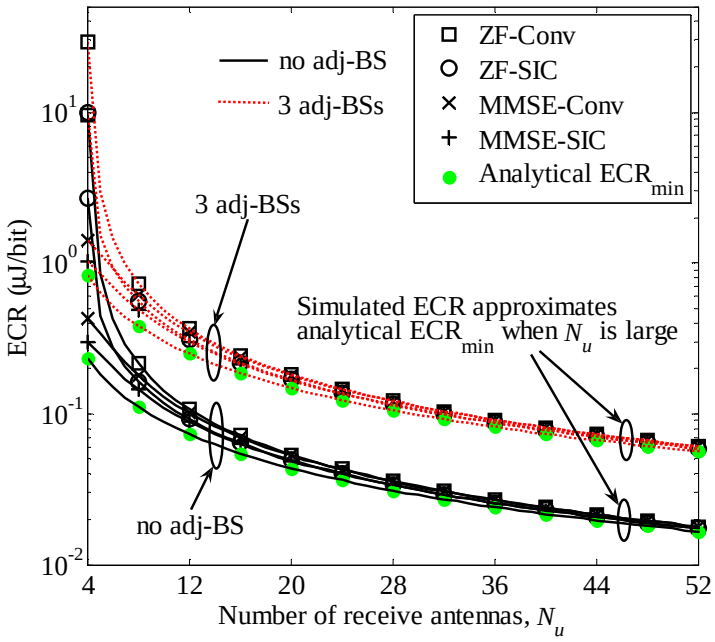

FIGURE 3.3: The ECR values of the desired BS (BS^A) with different receiver IC techniques versus the number of receive antennas ($N_b = 4$).

antennas increases further, the ECR converges to ECR_{min} regardless of the type of receiver used, thus, confirming the derivation of (3.26). This minimum energy is needed to overcome the remaining inter-cell interference plus noise which is present equally in all the receiver types. For the case without any adjacent base station, the minimum transmission energy is only used to overcome the background noise.

We also observe in Fig. 3.3 that there is always an energy gap between the case with no adjacent BS and with 3 adjacent BSs regardless of the number of receive antennas being deployed. This shows that increasing the number of receive antennas alone will not help in suppressing inter-cell interference as long as the receiver IC techniques treat inter-cell interference as only background noise. Furthermore, only a limited number of receive antennas can be installed in a mobile station due to its processing power and size constraint. When the number of receive antennas N_u is small, the choice of receiver IC techniques does make a difference in the required BS transmission energy as evident from Fig. 3.3. Therefore, this serves to emphasise the strong influence of receiver IC design on the BS transmission energy for a receiver with limited number of receive antennas. Note that we acknowledge the fact that the signal processing complexity, thus the energy consumption, of the receiver changes with the number of receive antennas and the type of IC being considered. However, in this work, we are only interested in the BS transmission energy consumption as it was shown in Section 2.3.2 that the energy consumption in current communication networks is largely attributed to the BSs.

In Fig. 3.4, the total power consumption of BS^A with different receiver IC techniques is illustrated for different number of receive antennas while considering the SP module which is operating at low circuit power consumption relative to that of the PA ($\varpi = 0.1$). It is observed that while receive diversity gain still contributes to the BS total power reduction as the number of receive antennas in the MMSE based receivers increases, the same advantage is not seen for the ZF based receivers. Specifically, there is no further reduction in the BS total power consumption for $N_u > 8$ as the power consumption of the SP module cancels out the transmission power savings

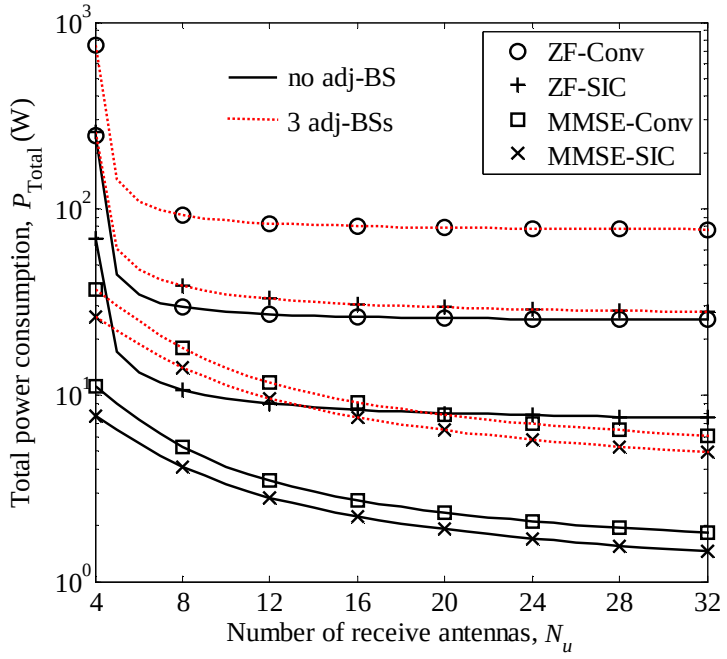

FIGURE 3.4: Total power consumption of BS^A with different receiver IC techniques v.s. the number of receive antennas for $\varpi = 0.1$ ($N_b = 4, \vartheta = 0.4$).

achieved through the ZF based receivers. This is contrary to the result obtained in Fig. 3.3 when no circuit power consumption is considered.

For the following results, we take the MMSE-SIC receiver as a case study since it delivers the most power savings among the receivers. In Fig. 3.5, the power consumption of the SP module versus the PA module of BS^A is illustrated at various ϖ values for a system employing the MMSE-SIC receiver. It is observed that the power consumption of the SP module at $\varpi > 1$ is always higher than that of the PA. Therefore, any power savings obtained through the combined use of MMSE-SIC technique and MIMO is very limited due to the high power consumption of the SP module. On the other hand, if $\varpi < 1$, there will be a certain number of receive antennas where the power consumption of both modules are equal, after which the power consumption of the SP module will once again dominate that of the PA module. For example, when $\varpi = 0.25$, the number of receive antennas that results in equal power consumption between the two modules is $N_u = 14$.

In Fig. 3.6, the total power consumption of BS^A at various ϖ values is illustrated for different number of receive antennas of the MMSE-SIC receiver. The ideal case

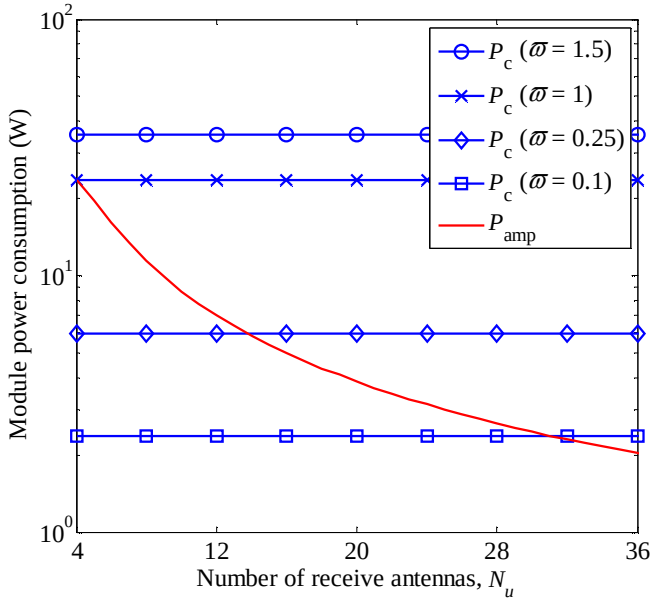

FIGURE 3.5: Power consumption of the SP and PA modules of BS^A at various ϖ values v.s. the number of receive antennas while considering the MMSE-SIC receiver with 3 adj-BS ($N_b = 4, \vartheta = 0.4$).

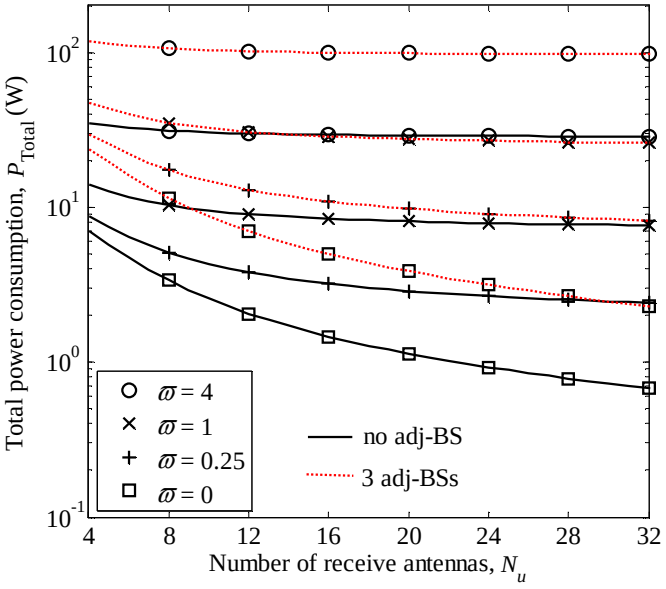

FIGURE 3.6: Total power consumption of BS^A at various ϖ values v.s. the number of receive antennas while considering the MMSE-SIC receiver ($N_b = 4, \vartheta = 0.4$).

where there is no power consumption for the SP module is shown when $\varpi = 0$. When ϖ increases, it is observed that increasing the number of receive antennas no longer reduces the BS total power consumption. It is also observed that the BS total power consumption without inter-cell interference but with dominant P_c (e.g.,

$\varpi = 4$) may even exceed that of the case with inter-cell interference but with lower P_c (e.g., $\varpi = 0.25$). This shows that the power consumed at the SP module may have a significant impact on the BS total power consumption as compared to the additional transmission power needed to overcome the detrimental effects of inter-cell interference to maintain the same SINR level.

3.8 Conclusions

The BS power consumption of the direct transmission scheme for a multicell cellular network has been investigated. Both the conventional and SIC receivers have been considered together with ZF and MMSE weight optimisation approaches. Besides the number of antennas, it has been shown that different weight optimisation approaches have an impact on the ECR of the BS. The ZF based receivers typically require up to 9 times the BS total power consumption of the MMSE based receivers in order to maintain the same SINR at the receiver output. Besides that, it has been demonstrated that treating the interference from adjacent BSs as background noise is not energy efficient as this requires roughly 4 times the transmission energy from the desired BS to maintain the targeted SINR. The impact of the circuit power consumption of the SP module on the BS total power consumption has also been investigated. In some cases, the circuit power consumption may exceed the transmission power savings obtained from receive diversity gains and receiver IC techniques. It may also contribute to the increase in the BS total power consumption more significantly than the additional transmission power needed in the presence of inter-cell interference to achieve the targeted SINR.

Chapter 4

Spectral-Energy Efficiency Trade-off in Conventional Relay Transmission

4.1 Introduction

The relay channel was first described by Van der Meulen [38]. Its capacity was thoroughly examined under various channel conditions in [119] and [120]. Today, relaying transmission has gained considerable attention and is envisaged to be a promising technology in future communication infrastructures.

The two-hop relaying transmission has been of particular interest [121]–[124]. During the first hop (broadcast phase), the source transmits its signal to the relay and sometimes the destination if it is near. The relay can then perform DF [125]–[128], AF [129]–[132] or CF [133]–[136] on the desired signal before relaying it to the destination during the second hop (relay phase). Inter-cell interference occurs when two or more sources at different cells simultaneously transmit, without cooperation, to their intended destinations via relays. This interference relay channel was first studied in [137] for a two-source one-relay two-destination configuration in a Gaussian channel where the achievable rate region was derived with rate splitting [138] performed at the sources. In [77], two DF relays were considered instead, turning the channel into a cascaded interference channel where the sources transmit to the relays via an

interference channel in the first hop and the relays transmit to the destinations via a subsequent interference channel in the second hop. The best transmission strategy for the first hop was again to use rate splitting. The work in [77] was then extended in [139] to include both DF and AF relaying with the RSs having the capability to switch transmission to another destination, effectively converting a strong interference channel to a weak one. A two-source two-relay two-destination configuration was also considered in [140] but with focus on the second hop where the available side information was utilised for partial relay cooperation strategies.

The performance of the relaying transmission can also be improved by applying some form of precoding to the transmitted information, thus, giving rise to a class of relaying schemes generally known as coded relay. Space-time coding is commonly applied to the transmitted information to achieve transmit diversity. For example, a form of space-time coding known as Distributed Time-Reversal Space-Time Block Code (D-TR-STBC) was proposed in [141] to guarantee the orthogonality of the transmitted codes at the destination. Both power gain and Symbol Error Rate (SER) improvement were demonstrated at optimum diversity order. Later, the authors combined transmit beamforming concepts with Distributed Orthogonal Space-Time Block Code (DOSTBC) in [142] to achieve both diversity gain and SER improvement. In [143], transmit beamforming concepts were also applied to the transmitted information in order to demonstrate improved array gains, leading to enhanced capacity performance. While in [144], relay selection method and turbo coding were utilised to improve the overall spectral efficiency of the relay network.

A different relaying paradigm was proposed by Dabora *et. al.* in [79]–[81] and most recently in [145]. In these works, the concept of interference forwarding was proposed. The RSs were utilised to forward a copy of the interference so that it is strong enough for the destination to cancel it. By doing so, the achievable rate region was able to be increased. In [146], both the training signal and the arrival time interval of the interference were utilised by the RS to assist in interference cancellation at the destination, thus, improving transmit efficiency.

The work thus far considered either the signal forwarding or the interference forwarding relaying paradigms, with direct transmission normally taken as the benchmark when performance gains were demonstrated. Therefore, there is insufficient study in comparing the two relaying paradigms. The authors in [147] attempted to address this by evaluating the capacity of the signal forwarding and the interference forwarding elements of the interference relay channel by utilising a relay infrastructure that transmits in orthogonal channels to the underlying interference channel with all nodes having single antenna.

Recently, there is an increased interest in green communication techniques that aim to design energy efficient communication networks. The concept of green communications encompasses the whole of wireless communication life cycle, including design and manufacturing, deployment, operation and decommissioning of the network. Our work focuses on the protocol design and operation cost of green communications, specifically for relay transmission techniques. Relay-aided cooperative communication, which is under consideration in the LTE–A standard, is an attractive technique towards realising the energy efficiency target. While energy efficiency was neglected in the work discussed so far, the authors in [148] considered energy efficiency to maximise the lifetime of a cooperative network through joint relay selection and power allocation strategies. The work was confined to AF relays without any source-destination direct link. In [149], the additional energy cost of implementing the relay selection schemes was considered and a strategy to minimise the corresponding cost was proposed. In [150], dynamically allocated mobile relays were deployed to minimise the energy consumption of a network of static nodes. A significant lifetime extension to the network was being reported. Besides that, a scheme that minimised the energy consumption of a DF relay network based on Bit Error Rate (BER) constraint was proposed in [151] while in [152], a cooperative broadcasting method was proposed that allowed destination nodes to accumulate signal energy from multiple source nodes to improve signal detection and reduce energy consumption. The authors in [153] proposed power allocation schemes that reduced the transmission power for several relay network configurations. In both [152] and [153], the relays were constrained to perform either DF or AF on the signal. In addition, the majority of works from the

aforementioned authors utilised either spectral efficiency or energy efficiency as a performance metric. Although the authors in [154]–[157] attempted to jointly consider them in their work, the trade-off between spectral efficiency and energy efficiency of relay networks is yet to be completely understood. Furthermore, circuit power consumption, a major power drain in MIMO systems, was not considered in [148]–[156] when evaluating energy efficiency.

We intend to address some of the shortcomings of previous work in this chapter. Our contributions are summarised as follows.

1. We investigate the performance of both the signal forwarding and interference forwarding relaying paradigms in a RACN. For each relaying paradigm, an adaptive MIMO relaying scheme [53] is considered where the RSs are able to perform both the DF and AF relaying mechanisms. The conventional DTCN scheme is compared to the relaying schemes. Our purpose is not to propose spectral efficient relaying mechanisms (for example, dynamic DF) but to investigate the signal forwarding and interference forwarding relaying paradigms incorporating the adaptive MIMO relaying scheme.

2. We consider both the spectral and energy efficiency of the schemes. The energy efficiency includes both the RF and circuit power consumption of the PA and SP modules, respectively. We demonstrate that there is a trade-off between spectral efficiency and energy efficiency of the relay schemes.

3. Inspired by [157], we propose the economic efficiency metric as a complementary performance measure to spectral and energy efficiency. The economic efficiency metric finds a point in the SEET region that provides maximum economic profitability. We differentiate our metric from [158] which mainly utilised one-off insertion and fixed costs as terms in their cost efficiency metric. These costs do not reflect the crucial operational power consumption cost and thus, the metric has limitation in representing the trade-off accurately.

4. Lastly, we also investigate the influence of the RS position on the spectral efficiency, energy efficiency and economic efficiency of the relay scheme.

The rest of the chapter is organised as follows. Section 4.2 describes the network topology, channel assumptions, the transmission protocol and the power consumption model of the RACN. In Section 4.3, the interference sources of the network are identified. Next, the relaying mechanisms are explained in Section 4.4 while in Section 4.5, the formulation for optimising energy efficiency is presented. In Section 4.6, the economic efficiency metric is proposed and its optimisation formulation is described. Following that, some numerical examples and discussions are presented in Section 4.7. Finally, concluding remarks are given in Section 4.8.

4.2 System Model

4.2.1 Network Topology

Let us consider a multicell cellular network consisting of a 7-cell wrap-around hexagonal structure as illustrated in Fig. 4.1 with the set $\mathcal{C} = \{1, \cdots, 7\}$ representing the hexagonal cells of the network structure. Each cell has a BS at its centre and is further divided into N_{Sec} sectors described by the set $\mathcal{S} = \{1, \cdots, N_{Sec}\}$. We assume M RSs are located at each sector. These equally spaced RSs are located at d_{RS} from the cell centre and are denoted by set $\mathcal{M} = \{1, \cdots, M\}$. A total of K UEs per sector defined by the set $\mathcal{K} = \{1, \cdots, K\}$ are selected to participate in the transmission. Furthermore, the indexes $b\,(i, j)$, $r\,(i, j, m)$ and $u\,(i, j, k)$ describe the BS from the ith sector of the jth cell, the mth RS from the ith sector of the jth cell and the kth user from ith sector of the jth cell, respectively. The performance of the base (centre) cell is of primary focus in this work. Each BS has N_b antennas per sector while the number of antennas of the RS and UE is N_r and N_u, respectively. Furthermore, we denote the system bandwidth as B_{sys}.

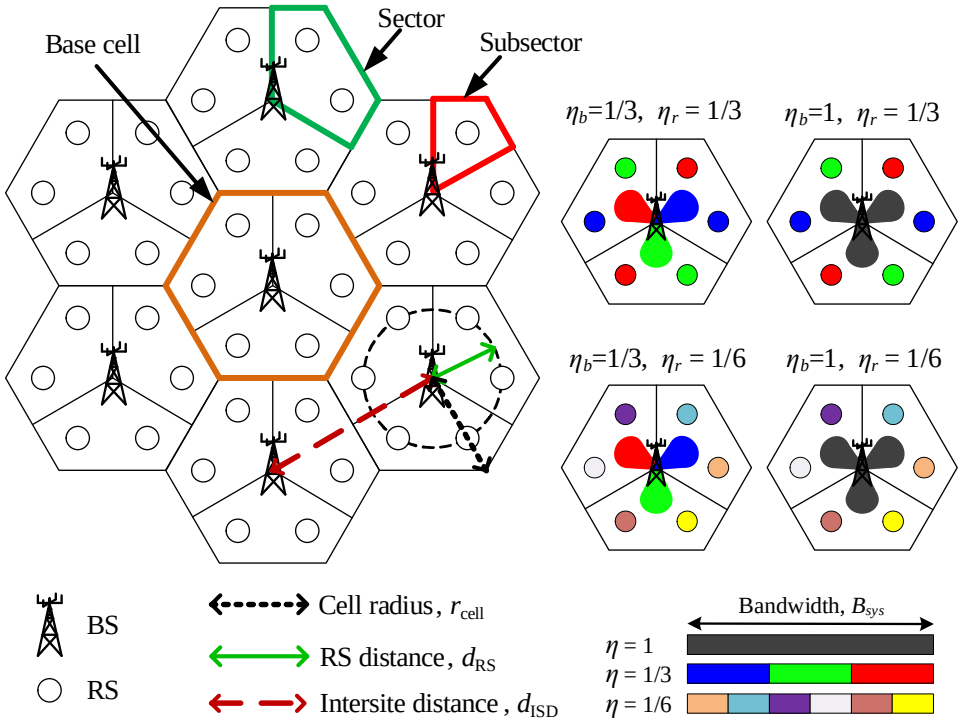

FIGURE 4.1: The RACN with its different frequency planning modes for both the broadcast and relay phases ($M = 2$).

4.2.2 Propagation Channel Model

Consider two nodes X and Y whereby X is transmitting data to Y. Let $\mathbf{H}_{X,Y} \in \mathbb{C}^{A \times B}$ be the channel matrix of size $A \times B$ between X and Y. The elements of $\mathbf{H}_{X,Y}$ are $h_{a,b}$ where $1 \leqslant a \leqslant A$ and $1 \leqslant b \leqslant B$. These elements are modelled as

$$h_{a,b} = G_X \cdot G_Y \cdot (L_{X,Y})^{-1} \cdot 10^{\frac{\xi_{X,Y}}{10}} \cdot \mu_{X,Y} \tag{4.1}$$

where G_X and G_Y are the transmit antenna gain of X and the receive antenna gain of Y, respectively. The path loss between X and Y is defined as $L_{X,Y}$. The following term is log-normal shadowing with $\xi_{X,Y}$ being a Gaussian random variable having zero mean and standard deviation, σ_s dB. The values for these terms depend on whether X and Y are BS, RS or UE nodes. These are shown in Table 4.1 with parameters selected from pp. 61–64 of [3]. Lastly, $\mu_{X,Y}$ denotes the complex Rayleigh fast fading coefficient with unit variance.

TABLE 4.1: Simulation parameters for the RACN.

Path loss model, $L_{X,Y}$ (d in km)	BS–RS	$125.2 + 36.3\log_{10}(d)$ dB
	BS–UE	$131.1 + 42.8\log_{10}(d)$ dB
	RS–UE	$145.4 + 37.5\log_{10}(d)$ dB
Shadowing standard deviation, σ_s	BS–RS	6 dB
	BS–UE	10 dB
	RS–UE	10 dB
Antenna pattern ($\theta_{3\text{dB}} = 70°, A_m = 20\,\text{dB}$)	BS	$\rho(\theta) = -\min\left(12\left(\frac{\theta}{\theta_{3\text{dB}}}\right)^2, A_m\right)$ dB
	RS–BS	$\rho(\theta) = -\min\left(12\left(\frac{\theta}{\theta_{3\text{dB}}}\right)^2, A_m\right)$ dB
	RS–UE	Omni
	UE	Omni
Antenna gain (boresight)	BS	14 dBi (including cable losses)
	RS–BS	7 dBi (including cable losses)
	RS–UE	5 dBi (including cable losses)
	UE	0 dBi
Noise power spectral density, N_0	-174 dBm	
Base service data rate (voice), r_{base}	10 kbps	
Revenue per bit, κ_r	1.54×10^{-6} pence/bit [159]	
Energy cost per Ws, κ_c	2.8×10^{-6} pence/Ws [160]	

4.2.3 Downlink Transmission Protocols

Let us consider the downlink transmission of a cellular mobile network. The transmission protocol is described for the RACN over a single transmission frame interval. The timeslot, T of each transmission frame is assumed to be shorter than the coherence time of the channel. In the RACN, both the BSs and RSs participate in data transmission. For practical reasons, a half-duplex transmission mode is assumed for the RSs. The transmission protocol is depicted in Fig. 4.2. We assume a single user scheduler to clearly demonstrate the benefit of relaying alone without any multiuser diversity gains typically obtained from a multiuser scheduler. In this case, one UE per subsector is selected to participate in the transmission while the corresponding RS at that subsector is assigned to serve the selected UE, giving $K = M$. A full traffic load is assumed so that there is at least one UE per subsector waiting to be served at any

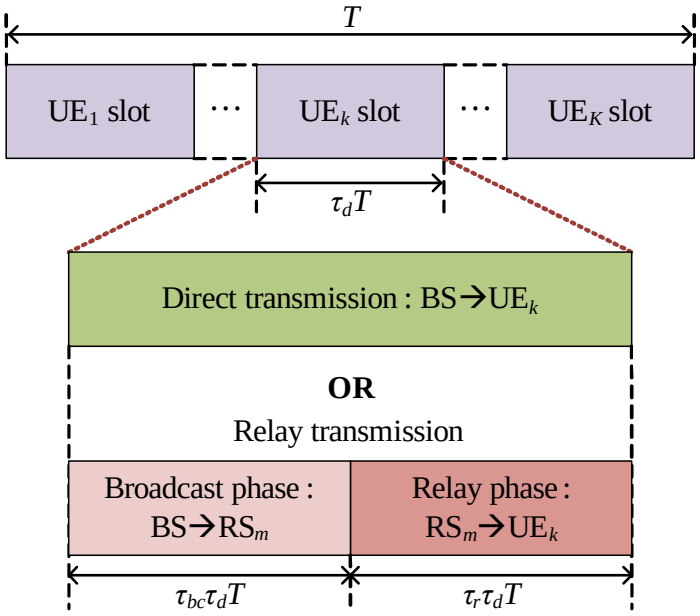

FIGURE 4.2: The downlink transmission protocol for the RACN.

given instant. In addition, the broadcast and relay channels are known to the RSs and UEs, respectively.

The downlink transmission at each sector uses Time Division Multiple Access (TDMA) whereby each of the K UEs is allocated equal fraction of the transmission frame timeslot denoted by $\tau_d T$, where $\tau_d = \frac{1}{K}$. Within $\tau_d T$, either a direct transmission or relay transmission will be performed, depending on which returns a higher throughput. While direct transmission utilises the whole $\tau_d T$, relay transmission further subdivides it into a broadcast phase and a relay phase having transmission duration $\tau_{bc}\tau_d T$ and $\tau_r \tau_d T$, respectively, given that $\tau_{bc} = 1 - \tau_r$ and $0 \leq \tau_{bc} \leq 1$. The mechanisms for the relay transmission will be described in Section 4.4.

We also implement frequency reuse planning for the transmission of both the BSs and RSs where the frequency reuse patterns are as illustrated in Fig. 4.1. For the BS transmission, a frequency reuse factor of η_b indicates a frequency reuse at every $1/\eta_b$ consecutive sectors in a cell while for the RS transmission, a frequency reuse factor of η_r suggests a frequency reuse after every $1/\eta_r$ consecutive RSs in a cell.

4.2.4 Power Consumption Model

In modelling the circuit power consumption, we adopt a methodology similar to [32]. The circuit power consumption of the BS and RSs is proportional to their allocated RF transmit power P_b and P_r, respectively. Thus, there is no circuit power consumption when no transmission is occurring. This is to emulate how future green BSs are expected to operate [161] when the hardware efficiency is improved. Let $P_{c,ref}$ be the circuit power consumption at a given RF transmit power P_{ref}. Therefore, the circuit power consumption of the BS is given as

$$P_{c,b} = \frac{P_b P_{c,ref}}{P_{ref}} \tag{4.2}$$

while the circuit power consumption of the RS is written as

$$P_{c,r} = \frac{P_r P_{c,ref}}{P_{ref}}. \tag{4.3}$$

The operational power of the system includes both the RF transmit power and the circuit power consumption. Considering the aggregate effects of the duplexer/feeder losses and the efficiencies of the antenna/amplifier modules, let the effective operational efficiencies of the BS and RS be represented by α_b and α_r, respectively. Therefore, the operational power utilised for transmission to the kth UE in a RACN is written as

$$P_{op}^{(k)} = \begin{cases} (1-\tau_r)\,\tau_d \alpha_b P_b + \tau_r \tau_d \alpha_r P_r + P_{c,b}/K + M P_{c,r}/K & \text{if relay,} \\ \tau_d \alpha_b P_b + P_{c,b}/K + M P_{c,r}/K & \text{if direct.} \end{cases} \tag{4.4}$$

The circuit power consumed by the RS is included in the second line of (4.4) even though direct transmission is selected. This is because in a RACN, the RS circuitry must be functioning at all times for fast response. We do not consider advanced methods like sleep modes, e.g., [162], where algorithms are designed mostly for green BSs to switch off non-essential circuit components while being idle. As for the conventional

DTCN which operates without employing RSs, the operational power is solely due to the BSs and is given by $\tau_d \alpha_b P_b + P_{c,b}/K$.

Energy Consumption Ratio

As described in Section 2.5.2.2, the ECR is used to measure the energy efficiency of the system. It is proportional to the ratio of the average operational power to the average capacity of the system under consideration. The ECR per sector of the system under consideration is, thus, given as

$$\mathrm{ECR}_{sys} = \frac{\mathbb{E}\left\{P_{op,sys}\right\}}{B_{sys} \cdot \mathbb{E}\left\{C_{sys}\right\}} \tag{4.5}$$

where C_{sys} is the spectral efficiency per sector of the system under consideration in bits/s/Hz while the total operational power per sector of the system under consideration is denoted as $P_{op,sys} = \sum_{k \in \mathcal{K}} P_{op}^{(k)}$, assuming that there are K UEs per sector as represented by set $\mathcal{K}$. Therefore, the ECR has units of Joules per bit (J/bit).

4.3 Interference Analysis

We will now briefly describe the interference sources of the RACN. Let $s \in \mathcal{S}$ be the current sector under consideration in the base cell. Also, let $f_{b(1,s)}$ be the BS transmitting frequency to the RSs and UEs at sector s of the base cell. The set of interference sources $\mathcal{X}$ experienced by the RSs during the broadcast phase of the relay transmission and by the UEs during direct transmission at sector s are from the other BSs transmitting to other sectors at frequency $f_{b(i,j)}$ equals to $f_{b(1,s)}$. This is illustrated in Fig. 4.3(a) for the case of $\eta_b = 1$ while considering sector $s = 1$ of the base cell. Therefore, we have

$$\mathcal{X} = \left\{(i,j) \,\middle|\, (i,j) \in \mathcal{C} \times \mathcal{S}, (i,j) \neq (1,s), f_{b(i,j)} = f_{b(1,s)}\right\}. \tag{4.6}$$

Thus, assuming the interference sources are independent, the interference covariance matrix at the mth RS at sector s of the base cell is given as

$$\mathbf{R}_{BC}^{r(1,s,m)} = \sum_{(i,j)\in\mathcal{X}} \frac{P_b}{N_b} \left(\mathbf{H}_{b(i,j),r(1,s,m)} \mathbf{H}_{b(i,j),r(1,s,m)}^{\mathrm{H}} \right) \tag{4.7}$$

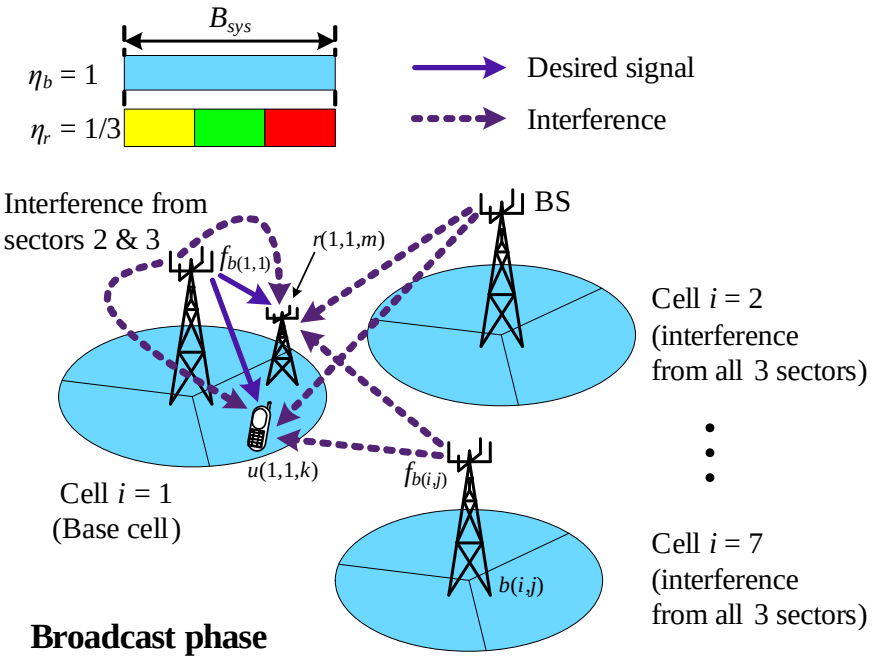

(a)

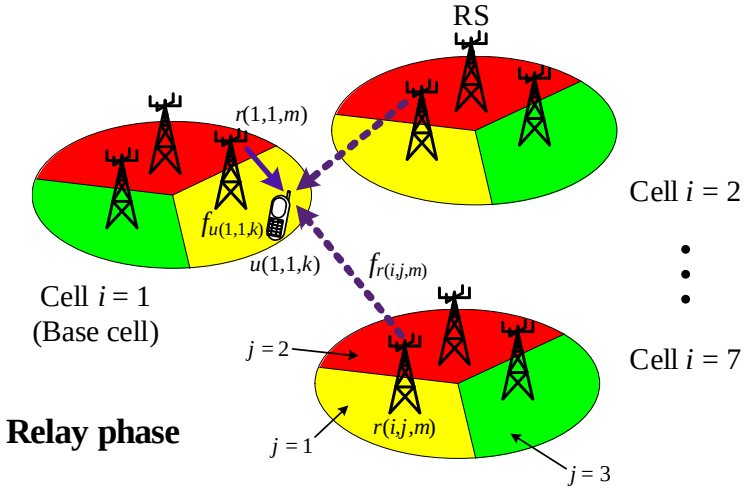

(b)

FIGURE 4.3: Interference sources at sector $s = 1$ of the base cell from (a) other BSs (transmitting to other sectors) experienced by the mth RS and kth UE during the broadcast phase where $f_{b(i,j)} = f_{b(1,1)}$ and (b) other RSs (located in other sectors) to the kth UE during the relay phase where $f_{r(i,j,m)} = f_{u(1,1,k)}$. The figure is illustrated for BS and RS frequency reuse factors of $\eta_b = 1$ and $\eta_r = 1/3$, respectively.

while for the kth UE at sector s of the base cell, the interference covariance matrix is given as

$$\mathbf{R}_D^{u(1,s,k)} = \sum_{(i,j)\in\mathcal{X}} \frac{P_b}{N_b} \left(\mathbf{H}_{b(i,j),u(1,s,k)} \mathbf{H}_{b(i,j),u(1,s,k)}^{\mathrm{H}}\right). \tag{4.8}$$

From (4.6), the strongest interfering BS to the kth UE at sector s of the base cell is identified as $b\left(i_0, j_0\right)$ where

$$\left(i_0, j_0\right) = \underset{(i,j)\in\mathcal{X}}{\arg\max} \left\|\mathbf{H}_{b(i,j),u(1,s,k)}\right\|_{\mathrm{F}}^2. \tag{4.9}$$

Let $\mathcal{X}_0 = \mathcal{X} \oplus \left(i_0, j_0\right)$ be the set of interfering BSs without the presence of the strongest interfering BS. Subsequently, the interference covariance matrix for the kth UE at sector s of the base cell without the strongest interfering BS is defined as

$$\bar{\mathbf{R}}_D^{u(1,s,k)} = \sum_{(i,j)\in\mathcal{X}_0} \frac{P_b}{N_b} \left(\mathbf{H}_{b(i,j),u(1,s,k)} \mathbf{H}_{b(i,j),u(1,s,k)}^{\mathrm{H}}\right). \tag{4.10}$$

Furthermore, let index $r\left(i_0, j_0, m_0\right)$ represent the RS that is designated to relay the interference of $b\left(i_0, j_0\right)$. Thus, the interference covariance matrix for $r\left(i_0, j_0, m_0\right)$ during the broadcast phase is written as

$$\mathbf{R}_{BC}^{r(i_0,j_0,m_0)} = \sum_{(i,j)\in\mathcal{X}_0\cup(1,s)} \frac{P_b}{N_b} \left(\mathbf{H}_{b(i,j),r(i_0,j_0,m_0)} \mathbf{H}_{b(i,j),r(i_0,j_0,m_0)}^{\mathrm{H}}\right). \tag{4.11}$$

When all the RSs are actively transmitting during the relay phase, the RSs interfering the kth UE with receiving frequency $f_{u(1,s,k)}$ at sector s of the base cell are the surrounding RSs from other sectors that are relaying at frequency $f_{r(i,j,m)} = f_{u(1,s,k)}$. This is depicted in Fig. 4.3(b). The set of RSs interfering the kth UE at sector s of the base cell is thus

$$\mathcal{P}_{u(1,s,k)} = \left\{(i,j,m) \,\middle|\, (i,j,m) \in \mathcal{C}\times\mathcal{S}\times\mathcal{M}, (i,j) \neq (1,s), f_{r(i,j,m)} = f_{u(1,s,k)}\right\}. \tag{4.12}$$

Consequently, its interference covariance matrix is given by

$$\mathbf{R}_R^{u(1,s,k)} = \sum_{(i,j,m)\in\mathcal{P}_{u(1,s,k)}} \frac{P_r}{N_r}\left(\mathbf{H}_{r(i,j,m),u(1,s,k)}\mathbf{H}^{\mathrm{H}}_{r(i,j,m),u(1,s,k)}\right) \tag{4.13}$$

while its interference covariance matrix in the absence of $r\left(i_0, j_0, m_0\right)$ is given by

$$\bar{\mathbf{R}}_R^{u(1,s,k)} = \mathbf{R}_R^{u(1,s,k)} - \frac{P_r}{N_r}\left(\mathbf{H}_{r(i_0,j_0,m_0),u(1,s,k)}\mathbf{H}^{\mathrm{H}}_{r(i_0,j_0,m_0),u(1,s,k)}\right). \tag{4.14}$$

The expressions presented in this section are utilised when describing the signal forwarding and interference forwarding paradigms in Section 4.4.

4.4 Spectral Efficiency of the Relaying Schemes

In this section, we describe the relaying mechanisms for the SFR and IFR paradigms, focusing on the kth UE and its assigned mth RS at sector s of the base cell. For conciseness, indexes $b\left(1,s\right)$, $r\left(1,s,m\right)$ and $u\left(1,s,k\right)$ are abbreviated to $\bar{b}$, $\bar{r}$ and $\bar{u}$, respectively, in subsequent channel matrix notations. Furthermore, the index for the strongest interfering BS, $b\left(i_0,j_0\right)$, is abbreviated to b_0 while the index $r\left(i_0,j_0,m_0\right)$, representing the RS that is designated to relay the interference caused by b_0, is abbreviated to r_0. Also, the noise power is represented by $\sigma^2 = N_0 B_{sys}$. The transmission diagrams for the relaying schemes are shown in Fig. 4.4

4.4.1 Signal Forwarding Relaying

The main idea of the SFR scheme is to increase the reliability of the desired signal at the destination by relaying a copy of it to the corresponding UE. The DF and AF relaying mechanisms are considered whereby the designated signal forwarding RS, $\bar{r}$ will select either one of the two relaying mechanisms depending on the channel

condition between $\bar{b}$ and $\bar{r}$. The received signal vector of $\bar{r}$ is

$$\mathbf{y}_{\bar{r}} = \sqrt{\frac{P_b}{N_b}}\mathbf{H}_{\bar{b},\bar{r}}\mathbf{s}_{\bar{b}} + \sum_{(i,j)\in\mathcal{X}} \sqrt{\frac{P_b}{N_b}}\mathbf{H}_{b(i,j),\bar{r}}\mathbf{s}_{b(i,j)} + \mathbf{n}_{\bar{r}} \tag{4.15}$$

where the first term is the desired signal component while, the second and third terms are the inter-cell interference and noise present at $\bar{r}$, respectively. Assuming that $\mathbb{E}\left\{\mathbf{s}_i\mathbf{s}_i^{\mathrm{H}}\right\} = \mathbf{I}_{N_b}$, the maximum supported transmission rate is, therefore, given by

$$R_{\bar{b},\bar{r}} = \log_2\det\left[\mathbf{I}_{N_r} + \frac{P_b}{N_b}\mathbf{H}_{\bar{b},\bar{r}}\mathbf{H}_{\bar{b},\bar{r}}^{\mathrm{H}}\left(\mathbf{R}_{BC}^{\bar{r}} + \eta_b\sigma^2\mathbf{I}_{N_r}\right)^{-1}\right]. \tag{4.16}$$

Given that the desired BS transmission rate is $R_{\bar{b}}$, the DF relaying mechanism is selected if $R_{\bar{b}} \leq R_{\bar{b},\bar{r}}$ in order for the signal to be decodable at the RS. At the destination, the UE achieves diversity gain by utilising both the direct and relay link signals. These signals are stacked before commencement of the decoding process. The transmission rate achieved by the UE is thus

$$R_{\bar{u},DF} = \log_2\det\left[\mathbf{I}_{2N_u} + \mathbf{Q}_{SFR,DF}\mathbf{W}_{SFR,DF}^{-1}\right]. \tag{4.17}$$

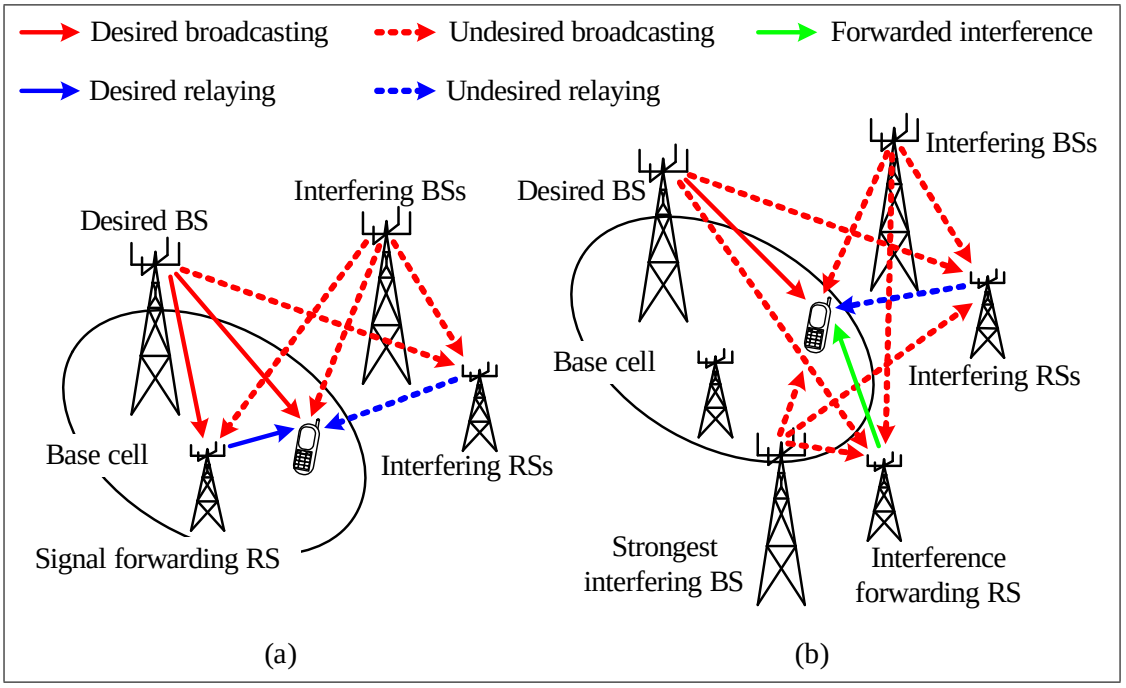

FIGURE 4.4: The transmission diagrams for (a) the SFR scheme, and (b) the IFR scheme.

Assuming the signal and interference sources are mutually independent, the covariance matrices $\mathbf{Q}_{SFR,DF}$ and $\mathbf{W}_{SFR,DF}$ in (4.17) can be defined as

$$\mathbf{Q}_{SFR,DF} = \begin{bmatrix} \frac{P_b}{N_b}\mathbf{H}_{\bar{b},\bar{u}}\mathbf{H}_{\bar{b},\bar{u}}^{\mathrm{H}} & \mathbf{0} \\ \mathbf{0} & \frac{P_r}{N_r}\mathbf{H}_{\bar{r},\bar{u}}\mathbf{H}_{\bar{r},\bar{u}}^{\mathrm{H}} \end{bmatrix} \tag{4.18}$$

and

$$\mathbf{W}_{SFR,DF} = \begin{bmatrix} \mathbf{R}_D^{\bar{u}} + \eta_b\sigma^2\mathbf{I}_{N_u} & \mathbf{0} \\ \mathbf{0} & \mathbf{R}_R^{\bar{u}} + \eta_r\sigma^2\mathbf{I}_{N_u} \end{bmatrix}. \tag{4.19}$$

If $R_{\bar{b}} > R_{\bar{b},\bar{r}}$, the RS is unable to decode the incoming signal. Hence, the AF relaying mechanism is selected whereby the RS will just amplify the signal before relaying it to the UE. The amplification factor is given as

$$g_{\bar{r}} = \frac{P_r}{\left\| \frac{P_b}{N_b}\mathbf{H}_{\bar{b},\bar{r}}\mathbf{H}_{\bar{b},\bar{r}}^{\mathrm{H}} \right\|_{\mathrm{F}}^2 + \eta_b\sigma^2 N_r}. \tag{4.20}$$

Hence, the transmission rate achieved by the UE is

$$R_{\bar{u},AF} = \log_2\det\left[\mathbf{I}_{2N_u} + \mathbf{Q}_{SFR,AF}\mathbf{W}_{SFR,AF}^{-1}\right] \tag{4.21}$$

where the covariance matrices $\mathbf{Q}_{SFR,AF}$ and $\mathbf{W}_{SFR,AF}$ are defined as

$$\mathbf{Q}_{SFR,AF} = \begin{bmatrix} \frac{P_b}{N_b}\mathbf{H}_{\bar{b},\bar{u}}\mathbf{H}_{\bar{b},\bar{u}}^{\mathrm{H}} & \mathbf{0} \\ \mathbf{0} & g_r\frac{P_b}{N_b}\mathbf{H}_{\bar{r},\bar{u}}\mathbf{H}_{\bar{b},\bar{r}}\mathbf{H}_{\bar{b},\bar{r}}^{\mathrm{H}}\mathbf{H}_{\bar{r},\bar{u}}^{\mathrm{H}} \end{bmatrix} \tag{4.22}$$

and

$$\mathbf{W}_{SFR,AF} = \begin{bmatrix} \mathbf{R}_D^{\bar{u}} + \eta_b\sigma^2\mathbf{I}_{N_u} & \mathbf{0} \\ \mathbf{0} & g_r\mathbf{H}_{\bar{r},\bar{u}}\left(\mathbf{R}_{BC}^{\bar{r}} + \eta_b\sigma^2\right)\mathbf{H}_{\bar{r},\bar{u}}^{\mathrm{H}} + \mathbf{R}_R^{\bar{u}} + \eta_r\sigma^2\mathbf{I}_{N_u} \end{bmatrix}. \tag{4.23}$$

The spectral efficiency of the kth UE for the SFR scheme is, thus, given as

$$C_{SFR}^{(k)} = \begin{cases} \tau_d \min\left\{\eta_b \tau_{bc} R_{\bar{b},\bar{r}}, \eta_r \tau_r R_{\bar{u},DF}\right\} & \text{if } R_{\bar{b}} \leq R_{\bar{b},\bar{r}}, \\ \eta_r \tau_r \tau_d R_{\bar{u},AF} & \text{otherwise.} \end{cases} \tag{4.24}$$

If the quality of the BS-UE direct link is high, e.g., when the UE is near the BS, it is desirable to perform direct transmission throughout the $\tau_d T$ transmission time duration that is allocated to the kth UE. The direct transmission spectral efficiency for the kth UE is given as

$$C_{Direct}^{(k)} = \eta_b \tau_d \log_2 \det\left[\mathbf{I}_{N_u} + \frac{P_b}{N_b} \mathbf{H}_{\bar{b},\bar{u}} \mathbf{H}_{\bar{b},\bar{u}}^{\mathrm{H}} \left(\mathbf{R}_D^{\bar{u}} + \eta_b \sigma^2 \mathbf{I}_{N_u}\right)^{-1}\right]. \tag{4.25}$$

Therefore, the SFR scheme adapts its transmission mode between direct and relay transmission according to the current channel conditions. Assuming there are K UEs per sector as represented by set $\mathcal{K}$, the system spectral efficiency per sector of the SFR scheme is, thus, given by

$$C_{sys,SFR} = \sum_{k \in \mathcal{K}} \max\left\{C_{SFR}^{(k)}, C_{Direct}^{(k)}\right\}. \tag{4.26}$$

We observe that the SFR scheme offers improvement to the Signal-to-Interference Ratio (SIR) by enhancing the strength of the desired signal. This increases the success rate of reliably detecting the desired signal in the presence of interference.

4.4.2 Interference Forwarding Relaying

The tenet behind the IFR scheme is to increase the received power of the strongest interfering signal at the UE so that it can be reliably detected and cancelled before the UE decodes the desired signal. This helps in improving the overall quality of the desired signal in the absence of the strongest interfering signal. Similarly, the designated interference forwarding RS, r_0 will select either the DF or AF relaying mechanism when forwarding a copy of the interfering signal to the UE. The received

signal vector of r_0 is

$$\mathbf{y}_{r_0} = \sqrt{\frac{P_b}{N_b}}\mathbf{H}_{b_0,r_0}\mathbf{s}_{b_0} + \sum_{(i,j)\in\mathcal{X}_0\cup(1,s)} \sqrt{\frac{P_b}{N_b}}\mathbf{H}_{b(i,j),r_0}\mathbf{s}_{b(i,j)} + \mathbf{n}_{r_0} \tag{4.27}$$

where the first term is the desired interfering signal to be forwarded by r_0 while, the second and third terms are the undesired inter-cell interference and noise present at r_0, respectively. Therefore, the maximum supported transmission rate between b_0 and r_0 is given as

$$R_{b_0,r_0} = \log_2\det\left[\mathbf{I}_{N_r} + \frac{P_b}{N_b}\mathbf{H}_{b_0,r_0}\mathbf{H}_{b_0,r_0}^{\mathrm{H}}\left(\mathbf{R}_{BC}^{R_0} + \eta_b\sigma^2\mathbf{I}_{N_r}\right)^{-1}\right] \tag{4.28}$$

while the transmission rate of b_0 itself be given as R_{b_0}. The RS will select the DF relaying mechanism if $R_{b_0} \leq R_{b_0,r_0}$ else the AF relaying mechanism will be selected instead.

At the destination, the UE will attempt to decode the interfering signal with the assistance of the relayed copy. The interfering signals received by the UE from both the direct and relay links are stacked before the decoding process is attempted. For successful interference decoding, the transmission rate, R_{b_0} must further satisfy

$$R_{b_0} \leq \log_2\det\left[\mathbf{I}_{2N_d} + \mathbf{Q}_{IFR}\mathbf{W}_{IFR}^{-1}\right] \tag{4.29}$$

where $\mathbf{Q}_{IFR}$ and $\mathbf{W}_{IFR}$ are the covariance matrices of the stacked signals representing the desired interfering signal and other residual interference, respectively. The expressions for these covariance matrices will depend on the type of relaying mechanism that the RS employed when performing interference forwarding and are given as

$$\mathbf{Q}_{IFR} = \begin{cases} \begin{bmatrix} \frac{P_b}{N_b}\mathbf{H}_{b_0,\bar{u}}\mathbf{H}_{b_0,\bar{u}}^{\mathrm{H}} & \mathbf{0} \\ \mathbf{0} & \frac{P_r}{N_r}\mathbf{H}_{r_0,\bar{u}}\mathbf{H}_{r_0,\bar{u}}^{\mathrm{H}} \end{bmatrix} & \text{if DF,} \\ \begin{bmatrix} \frac{P_b}{N_b}\mathbf{H}_{b_0,\bar{u}}\mathbf{H}_{b_0,\bar{u}}^{\mathrm{H}} & \mathbf{0} \\ \mathbf{0} & g_{r_0}\frac{P_b}{N_b}\hat{\mathbf{H}}_{r_0}\hat{\mathbf{H}}_{r_0}^{\mathrm{H}} \end{bmatrix} & \text{otherwise} \end{cases} \tag{4.30}$$

where $\hat{\mathbf{H}}_{r_0} = \mathbf{H}_{r_0,\bar{u}}\mathbf{H}_{b_0,r_0}$ and

$$\mathbf{W}_{IFR} = \begin{cases} \begin{bmatrix} \frac{P_b}{N_b}\mathbf{H}_{\bar{b},\bar{u}}\mathbf{H}_{\bar{b},\bar{u}}^{\mathrm{H}} + \bar{\mathbf{R}}_D^{\bar{u}} + \eta_b\sigma^2\mathbf{I}_{N_u} & \mathbf{0} \\ \mathbf{0} & \bar{\mathbf{R}}_R^{\bar{u}} + \eta_r\sigma^2\mathbf{I}_{N_u} \end{bmatrix} & \text{if DF,} \\ \begin{bmatrix} \frac{P_b}{N_b}\mathbf{H}_{\bar{b},\bar{u}}\mathbf{H}_{\bar{b},\bar{u}}^{\mathrm{H}} + \bar{\mathbf{R}}_D^{\bar{u}} + \eta_b\sigma^2\mathbf{I}_{N_u} & \mathbf{0} \\ \mathbf{0} & g_{r_0}\mathbf{H}_{r_0,\bar{u}}\hat{\mathbf{R}}_{BC}\mathbf{H}_{r_0,\bar{u}}^{\mathrm{H}} + \bar{\mathbf{R}}_R^{\bar{u}} + \eta_r\sigma^2\mathbf{I}_{N_u} \end{bmatrix} & \text{otherwise} \end{cases} \tag{4.31}$$

where $\hat{\mathbf{R}}_{BC} = \mathbf{R}_{BC}^{r_0} + \eta_b\sigma^2\mathbf{I}_{N_u}$.

If the condition in (4.29) is not satisfied, the interference is not decodable. Instead, the UE will calculate a scaled version of the relayed interference signal. After detection by either decoding or scaling, the desired interfering signal will then be reconstructed to match the one originally received by the UE during the broadcast phase. Subsequently, the reconstructed interference is subtracted from that originally received signal.

We observe that there are 4 outcomes that can transpire, each contributing to a different spectral efficiency of the IFR scheme. The observed outcomes are

1. RS r_0 does DF interference relaying while UE $\bar{u}$ successfully decodes it.
2. RS r_0 does DF interference relaying while UE $\bar{u}$ is unsuccessful in decoding it.
3. RS r_0 does AF interference relaying while UE $\bar{u}$ successfully decodes it.
4. RS r_0 does AF interference relaying while UE $\bar{u}$ is unsuccessful in decoding it.

Specifically, these 4 outcomes determine the final amount of residual interference and therefore, influence the interference covariance matrix embedded in the spectral efficiency expression of the IFR scheme. The general spectral efficiency expression of the kth UE for the IFR scheme that encompasses the 4 outcomes is, thus, given as

$$C_{IFR}^{(k)} = \eta_b\tau_d\tau_{bc}\log_2\det\left[\mathbf{I}_{N_u} + \frac{P_b}{N_b}\mathbf{H}_{\bar{b},\bar{u}}\mathbf{H}_{\bar{b},\bar{u}}^{\mathrm{H}}\mathbf{W}_0^{-1}\right] \tag{4.32}$$

where $\mathbf{W}_0$ is the said interference covariance matrix. Its elements are shown in Table 4.2 for the 4 different outcomes. Likewise, the IFR scheme adapts its transmission

TABLE 4.2: Interference covariance matrix, $\mathbf{W}_0$, of the IFR scheme.

Outcome:		**RS r_0 relaying mechanism**	
		DF	AF
Is UE $\bar{u}$ able to decode?	Yes	$\bar{\mathbf{R}}_D^{\bar{u}} + \eta_b\sigma^2\mathbf{I}_{N_u}$	$\bar{\mathbf{R}}_D^{\bar{u}} + \eta_b\sigma^2\mathbf{I}_{N_u}$
	No	$\frac{P_b N_r}{P_r N_b}\mathbf{V}\left(\bar{\mathbf{R}}_R^{\bar{u}} + \eta_r\sigma^2\mathbf{I}_{N_u}\right)\mathbf{V}^{\mathrm{H}}$ $+\bar{\mathbf{R}}_D^{\bar{u}} + \eta_b\sigma^2\mathbf{I}_{N_u}$	$\mathbf{F}\left(\mathbf{R}_{BC}^{r_0} + \eta_b\sigma^2\mathbf{I}_{N_u}\right)\mathbf{F}^{\mathrm{H}}$ $+\frac{1}{g_{r_0}}\mathbf{G}\left(\bar{\mathbf{R}}_R^{\bar{u}} + \eta_r\sigma^2\mathbf{I}_{N_u}\right)\mathbf{G}^{\mathrm{H}}$ $+\bar{\mathbf{R}}_D^{\bar{u}} + \eta_b\sigma^2\mathbf{I}_{N_u}$
Definitions: $\mathbf{V} = \mathbf{H}_{b_0,\bar{u}}\mathbf{H}_{r_0,\bar{u}}^{\dagger}$, $\mathbf{F} = \mathbf{H}_{b_0,\bar{u}}\mathbf{H}_{b_0,r_0}^{\dagger}$, $\mathbf{G} = \mathbf{H}_{b_0,\bar{u}}(\mathbf{H}_{r_0,\bar{u}}\mathbf{H}_{b_0,r_0})^{\dagger}$			

mode between direct and relay transmissions according to the current channel conditions. Assuming we have K UEs per sector as given in set $\mathcal{K}$, the system spectral efficiency per sector of the IFR scheme is

$$C_{sys,IFR} = \sum_{k\in\mathcal{K}} \max\left\{C_{IFR}^{(k)}, C_{Direct}^{(k)}\right\} \tag{4.33}$$

where $C_{Direct}^{(k)}$ is the direct transmission spectral efficiency for the kth UE as defined in (4.25). Contrary to the SFR scheme, the IFR scheme does not offer SIR gains by increasing the desired signal strength but rather by removing the strongest interfering signal to improve the reliability of the received signal for successful detection.

The conventional DTCN employs only direct transmission throughout its operation. Its system spectral efficiency per sector is given as

$$C_{sys,DIRECT} = \sum_{k\in\mathcal{K}} C_{Direct}^{(k)}. \tag{4.34}$$

4.5 Energy Efficiency Optimisation

In this section, we present the formulation to optimise the energy efficiency of a given relay scheme, $\wp$, with a targeted spectral efficiency identical to that achieved by the DIRECT scheme which is taken as the baseline. With the ECR_{sys} being defined in

(4.5), the energy efficiency optimisation problem is formulated as

$$\begin{aligned} \underset{\{P_b,P_r\}}{\text{minimise}} \quad & \text{ECR}_{sys,\wp} \\ \text{subject to} \quad & C_{sys,\wp} = C_{sys,DIRECT} \\ & P_b + MP_r \leq P_0 \\ & P_{b,DIRECT} = P_0 \\ & P_b, P_r > 0 \end{aligned} \tag{4.35}$$

where P_b and P_r are the transmit powers for the BS and RS of the relay scheme, $\wp$, respectively, while $P_{b,DIRECT}$ is the transmit power for the BS of the DIRECT scheme, given that the available transmit power is P_0. We perform an exhaustive search for the values of the $\{P_b, P_r\}$ pair that will minimise $\text{ECR}_{sys,\wp}$ as our objective is not to implement the optimisation algorithm but rather to investigate the interplay between spectral efficiency and energy efficiency. We symbolise the minimised $\text{ECR}_{sys,\wp}$ of the relay scheme, $\wp$, as $\Omega_{0,\wp}$.

4.6 Economic Efficiency

As there is a trade-off between spectral and energy efficiency, neither quantity may be optimised without constricting the other. A system that solely relies on one of them as a performance measure may not yield the best overall network performance. Motivated by the idea first introduced in [157], the economic efficiency metric is proposed as a possible complementary measure to the spectral efficiency and energy efficiency performance metrics.

The economic efficiency metric was also proposed in [158]. However, the authors in [158] did not consider the potential revenue generated from the spectral efficiency provided by the investigated scheme as a viable source to mitigate costs. Furthermore, the CAPEX and OPEX costs in the proposed cost efficiency metric shown in (12) of [158] were mostly decoupled from the spectral and energy efficiency metrics. While the CAPEX cost was a one-off insertion cost to initially set up the network, most of

the utilised OPEX costs were fixed rental costs which have little to do with the cost incurred due to the operational power consumption. This decreases the effectiveness of the proposed cost efficiency metric to represent the trade-off between spectral and energy efficiency.

The spectral efficiency and energy efficiency can be sufficiently characterised by both C_{sys} and $P_{op,sys}$. By jointly considering both parameters, a suitable SEET point that will deliver the maximum economic profitability can be found. We define the economic efficiency metric as

$$U_{sys} = \kappa_r r_{base} \log_2 \left(1 + \frac{B_{sys} C_{sys}}{r_{base}}\right) - \kappa_c P_{op,sys} \tag{4.36}$$

where r_{base} is the base service data rate which refers to the essential service expected by every mobile user, while κ_r and κ_c are the revenue per bit and energy cost per Watt-second (Ws), respectively. Both revenue and cost are measured in the same monetary unit (m.u.), e.g., in pence. We do not consider the CAPEX costs, e.g., planning, equipment and installation costs, as they are usually one off insertion costs in setting up the network. Also, we do not consider the OPEX costs that are related to the rental costs, e.g., cell site and back-haul rentals as they are fixed costs. However, our cost is related to the electricity cost component of the OPEX as it is due to the operational power consumption of the scheme under investigation. Therefore, unlike the CAPEX costs and the fixed rental costs of the OPEX, the electricity cost in the OPEX is variable as it depends on the performance of the network and thus, provides the opportunity for further optimisation.

Taking a closer look at the economic efficiency metric, we see that the first term on the Right Hand Side (RHS) of (4.36) represents the revenue attainable with that scheme in the chosen m.u. per second (m.u./s). Based on the observation in [157], a user is only willing to pay a small additive premium on top of the basic service for a multiplicative increase in the attainable data rate. Thus, the attainable revenue grows incrementally with every new service enabled by the scheme rather than following the multiplicative growth in data rate attainable by such a scheme. This economic trend is known as the law of diminishing returns and this leads to a logarithmic relationship

between the attainable revenue and attainable data rate. The second term on the RHS of (4.36) represents the operational cost, also in m.u./s, incurred by the scheme and unlike the revenue growth, is linearly proportional to $P_{op,sys}$. The values used for the economic efficiency parameters are shown in Table 4.1.

Although the proposed economic efficiency metric is illustrated for the relay-aided cellular network, its framework can also be employed as a practical engineering tool to optimise the economic profitability of any network architecture. Another advantage of the parameterised economic efficiency metric is that it is applicable to different mobile standards and economic conditions. The mobile operators only need to assign different parameter values in order to represent that particular change. For example, r_{base} may change from voice to multimedia in future standards as the complete migration towards wireless internet access occurs [10]. Furthermore, κ_r and κ_c may also be adapted to reflect the change in future electric tariffs.

4.6.1 Economic Efficiency Optimisation

In this section, we present the formulation for the optimisation of the economic efficiency metric which takes into account the SEET. This approach differs from the optimisation presented in (4.35) which attempts to maximise energy efficiency by minimising the ECR, given a targeted spectral efficiency value. In contrast, the spectral efficiency and ECR are now left as variables to be suitably chosen to maximise the economic profitability of the network. Therefore, the economic efficiency metric can be utilised as a common reference point to compare the performance of schemes with different spectral and energy efficiency values. The optimisation of the economic efficiency metric of (4.36) for a given relay scheme $\wp$, can be written as

$$\begin{aligned} \underset{\{P_b,P_r\}}{\text{maximise}} \quad & U_{sys,\wp} \\ \text{subject to} \quad & P_b + MP_r \leq P_0 \\ & P_b, P_r > 0. \end{aligned} \tag{4.37}$$

As we are interested to investigate the interplay of these metrics rather than to implement an actual optimisation algorithm in real time, we choose to solve (4.37) by performing an exhaustive search for the values of the $\{P_b, P_r\}$ pair to find one that maximises $U_{sys,\wp}$. We symbolise the maximum of $U_{sys,\wp}$ as $\zeta_{0,\wp}$.

4.7 Simulation Results and Discussions

We now present some numerical results of the relaying schemes for downlink transmission. The link level and system level performance in terms of spectral efficiency, ECR and economic efficiency are evaluated for these schemes. We assume a cell radius of $r_{cell} = 2000$ m and inter-site distance of $d_{ISD} = \sqrt{3}r_{cell}$ Furthermore, we set $\tau_r = 1/2$, $B_{sys} = 10$ MHz, $\alpha_b = \alpha_r = 2.84$ and $P_{c,ref} = 577$ W at $P_{ref} = 40$ W. The rest of the simulation parameters are listed in Table 4.1.

4.7.1 Link Level Performance

We begin by evaluating the link level performance of the relaying schemes. This is to initially demonstrate the advantage of one scheme over the other in a simple setting. The link level depiction can also loosely represent the network topology of Fig. 4.1 with frequency planning having parameters of $\eta_b = \eta_r = 1/2$.

In Fig. 4.5, the maximum spectral efficiency for the SFR and IFR schemes are illustrated at various normalised relay distances, d_{RS}, as compared to the DIRECT scheme. The maximum spectral efficiency refers to the highest possible spectral efficiency attainable by each scheme regardless of its energy consumption. The IFR scheme maintains a fairly constant maximum spectral efficiency at $0.1 \leq d_{RS} \leq 0.4$ when the chances of the UE in decoding the interference source are fairly high but it begins to drop at $d_{RS} > 0.4$ as the performance is now constrained by relay phase when the RS is positioned farther away from the UE. It is also observed that the spectral efficiency of the IFR scheme never exceeds that of the DIRECT scheme. The

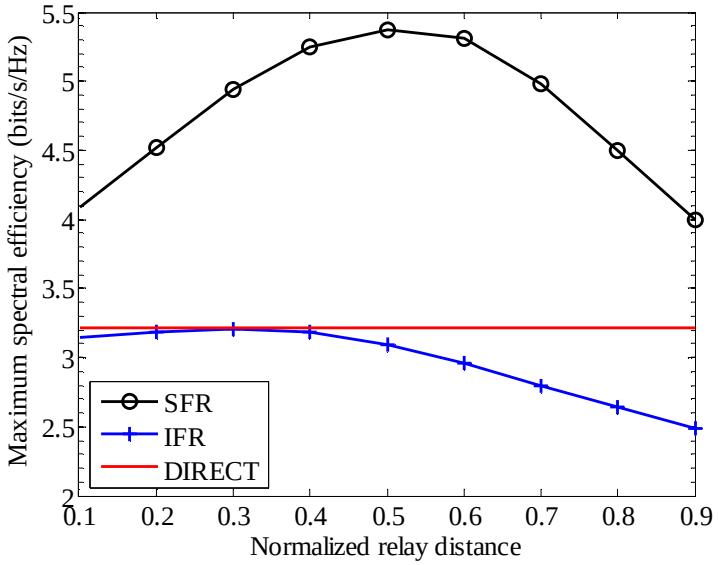

FIGURE 4.5: The maximum spectral efficiency of the SFR and IFR schemes v.s. the normalised relay distance with the DIRECT scheme taken as the baseline.

SIR improvement of the IFR scheme over the DIRECT scheme, whenever the interference is successfully removed, is unfortunately not enough to compensate for the multiplexing loss due to the necessary two-hop relaying protocol. In contrast, the SIR improvement of the SFR scheme outweighs the multiplexing loss and thus, it is able to deliver higher spectral efficiency than both the IFR and DIRECT schemes. This shows that SIR improvement through the desired signal enhancement is more effective than trying to remove interference from the received signal at the UE designated for relay transmission. The SFR scheme is able to obtain roughly a 67% spectral efficiency improvement over the DIRECT scheme at $d_{RS} = 0.5$.

Next, the relation between spectral efficiency and energy efficiency (represented by ECR) is shown in Fig. 4.6 for the SFR and IFR schemes at $d_{RS} = 0.5$. The SEET region is formed for both schemes when different combinations of $\{P_b, P_r\}$ pairs satisfying the constraints in (4.35) are considered. Each $\{P_b, P_r\}$ pair maps to a unique point in the region of a given relay scheme. For the DIRECT scheme, there is only one point in the figure since only one transmit power value, $P_{b,DIRECT} = P_0$, is considered. We observe that the IFR SEET region is confined to the left, covering a wide ECR range, while the SFR SEET region elongates narrowly to the right with its ECR having smaller range and values. This suggests that the SFR scheme is generally able

to attain higher spectral efficiency at lower energy consumption than the IFR scheme which is unable to deliver spectral efficiency in excess of 3.3 bits/s/Hz. Furthermore, the DIRECT scheme point is outside the IFR SEET region, indicating that the IFR scheme also performs poorly in comparison to the DIRECT scheme.

A trade-off between spectral efficiency and energy efficiency is illustrated with the SEET curves in the inset of Fig. 4.6 for both the SFR and IFR schemes at $P_b = 2$ W. It is observed that initially the ECR does not change much when spectral efficiency gains are registered. However, the ECR begins to increase with each marginal improvement in spectral efficiency. This quickly culminates to an accelerated growth in ECR beyond the knee of the curves which is at around 4.5 bits/s/Hz and 1.75 bits/s/Hz for the SFR and IFR schemes, respectively. Past this, very negligible spectral efficiency gains are observed for a large increase in ECR. The SEET curve for the SFR scheme is also more favourable than the IFR scheme.

It is interesting to note that there is a clear trade-off between spectral and energy efficiency if one parameter in $\{P_b, P_r\}$ is fixed while the other is varied, thus, producing a particular SEET curve. However, if the network is flexible enough so that both P_b and P_r can be freely tuned, it is then possible for the SFR or IFR scheme to operate

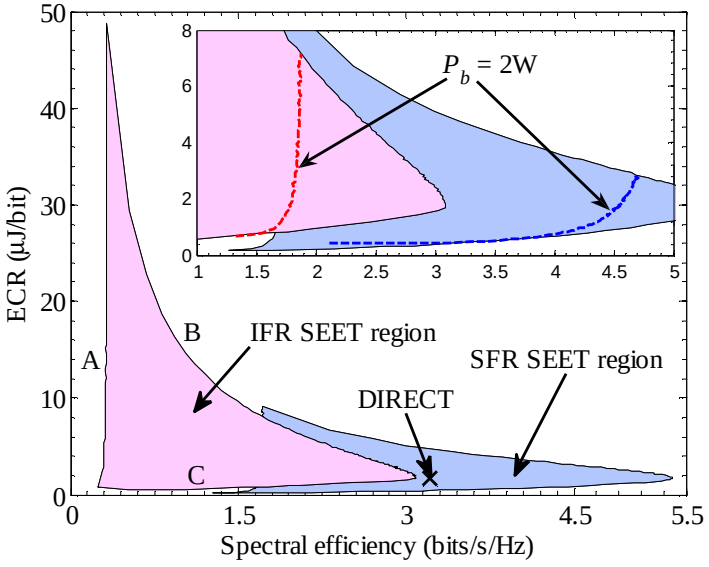

FIGURE 4.6: The SEET region for the SFR and IFR schemes with the inset illustrating a specific trade-off at $P_b = 2$ W. The DIRECT scheme is shown for comparison.

along the three boundaries of its SEET region in Fig. 4.6. The three boundaries are essentially SEET curves, each representing a distinct trade-off characteristic. While they are labelled as A, B and C for the IFR scheme, the same labelling sequence can be applied correspondingly to the SFR scheme. For SEET curve A, a hard trade-off is observed whereby the ECR increases sharply with almost no increase in spectral efficiency. Thus, it is a highly undesirable operation mode. For SEET curve B, the ECR decreases as spectral efficiency increases, indicating that energy efficiency actually improves with spectral efficiency. Although this seems to be desirable initially, a closer inspection shows that the ECR values are at the highest given a particular spectral efficiency. Therefore, while the energy efficiency does improve with spectral efficiency, the network consumes more energy under this operation mode. A lower energy consumption is achievable given a particular spectral efficiency where its minimum value is represented along the line of SEET curve C. Under this operation mode, a soft trade-off is observed whereby the ECR gently increases as spectral efficiency increases. Therefore, this is the most desirable operation mode for the network and, as we shall see later, this is where we would expect to find $\{P_b, P_r\}$ pairs that maximise energy efficiency and economic efficiency.

As the SFR scheme is more superior than the IFR scheme, it is selected for further investigation in the results that follow. In Fig. 4.7, the spectral efficiency and ECR values of the SFR scheme are given for several $\{P_b, P_r\}$ pairs. For clarity of illustration, only key $\{P_b, P_r\}$ pairs are shown although a much wider range were simulated. It is observed that the minimum ECR, corresponding to the maximum energy efficiency, is obtained at $\Omega_0 = 0.44\mu$J/bit where it consumes 3.7 times less energy than the Direct scheme. Again due to the inherent trade-off, lower ECR than Ω_0 is attainable but with loss incurred to its spectral efficiency.

The economic efficiency metric in (4.36) is employed to measure the economic profitability of the SFR scheme in Fig. 4.8. The same set of $\{P_b, P_r\}$ pairs used to generate Fig. 4.6 is used to produce the economic efficiency region of Fig. 4.8. For comparison, the economic profitability of the SFR scheme when operating at maximum energy efficiency of Ω_0 is also shown with its corresponding economic efficiency of 0.179 pence/s.

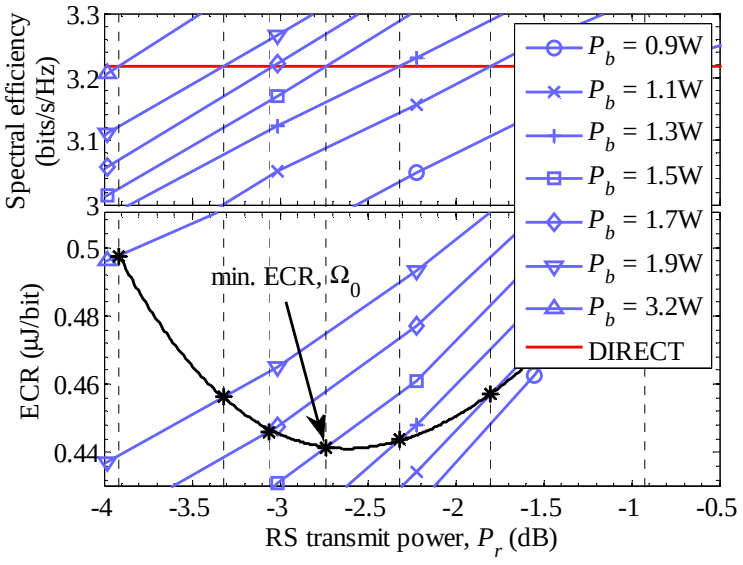

FIGURE 4.7: The spectral efficiency and ECR of the SFR scheme at various $\{P_b, P_r\}$ pairs. The min. ECR of the SFR scheme with the same spectral efficiency as the DIRECT scheme is shown as Ω_0 ($d_{RS} = 0.5$).

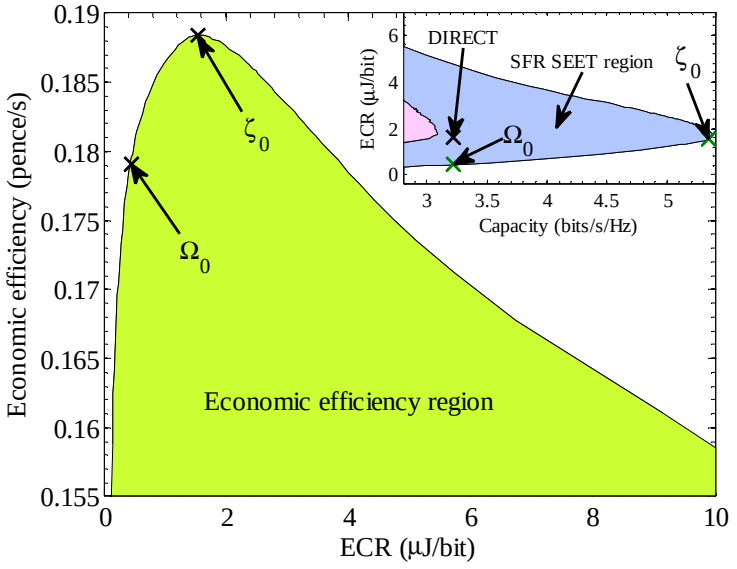

FIGURE 4.8: The economic efficiency v.s. ECR of the SFR scheme at various $\{P_b, P_r\}$ pairs. The min. ECR Ω_0 and max. economic efficiency ζ_0 are shown with the inset indicating their corresponding locations in the SEET region.

Immediately, we see that operating at Ω_0 is not economically optimum. The maximum economic efficiency, ζ_0 is obtained at 0.188 pence/s with the corresponding ECR and spectral efficiency of around 1.55μJ/bit and 5.35 bits/s/Hz, respectively. Moving from Ω_0 to ζ_0 in the SEET region as shown in the inset of Fig. 4.8 maximises the economic efficiency but, due to the trade-off, incurs a 3.5 times increase in ECR while

the spectral efficiency improves by 1.7 times. Therefore by tolerating a decrease in energy efficiency, the SFR scheme stands to gain further in terms of economic efficiency and spectral efficiency. In Fig. 4.9, the maximum economic efficiency and its corresponding ECR is investigated for the SFR scheme at various normalised relay distances. The optimum economic profitability is obtained when $d_{RS} = 0.4$.

4.7.2 System Level Performance

We further study the performance of the SFR scheme under more realistic conditions of a RACN. In Fig. 4.10, the spectral efficiency of the SFR scheme while employing frequency reuse planning modes η_b and η_r for the BS and RS transmission, respectively, is illustrated at different BS transmit power, P_b. It is observed that the SFR scheme with full BS frequency reuse ($\eta_b = 1$) delivers higher spectral efficiency than partial BS frequency reuse ($\eta_b = 1/3$) as the system bandwidth is utilised more efficiently in the former. However, as the BS transmit power increases, the SFR scheme with $\eta_b = 1/3$ is able to obtain larger improvement in spectral efficiency as compared to $\eta_b = 1$ as the performance of full BS frequency reuse is interference limited. A similar observation is made while investigating the RS frequency planning modes, η_r for a given η_b. The more bandwidth efficient RS frequency reuse mode of $\eta_r = 1/3$

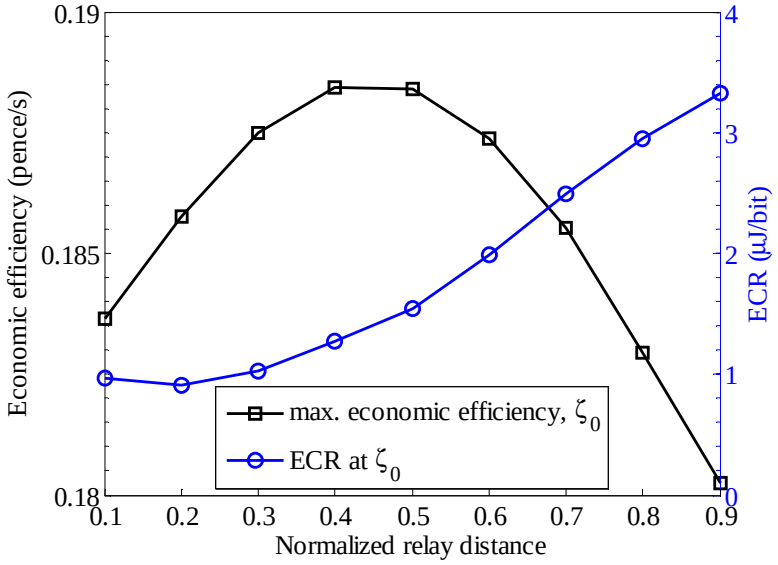

FIGURE 4.9: The maximum economic efficiency ζ_0 at various normalised relay distances of the SFR scheme with the corresponding ECR shown.

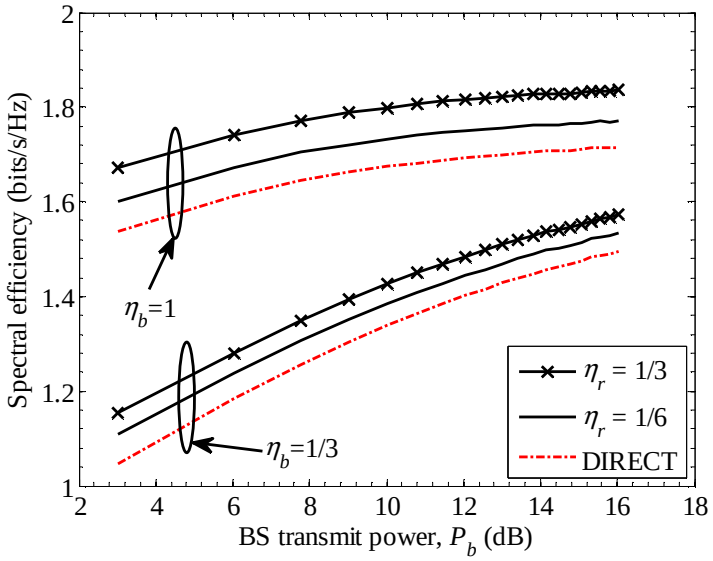

FIGURE 4.10: The system spectral efficiency v.s. BS transmit power of the SFR scheme at different frequency planning modes of both the broadcast and relay phases. The DIRECT scheme is taken as the baseline.

delivers higher system spectral efficiency than the $\eta_r = 1/6$ mode which is designed to avoid RS interference during the relay phase. However, further spectral efficiency improvement is determined by the type of BS frequency planning mode during the broadcast phase. In all cases, the DIRECT scheme underperforms the SFR scheme but even here, we see that the $\eta_b = 1$ mode provides better spectral efficiency than the $\eta_b = 1/3$ mode.

Next, we investigate the economic profitability of the SFR scheme versus its energy efficiency as depicted in Fig. 4.11 while considering both the BS and RS frequency reuse planning modes. The energy efficiency corresponds to the spectral efficiency spanned in Fig. 4.10. From Fig. 4.11, the SFR scheme with $\eta_b = 1$ generally has higher economic efficiency than with $\eta_b = 1/3$ as more bandwidth is being translated to spectral efficiency for revenue generation. However, as $\eta_b = 1$ is interference limited during the broadcast phase, the spectral efficiency improves only slightly even though more energy is expended per bit. As a result, the economic efficiency increases slightly until reaching ECR of around 1.5μJ/bit and 1.6μJ/bit for $\eta_r = 1/3$ and $\eta_r = 1/6$, respectively, before declining as the operational power consumption cost escalates further while revenue remains almost stagnant.

Conversely, regardless of the RS frequency planning mode, the economic efficiency increases sharply for the SFR scheme with $\eta_b = 1/3$, though at lower values, than that of $\eta_b = 1$ as the system has less interference during the broadcast phase. However, the marginal gains quickly decrease as the ECR continues to increase to a point where profitability is now limited by the operational power consumption cost. We now look at the influence of the RS frequency planning mode. Unlike operating at $\eta_b = 1$ during the broadcast phase where the relay phase having $\eta_r = 1/3$ performs consistently better than $\eta_r = 1/6$, it is observed that the economic efficiency is separated into two distinct ECR regimes for $\eta_r = 1/3$ and $\eta_r = 1/6$ when the SFR scheme adopts $\eta_b = 1/3$. At the lower ECR regime, the relay phase with $\eta_r = 1/6$ requires less energy per bit than the relay phase with $\eta_r = 1/3$ to achieve the same economic efficiency as the former has a lower RS interference level. When the SFR scheme migrates to the higher ECR regime where the operational power consumption cost becomes more significant, it is more essential for the SFR scheme to operate at higher bandwidth efficiency in order to deliver higher spectral efficiency to be generated as revenue to compensate the increased cost. Thus, the more aggressive bandwidth use of $\eta_r = 1/3$ performs better than $\eta_r = 1/6$ in the higher ECR regime.

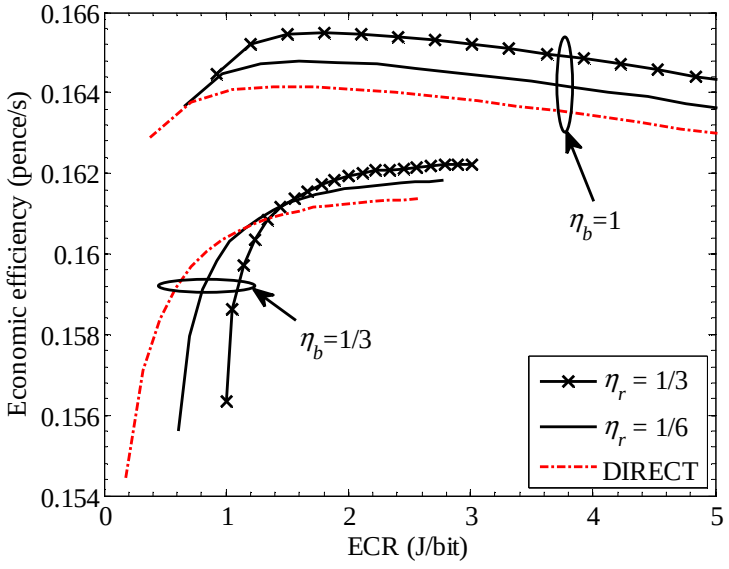

FIGURE 4.11: The system economic efficiency v.s. ECR of the SFR scheme at different frequency planning modes of both the broadcast and relay phases. The DIRECT scheme is taken as the baseline.

4.8 Conclusions

The signal forwarding and interference forwarding relaying paradigms of a RACN have been compared. Both relaying paradigms utilised the adaptive MIMO relay scheme. The spectral, energy and economic efficiency values have been considered. Both the RF and circuit power consumption values have been included in the energy efficiency. Simulation results have shown that the SFR scheme outperforms the IFR scheme. Specifically, the SFR scheme has been shown to deliver a 1.6 times improvement in spectral efficiency over the IFR scheme when both schemes are having optimum relay locations. This indicates that enhancing the desired signal strength is more favourable than attempting to remove the interference from the received signal. Furthermore, the SFR scheme has been shown to achieve up to 3.7 times of energy reduction over the direct transmission scheme for the same spectral efficiency. Next, the economic efficiency metric has been proposed to select a balance point in the SEET in order to maximise the economic profitability. It has been demonstrated that operating the SFR scheme at maximum energy efficiency may not be economically optimum. Due to the trade-off, it has been shown that maximising economic efficiency requires a 3.5 times decrease in energy efficiency while the spectral efficiency is increased by 1.7 times. Investigation into frequency reuse planning modes of the SFR scheme has shown that full bandwidth utilisation delivers higher performance than bandwidth allocation strategies that avoid interference with results demonstrating a 41% and 16% spectral efficiency improvements at low and high BS transmit power, respectively.

Chapter 5

Relay Cooperation for Improved Spectral-Energy Efficiency Trade-off

5.1 Introduction

For a network with more RSs, relay spectrum planning [68]–[71] is essential to avoid relay interference. Although this improves the link level performance, limited gain is observed at the system level as orthogonal frequency reuse schemes do not efficiently utilise the scarce radio resources. Sharing of relay slots can improve resource utilisation but introduces relay interference that has to be mitigated [72]–[77].

Relay interference arises because conventional RSs transmit independently. Recent research in cooperative communication shows that significant throughput improvement is possible when network nodes cooperate with each other [163]. While CoMP for cooperation among BSs has been widely investigated [164], the attractive idea of relay cooperation still remains largely unexplored. In relay cooperation, the RSs share cooperative information to perform *joint relay transmission* to the UEs. We differentiate this concept from those commonly referenced in the literature where relay cooperation often means that both the direct and relay transmissions are used by the UE for reliable signal decoding, i.e., receive diversity [165]–[167]. In [168], the authors proposed an inter-cell relay cooperation scheme to form the uplink joint

precoders. The transmission rate of such a scheme was then evaluated in a linear three-cell topology. Here, a linear topology means that the communication nodes are arranged in a straight line. The authors in [169] evaluated the spectral efficiency of a single-cell topology for a flexible downlink resource management scheme whereby the RSs cooperate to meet a minimum QoS requirement at the UE. Fractional coded relay cooperation was proposed in [170] whereby each RS offers a fraction of its radio resources to relay the data from its neighboring RSs. The BER performance of the scheme was then evaluated for a linear topology. The cooperating RSs have also been shown to utilise the interference alignment [171]–[175] and block diagonalisation [176]–[178] methods to decompose the relay channel into several parallel streams for improved multiplexing gains. In [179], relay cooperation was achieved through the implementation of network coding techniques derived from eXclusive OR (XOR) coding or Reed Solomon coding. The outage probability and the BLock Error Rate (BLER) performance were then evaluated for a linear topology. In [180], the authors proposed a scheme to select the best transmit antennas distributed across multiple RSs for simultaneous relay transmissions. The outage capacity of this scheme was evaluated for a linear topology. Again, a linear topology with two BSs, two RSs and two UEs was considered in [181] where relay cooperation was implemented between the two RSs. Different levels of relay cooperation in terms of different degrees of RS decoding in the broadcast phase were explored. During the relay phase, it was assumed that the RSs have access to global CSI of all relay channels and are thus able to jointly design the precoders for joint relay transmission.

Until recently, most works in relay cooperation focused on the spectral efficiency or throughput performance of a system while others solely focused on energy efficiency. For example in [149], energy efficiency improvement was shown by combining relay selection with cooperative relay beamforming for a linear topology. However, given the significance of energy efficiency for future mobile networks [118] where both power and bandwidth constrict the achievable gains, a joint spectral-energy efficiency performance evaluation, e.g., [155], [156], [182], is imperative. However, [155], [156], [182] evaluated the spectral-energy efficiency performance of their proposed relay cooperation schemes using only the RF transmit power. Circuit power, especially in MIMO

systems, drains a considerable amount of the input power and this necessitates its adoption in energy efficiency evaluation, e.g., [31]–[33], to provide realistic results. In this chapter, we propose a relay cooperation scheme for downlink multicell MIMO cellular networks to address some of the shortcomings of the previous schemes. The following summarises our contributions.

1. Different cooperation levels among the RSs are investigated in our proposed scheme. We consider different RS decoding strategies for the broadcast phase and joint relay transmission with different degrees of CSI sharing for the relay phase. This is different from [181] which only considered several RS decoding strategies for the broadcast phase.

2. We extend the work in [33] and [181] to include multiuser diversity gain by proposing a low complexity norm-based user selection method for the relay cooperation scheme. It is designed to operate without excessively loading the cooperative links as it is well-known that this is a major limitation for cooperative systems [42]. To the best of our knowledge, our user selection method is new as none of the existing relay cooperation work addressed this issue and most existing methods were designed for the point-to-point multiuser MIMO systems, e.g. [183]–[185], with the intention of maximising capacity.

3. We consider both the spectral and energy efficiency performance of the schemes. The operational power is utilised to measure the system energy efficiency. In calculating the operational power, we take into account the RF transmit power and the circuit power consumption of the PA and SP modules, respectively.

4. We quantify the cost of different cooperation levels in terms of the bit rate needed at the cooperative links to sustain the performance gains that these cooperative strategies provide. The average power consumption of the cooperative links is also given to further emphasise the cooperative costs involved.

The rest of the chapter is organised as follows. Section 5.2 describes the system model of the multicell cellular network. In Section 5.3, the interference sources of the network

are identified. A description of the relaying schemes is then presented in Section 5.4, while the user selection methods for relay cooperation are outlined in Section 5.5. In Section 5.6, the cooperative cost of the RS cooperation link is quantified and incorporated into the formulation to optimise energy efficiency in Section 5.7. Next, the economic efficiency of the schemes is presented in Section 5.8. Its optimisation formulation is also described while considering the cooperative cost. Some simulation results and discussions are presented in Section 5.9. Finally, concluding remarks are given in Section 5.10.

5.2 System Model

Let us consider a multicell cellular network shown in Fig. 5.1 with a 7-cell wrap-around hexagonal structure represented by the set $\mathcal{C} = \{1, \cdots, 7\}$. Each cell is divided into N_{Sec} sectors denoted by the set $\mathcal{S} = \{1, \cdots, N_{Sec}\}$. In each sector, M equally spaced RSs are positioned at a distance d_{RS} from the cell centre, thus forming an arc. The relay set is denoted as $\mathcal{M} = \{1, \cdots, M\}$. A total of K UEs given by the set $\mathcal{K} = \{1, \cdots, K\}$ are uniformly distributed in each sector. We define indexes $b\,(i, j)$,

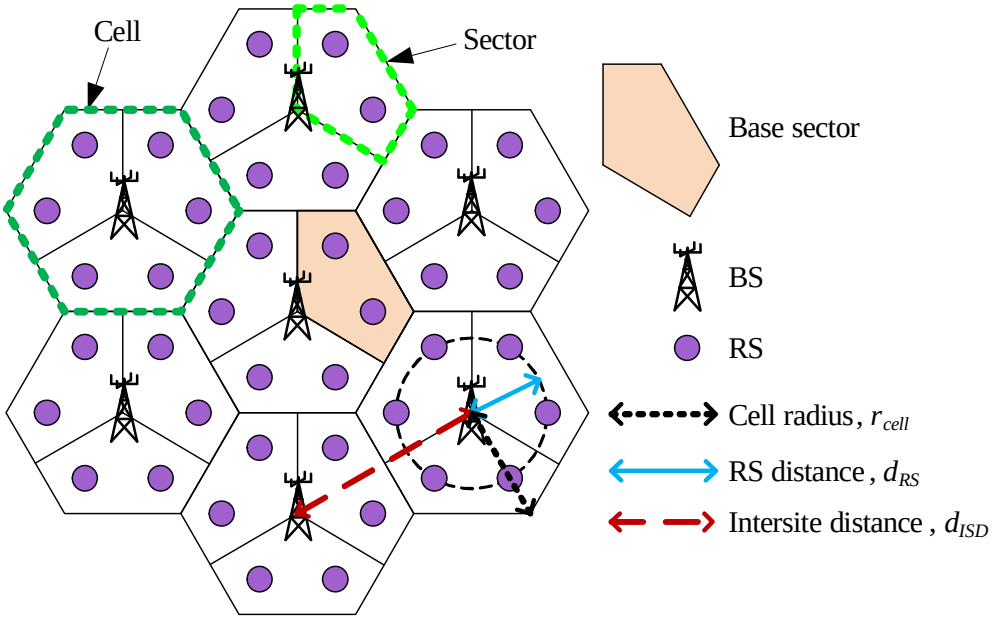

FIGURE 5.1: Topology of the multicell MIMO cellular network with $M = 2$ RSs per sector.

$r\,(i,j,m)$ and $u\,(i,j,k)$ to represent the BS of the jth cell serving the ith sector, the mth RS from the ith sector of the jth cell and the kth user from the ith sector of the jth cell, respectively. It is sufficient to focus on one sector of the central cell as the performance of other sectors is identical on average. We assign $(i,j) = (1,1)$ as the base sector being in focus. Each BS has N_b antennas per sector while the number of antennas at the RSs and UEs are N_r and N_u, respectively. The system bandwidth is given as B_{sys}.

Let $\mathbf{H}_{X,Y} \in \mathbb{C}^{A\times B}$ be the $A \times B$ channel matrix between nodes X and Y, where A and B are the number of antennas at X and Y, respectively. The elements of $\mathbf{H}_{X,Y}$ are $h_{a,b} = G_X \cdot G_Y \cdot (L_{X,Y})^{-1} \cdot 10^{\frac{\xi_{X,Y}}{10}} \cdot \mu_{X,Y}$, $(1 \leqslant a \leqslant A, 1 \leqslant b \leqslant B)$, where G_X and G_Y are the transmit antenna gain of X and the receive antenna gain of Y, respectively. The path loss between X and Y is $L_{X,Y}$. Next is the log-normal shadowing term with $\xi_{X,Y}$ being a Gaussian distributed random variable having zero mean and standard deviation, σ_s dB. The values for these terms depend on whether X and Y are BS, RS or UE nodes. These are shown in Table 5.1 with parameters selected from pp. 61–64 of [3]. Lastly, $\mu_{X,Y}$ denotes the complex Rayleigh fast fading coefficient with unit variance.

5.2.1 Downlink Transmission Protocols

5.2.1.1 Relay-Aided Cellular Network

For practical reasons, a half-duplex transmission mode is assumed for the RSs since they typically cannot transmit and receive simultaneously on the same time and frequency. Before transmission, the K UEs are assigned into either the direct transmission group denoted by set $\mathcal{G}_{Direct}$ or the relay transmission group denoted by set $\mathcal{G}_{Relay}$ based on whether direct transmission or relay transmission (using a single RS with the best channel condition) provides better throughput (Fig. 5.2(a)).

In actual relay cooperation transmission using a group of RSs, a user might benefit more from relay transmission rather than direct transmission even though its relay

TABLE 5.1: Simulation parameters for CMP relaying.

Path loss, $L_{X,Y}$ (d in km)	BS–RS	$[125.2 + 36.3\log_{10}(d)]$ dB
	BS–UE	$[131.1 + 42.8\log_{10}(d)]$ dB
	RS–UE	$[145.4 + 37.5\log_{10}(d)]$ dB
	RS–RS	$[125.2 + 36.3\log_{10}(d)]$ dB
Shadowing standard deviation, σ_s	BS–RS	6 dB
	BS–UE	10 dB
	RS–UE	10 dB
	RS–RS	16.4 dB shadow margin at $\sigma_s = 10$ dB
Antenna pattern ($\theta_{3\text{dB}} = 70°, A_m = 20\,\text{dB}$)	BS	$\rho(\theta) = -\min\left(12\left(\frac{\theta}{\theta_{3\text{dB}}}\right)^2, A_m\right)$ dB
	RS–BS	$\rho(\theta) = -\min\left(12\left(\frac{\theta}{\theta_{3\text{dB}}}\right)^2, A_m\right)$ dB
	RS–UE	Omni
	UE	Omni
Antenna gain (boresight)	BS	14 dBi (including cable losses)
	RS–BS	7 dBi (including cable losses)
	RS–UE	5 dBi (including cable losses)
	UE	0 dBi
Noise power spectral density, N_0	-174 dBm	
Relay time fraction, τ_r	1/2	
Transmit time interval, T_{TTI}	1 ms	
Cooperative time fraction, τ_{coop}	0.1	
Quantisation bits, θ	4 bits per sample	

transmission with single RS performs worse than direct transmission. Nevertheless, the single RS approach is used to avoid the high complexity of sharing the CSIs of all the K UEs among all the M RSs. Thus, we introduce the relay confidence parameter $\beta_R\,(0 \leq \beta_R \leq 1)$ in the transmission group assignment stage to take into account the potential gain of relay cooperation while using the relay transmission with single RS approach. This is achieved by multiplying the direct transmission throughput with a penalising factor of $(1 - \beta_R)$ before comparing it to the relay transmission throughput. By varying β_R, this allows the performance of conservative and aggressive strategies for allocating users to relay transmission to be studied.

The TDMA protocol is utilised for the UEs in $\mathcal{G}_{Direct}$ over $t_D T\,(0 \leq t_D \leq 1)$ duration where T is the transmission frame interval (Fig. 5.2(b)). As for the $\mathcal{G}_{Relay}$ UEs,

the two-hop relay transmission protocol is employed as it provides a good trade-off between performance and complexity. Relay transmission occurs over the remaining time interval $t_R T = T - t_D T$ with $0 \leq t_R \leq 1$. We select L UEs from $\mathcal{G}_{Relay}$ for transmission where L is defined in Section 5.4. The relay transmission time period $t_R T$ is further divided into two time durations. During the first $\tau_{bc} t_R T \, (0 \leq \tau_{bc} \leq 1)$ duration (broadcast phase), the BS broadcasts the information packets of the L selected UEs to all the M RSs. During the second $\tau_r t_R T \, (0 \leq \tau_r \leq 1)$ duration (relay phase), the RSs then relay these packets to the UEs. Here, we define $\tau_{bc} = 1 - \tau_r$ and $t_R = \frac{L}{|\mathcal{G}_{Direct}|+L}$ where $|\mathcal{G}_{Direct}| + L$ is the the total number of UEs actually selected for transmission during time interval T.

5.2.1.2 Direct Transmission Cellular Network

Here, only the BSs participate in data transmission. The BS will transmit directly to the K UEs of each sector in a TDMA arrangement whereby each UE is allocated a

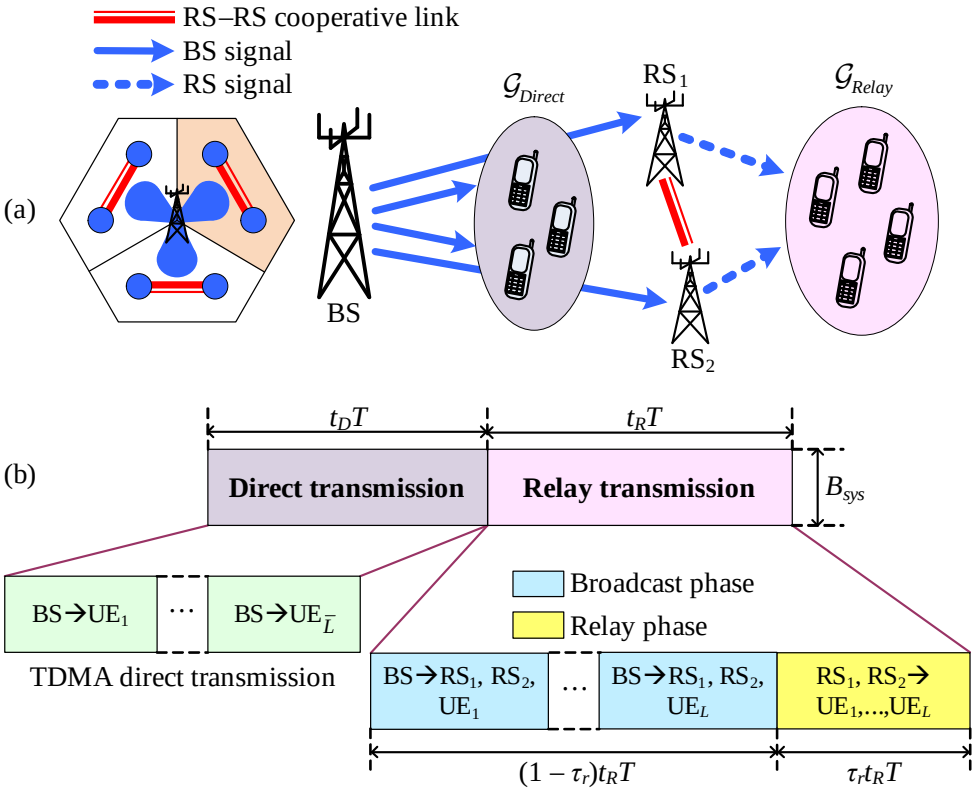

FIGURE 5.2: (a) The relaying structure and (b) the transmission protocol of a RACN employing relay cooperation with $M = 2$ RSs per sector.

transmission duration of $\frac{T}{K}$.

5.2.2 Power Consumption Model

Let P_{BS} be the RF transmit power allocated to the BS in each cell. Assuming that P_{BS} is equally allocated among the sectors and the BSs utilise full bandwidth to transmit, the effective RF transmit power at each sector is $P_b = \frac{P_{BS}}{N_{Sec}}$. Full bandwidth is employed during BS transmission as it was shown in Section 4.7.2 to deliver better performance. Also, let P_{RS} be the RF transmit power allocated to each RS. We assume that equal power is assigned to each sub-channel during relay transmission. Consequently, each RS will utilise a fraction, $\eta_r\,(0 \leq \eta_r \leq 1)$, of its allocated RF transmit power for relaying in its designated sub-channel(s). Thus, the effective RF transmit power of each RS is $P_r = \eta_r P_{RS}$.

In modelling the circuit power consumption, we assume that the circuit power consumption of the BS and RSs is proportional to P_b and P_r, respectively, as described in Section 2.5.2.1. Let $P_{c,ref}$ be the circuit power consumption at a given RF transmit power P_{ref}. Therefore, the circuit power consumption of the BS and RS is defined as $P_{c,b} = \frac{P_b P_{c,ref}}{P_{ref}}$ and $P_{c,r} = \frac{P_r P_{c,ref}}{P_{ref}}$, respectively.

When measuring total power consumption, we consider the operational power of the system which includes both the RF transmit power and the circuit power consumption of the PA and SP modules, respectively. Considering the aggregate effect of the duplexer/feeder losses and the efficiency of the antenna/amplifier modules, let the effective operational efficiency of the BS and RS be given as α_b and α_r, respectively. Therefore, the operational power per sector of a relay transmission is

$$P_{op,relay} = (1 - \tau_r)\,\alpha_b P_b + M\tau_r \alpha_r P_r + P_{c,b} + M P_{c,r} \tag{5.1}$$

while the operational power per sector of a direct transmission is given as

$$P_{op,direct} = \alpha_b P_b + P_{c,b}. \tag{5.2}$$

A RACN consists of both direct and relay transmissions. Thus, the total operational power per sector of the RACN is

$$P_{op,total}^{Relay} = t_D \left(P_{op,direct} + M P_{c,r} \right) + t_R P_{op,relay} \tag{5.3}$$

while that of the DTCN is given as

$$P_{op,total}^{Direct} = P_{op,direct}. \tag{5.4}$$

From (5.1) and (5.3), we observe that in a relay transmission the circuit power consumption of the M RSs is the additional power cost that must be accommodated. This additional power cost can quickly become substantial in a network architecture that employs many transmission nodes.

Energy Consumption Ratio

As described in Section 2.5.2.2, the ECR is used as a performance metric for the energy efficiency of a system. It is proportional to the ratio of the average total operational power to the average capacity of the system under consideration. Thus, the ECR is

$$ECR_{sys} = \frac{\mathbb{E}\left\{ P_{op,total}^{sys} \right\}}{B_{sys} \cdot \mathbb{E}\left\{ C_{sys} \right\}} \tag{5.5}$$

where $P_{op,total}^{sys}$ can be either (5.3) or (5.4) and C_{sys} is the spectral efficiency of the system under consideration in bits/s/Hz. Therefore, the ECR has units of J/bit.

5.3 Interference Analysis

When all BSs are actively transmitting at full bandwidth, the set of interference sources $\mathcal{X}$ experienced by the RSs during the broadcast phase of the relay transmission and by the UEs during direct transmission are from the BSs transmitting to all sectors of all cells except the base sector, that is, $\mathcal{X} = \{(i,j) \,|(i,j) \in \mathcal{C} \times \mathcal{S}, (i,j) \neq (1,1)\}$.

Assuming the interference sources are independent, the interference covariance matrix for JDEC is a block diagonal matrix given as

$$\mathbf{R}_{BC}^{JDEC} = \text{diag}\left(\mathbf{U}_m \,|m = 1, \cdots, M\right) \tag{5.6}$$

where $\mathbf{U}_m = \sum_{(i,j)\in\mathcal{X}} \frac{P_b}{N_b}\left(\mathbf{H}_{b(i,j),r(1,1,m)}\mathbf{H}_{b(i,j),r(1,1,m)}^{\text{H}}\right)$. For IDEC, the interference covariance matrix at the mth RS is given as

$$\mathbf{R}_{BC}^{(m)} = \mathbf{U}_m \tag{5.7}$$

while for the kth UE, the interference covariance matrix is given as

$$\mathbf{R}_{D}^{(k)} = \sum_{(i,j)\in\mathcal{X}} \frac{P_b}{N_b}\left(\mathbf{H}_{b(i,j),u(1,1,k)}\mathbf{H}_{b(i,j),u(1,1,k)}^{\text{H}}\right). \tag{5.8}$$

When all the RSs are actively transmitting, the interference at the kth UE which is receiving at frequency $f_{u(1,1,k)}$ is from the surrounding RSs, other than the base sector, that are relaying at frequency $f_{r(i,j,m)} = f_{u(1,1,k)}$. Thus, the set of RSs interfering the kth UE is $\mathcal{P}_{u(1,1,k)} = \left\{(i,j,m)\,\middle|(i,j,m) \in \mathcal{X}\times\mathcal{M}, f_{r(i,j,m)} = f_{u(1,1,k)}\right\}$. Following that, the interference covariance matrix at the kth UE is given by

$$\mathbf{R}_{R}^{(k)} = \sum_{(i,j,m)\in\mathcal{P}_{u(1,1,k)}} \frac{P_r}{N_r}\left(\mathbf{H}_{r(i,j,m),u(1,1,k)}\mathbf{H}_{r(i,j,m),u(1,1,k)}^{\text{H}}\right). \tag{5.9}$$

5.3.1 Relay Frequency Reuse Pattern Analysis

As the RSs' antennas are usually omni-directional, careful RFR planning is essential to mitigate interference in the relay phase. Three types of RFR patterns are investigated. We introduce the $\eta_r = 1/3$ RFR pattern of Fig. 5.3(a) (Type I) to work with the proposed relay cooperation scheme. The $\eta_r = 1/3$ RFR pattern of Fig. 5.3(b) (Type II) is commonly utilised by conventional independent relaying and will be used for comparison purposes. We are also interested in the performance of $\eta_r = 1$ RFR pattern of Fig. 5.3(c) (Type III) whereby the RSs utilise the full bandwidth for relaying. The

transmission protocol of Type I RFR pattern is illustrated in Fig. 5.3(d) while that of Type III is shown in Fig. 5.2(b).

Firstly, we consider the Type I RFR pattern used in the relay cooperation scheme. With this RFR pattern, inter-cell interference coming from the immediately adjacent sectors around the the base cell can be avoided. The intra-cell interference in each sector due to co-location of the same frequency band is further eliminated through the proposed relay cooperation scheme which also simultaneously provides additional diversity gain through cooperative relaying. The only interference sources are those coming from the surrounding cells with distances of at least one sector away from the

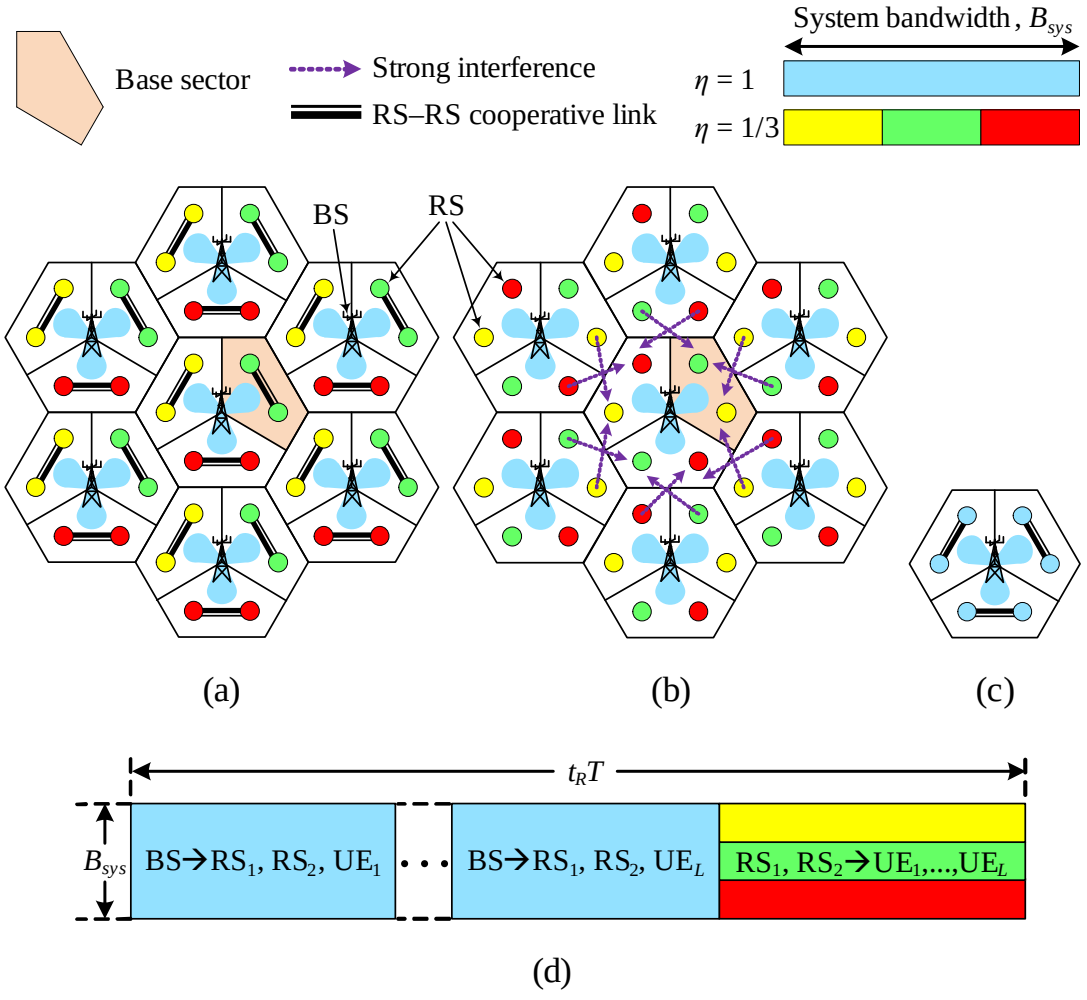

FIGURE 5.3: (a) Type I RFR pattern for the relay cooperation scheme, (b) Type II RFR pattern for the conventional independent relaying scheme and (c) Type III RFR pattern for both schemes, while (d) shows the transmission protocol of the relay cooperation scheme for Type I RFR pattern ($M = 2$ RSs per sector).

base sector. Given the finite exponent decay of path loss, the outer inter-cell interference sources are usually weak. In contrast, the Type II RFR pattern is adopted by conventional relaying to minimise (but not completely eradicate) intra-cell interference when the RSs independently transmit their signals during the relay phase. However, it is not able to avoid inter-cell interference from the immediately adjacent cell sites when a system level perspective is considered as illustrated in Fig. 5.3(b). Thus, the accumulated interference power in (5.9) is smaller for the Type I RFR pattern as compared to the Type II RFR pattern. As for the Type III RFR pattern, all the RSs are using the same frequency and time slot for transmission. Because of this, it has the highest efficiency in bandwidth utilisation but incurs the highest accumulated interference power. Therefore, we have

$$\left\|\mathbf{R}^{k}_{\mathrm{R,Type\,I}}\right\|^{2}_{\mathrm{F}} < \left\|\mathbf{R}^{k}_{\mathrm{R,Type\,II}}\right\|^{2}_{\mathrm{F}} < \left\|\mathbf{R}^{k}_{\mathrm{R,Type\,III}}\right\|^{2}_{\mathrm{F}}. \tag{5.10}$$

To avoid an excessive level of interference, conventional independent relaying schemes do not usually use the Type III RFR pattern. Nevertheless, the benefit of full bandwidth utilisation in Type III RFR pattern can be exploited in the proposed relay cooperation scheme as it is able to remove interference from within its own sector.

5.4 Spectral Efficiency of the Relaying Techniques

We now describe the relaying functions at both the broadcast and relay phases. We utilise the DF mechanism whereby the RSs will attempt to decode the received signals before relaying them to the selected UEs. The focus is largely at the relay phase where our proposed relay cooperation technique is implemented. Two other key relaying techniques with contrasting packet forwarding paradigms are also described. For clarity, the index $(i, j) = (1, 1)$ is dropped henceforth. Each RS is assumed to only know the CSIs between itself and all the UEs in $\mathcal{G}_{Relay}$. All other forms of CSIs information must be exchanged with other RSs.

5.4.1 Broadcast Phase: Relay Decoding Techniques

5.4.1.1 Joint RS Decoding

In the JDEC strategy, each RS will share its received signals and CSI with all the other RSs through the cooperative links so that they are able to perform joint decoding for all the L selected UE signals. The expressions for L will be defined in Section 5.4.2 and Section 5.4.3. The cooperative link between the RSs can be a reliable wireless conference channel that utilises a different bandwidth to the underlying cellular network. The cooperative cost of this strategy will be addressed in Section 5.6. Let us define the concatenated broadcast channel matrix, $\mathbf{G} = \left[\mathbf{H}^{\mathrm{T}}_{b,r(1)} \cdots \mathbf{H}^{\mathrm{T}}_{b,r(M)}\right]^{\mathrm{T}}$. Assuming that the CSI does not change during one transmission frame, the achievable spectral efficiency at the source-relay link for the JDEC strategy is given as

$$C_{BC,JDEC} = (1-\tau_r)\, t_R \log_2 \det\left[\mathbf{I}_{MN_r} + \frac{P_b}{N_b}\left(\frac{\mathbf{G}\mathbf{G}^{\mathrm{H}}}{\mathbf{R}^{JDEC}_{BC} + N_0 B_{sys}\mathbf{I}_{MN_r}}\right)\right] \tag{5.11}$$

where the interference covariance matrix $\mathbf{R}^{JDEC}_{BC}$ is defined in (5.6).

5.4.1.2 Independent RS Decoding

In the IDEC strategy, the RSs will not share their received signals and CSI values to keep complexity low. However, they will still attempt to decode the signals of all the L selected UEs. For successful decoding, the transmission rate of each received signal will be constrained to the minimum spectral efficiency among all M RSs that attempt to decode it. Thus, the achievable spectral efficiency at the source-relay link for the IDEC strategy is

$$C^{all}_{BC,IDEC} = \min\left\{(1-\tau_r)\, t_R \log_2 \det\left[\mathbf{I}_{N_r} + \frac{P_b}{N_b}\left(\frac{\mathbf{H}_{b,r(m)}\mathbf{H}^{\mathrm{H}}_{b,r(m)}}{\mathbf{R}^{(m)}_{BC} + N_0 B_{sys}\mathbf{I}_{N_r}}\right)\right]; \forall m \in \mathcal{M}\right\} \tag{5.12}$$

where the interference covariance matrix $\mathbf{R}^{(m)}_{BC}$ is defined in (5.7).

On the other hand, each RS can choose to only decode the signals of the selected UEs that it is assigned to. Let L_m be the number of selected UEs for the mth RS

where $\sum_{m=1}^{M} L_m = L$. The achievable spectral efficiency at the source-relay link is, alternatively, given as

$$C_{BC,IDEC}^{select} = \frac{1}{L}\sum_{m=1}^{M} L_m\left(1-\tau_r\right) t_R \log_2 \det\left[\mathbf{I}_{N_r} + \frac{P_b}{N_b}\left(\frac{\mathbf{H}_{b,r(m)}\mathbf{H}_{b,r(m)}^{\mathrm{H}}}{\mathbf{R}_{BC}^{(m)} + N_0 B_{sys}\mathbf{I}_{N_r}}\right)\right]. \quad (5.13)$$

5.4.2 Relay Phase: Cooperative Multi-Processing Relaying

In this section, we describe our proposed relay cooperation technique which is an improvement over existing relaying techniques. Here, the RSs will occupy the same relay slot and cooperatively relay the signals received during the broadcast phase to achieve higher spatial multiplexing gain while mitigating multiuser interference, thus, providing higher spectral efficiency improvement over other relaying techniques. Let L_C be the number of UEs than can be supported in CMP relaying. The RSs will design the precoder matrix of the lth UE so that its signal is relayed in the null spaces of the remaining $L_C - 1$ UEs. Thus, the total spatial dimensions of any $L_C - 1$ UEs must be less than that of the RSs, that is,

$$\left(L_C - 1\right) N_u < MN_r \Rightarrow L_C < \frac{MN_r}{N_u} + 1 \quad (5.14)$$

$$\Rightarrow L_C^* = \left\lceil \frac{MN_r}{N_u} \right\rceil \quad (5.15)$$

where L_C^* denotes the smallest integer not less than $\frac{MN_r}{N_u}$ and satisfies the inequality in (5.14). Considering the actual UEs in $\mathcal{G}_{Relay}$ that are available to participate in the transmission, the effective L_{CMP} UEs are selected based on the minimum between L_C^* and $|\mathcal{G}_{Relay}|$, that is,

$$L_{CMP} = \min\left\{L_C^*, |\mathcal{G}_{Relay}|\right\}. \quad (5.16)$$

From (5.14), we see that each RS selects the total UEs based on the assumption that MN_r antennas are available for cooperative relaying, thus, increasing the number of UEs that can be served at a time. The user selection methods for the L_{CMP} UEs will be presented in Section 5.5.

Let $\mathcal{U}^{CMP} = \{u(l) | u(l) \in \mathcal{G}_{Relay}, l = 1, \cdots, L_{CMP}\}$ be the set of L_{CMP} selected UEs. Their CSI between each RS are shared among all the RSs. The cooperative cost incurred from this step is investigated in Section 5.6. Also define the concatenated relay channel matrix as seen by the lth UE of set $\mathcal{U}^{CMP}$ as $\mathbf{F}_{u(l)} = \left[\mathbf{H}_{r(1),u(l)} \dots \mathbf{H}_{r(M),u(l)}\right]$. The RSs jointly calculate the precoder matrix $\mathbf{W}_{u(l)}$ for $l = 1, \cdots, L_{CMP}$, to maximise the relay-destination link spectral efficiency of

$$C_{R,CMP} = \max \sum_{u(l) \in \mathcal{U}^{CMP}} \bar{\tau} \log_2 \det \left[\mathbf{I}_{N_u} + MP_r \left(\frac{\mathbf{F}_{u(l)} \mathbf{W}_{u(l)} \mathbf{W}_{u(l)}^{\mathrm{H}} \mathbf{F}_{u(l)}^{\mathrm{H}}}{\mathbf{R}_R^{u(l)} + N_0 B_{sys} \mathbf{I}_{N_u}} \right) \right] \tag{5.17}$$

where $\bar{\tau} = \tau_r t_R$ and $\mathbf{R}_R^{u(l)}$ is defined in (5.9). To ensure no multiuser interference, we must have $\mathbf{F}_{u(k)} \mathbf{W}_{u(l)} = \mathbf{0}$ for all $k = 1, \cdots, L_{CMP}$ where $k \neq l$. The solution for $\mathbf{W}_{u(l)}$ that will maximise the spectral efficiency of (5.17) and simultaneously suppress multiuser interference is obtained through a combination of the SVD and water-filling approaches. Define $\tilde{\mathbf{F}}_{u(l)} = \left[\mathbf{F}_{u(1)}^{\mathrm{T}} \cdots \mathbf{F}_{u(l-1)}^{\mathrm{T}} \mathbf{F}_{u(l+1)}^{\mathrm{T}} \cdots \mathbf{F}_{u(L_{CMP})}^{\mathrm{T}}\right]^{\mathrm{T}}$. First, we obtain the right singular null space vectors of $\tilde{\mathbf{F}}_{u(l)}$, denoted by the column vectors of matrix $\tilde{\mathbf{V}}_{u(l)}^{null}$. Next, the r singular values of $\left(\mathbf{F}_{u(l)} \tilde{\mathbf{V}}_{u(l)}^{null}\right)$ are extracted and represented as the diagonals of the $r \times r$ diagonal matrix, $\mathbf{\Gamma}_{u(l)}$. Here, r is the rank of $\left(\mathbf{F}_{u(l)} \tilde{\mathbf{V}}_{u(l)}^{null}\right)$. The right singular vectors corresponding to the r singular values are then found and denoted as the column vectors of matrix $\mathbf{V}_{u(l)}^{base}$. Next, water-filling is carried out based on $\mathbf{\Gamma}_{u(l)}$ to obtain the diagonal power loading matrix $\mathbf{\Pi}_{u(l)}$. Finally, the precoder matrix for the lth UE is given as $\mathbf{W}_{u(l)} = \tilde{\mathbf{V}}_{u(l)}^{null} \mathbf{V}_{u(l)}^{base} \left(\mathbf{\Pi}_{u(l)}\right)^{\frac{1}{2}}$. Thus, the overall spectral efficiency of the relay cooperation is given as

$$C_{CMP} = \begin{cases} \min\left\{C_{BC,JDEC}, C_{R,CMP}\right\} & \text{if JDEC,} \\ \min\left\{C_{BC,IDEC}^{all}, C_{R,CMP}\right\} & \text{if IDEC.} \end{cases} \tag{5.18}$$

In theory, CMP relaying is designed to operate with an arbitrary number of M RSs. However, in practice, the value of M has to be restricted to a small integer as the number of RS cooperative links, which is given as $\frac{M(M-1)}{2}$, increases rapidly with M. Thus, the complexity for cooperative information sharing among the RSs does not

scale linearly with M. For this reason, a topology with $M = 2$ is selected which, incidentally, also coincides with the ones commonly found in the literature, for example, in [71], [72], [186].

5.4.3 Other Relay Phase Techniques

5.4.3.1 Interference Free Relaying

The "cause no harm" altruistic policy is the principle of this relaying technique. During relay transmission, each RS transmits to its UE group while nulling its transmission towards the other UE groups of the other RSs [187]. Therefore, cooperative information relating to the currently served members in each UE group needs to be exchanged among the RSs. Define K_m as the number of UEs assigned to the mth RS where $\sum_{m=1}^{M} K_m = |\mathcal{G}_{Relay}|$. Furthermore, let L_I be the number of UEs that each RS can support in IF relaying. Each RS must reserve $(M-1)\,L_I N_u$ of its spatial dimensions to null interference towards the other UE groups. The remaining $N_r - (M-1)\,L_I N_u$ spatial dimensions are used to transmit interference free information to its intended L_I UEs. To achieve this, the total spatial dimensions of any $L_I - 1$ intended UEs must be less than the available total spatial dimensions. Thus,

$$(L_I - 1)\,N_u < N_r - (M-1)\,L_I N_u \;\Rightarrow\; L_I < \frac{Nr + Nu}{MN_u} \tag{5.19}$$

$$\Rightarrow\; L_I^* = \left\lceil \frac{Nr + Nu}{MN_u} \right\rceil - 1 \tag{5.20}$$

where L_I^* denotes the smallest integer not less than $\frac{Nr+Nu}{MN_u}$ minus one and satisfies the inequality in (5.19). Considering the actual K_m UEs that are available to participate in the transmission, the $L_{IF,m}$ UEs that are effectively selected by the mth RS is given by the minimum between L_I^* and K_m, that is,

$$L_{IF,m} = \min\left\{L_I^*, K_m\right\}. \tag{5.21}$$

As each RS must have sufficient spatial dimensions to null interference towards other UEs while still being able to relay useful information to its own UEs, the total number of UEs served by all the M RSs will be less than that of the proposed CMP relaying technique in Section 5.4.2. Let the set of $L_{IF,m}$ selected UEs by the mth RS be $\mathcal{U}_m^{IF} = \{u(l) \,|u(l) \in \mathcal{G}_{Relay}, l = 1, \cdots, L_{IF,m}\}$. Thus, the relay-destination link spectral efficiency of this relay technique is written as

$$C_{R,IF} = \sum_{m \in \mathcal{M}} \sum_{u(l) \in \mathcal{U}_m^{IF}} \bar{\tau} \log_2 \det \left[\mathbf{I}_{N_u} + \frac{P_r}{L_{IF,m}} \left(\frac{\mathbf{H}_{r(m),u(l)} \mathbf{W}_{u(l),m} \mathbf{W}_{u(l),m}^{\mathrm{H}} \mathbf{H}_{r(m),u(l)}^{\mathrm{H}}}{\mathbf{R}_R^{u(l)} + N_0 B_{sys} \mathbf{I}_{N_u}} \right) \right] \tag{5.22}$$

where $\mathbf{W}_{u(l),m}$ is the mth RS precoder of the lth UE. The design of $\mathbf{W}_{u(l),m}$ was given in [187] for a MISO system. We extend it here to a MIMO system as follows. Let us define the group of other UEs not served by the mth RS as the set given as $\bar{\mathcal{U}}_m^{IF} = \{\cup \mathcal{U}_n^{IF} \,| n \neq m, n \in \mathcal{M}\} = \{\bar{u}(1), \cdots, \bar{u}\left(|\bar{\mathcal{U}}_m^{IF}|\right)\}$. By using SVD, the right singular null space vectors of the vertically stacked channel matrix $\left[\mathbf{H}_{r(m),\bar{u}(1)}^{\mathrm{T}} \cdots \mathbf{H}_{r(m),\bar{u}\left(|\bar{\mathcal{U}}_m^{IF}|\right)}^{\mathrm{T}}\right]^{\mathrm{T}}$ between the mth RS and the UEs in set $\bar{\mathcal{U}}_m^{IF}$ is obtained as the column vectors of matrix $\tilde{\mathbf{V}}_{\bar{\mathcal{U}}_m^{IF}}^{null}$. Next, the concatenated channel between the mth RS and the intended UEs in set $\mathcal{U}_m^{IF}$ is obtained as $\mathbf{J}_m = \left[\mathbf{H}_{r(m),u(1)}^{\mathrm{T}} \cdots \mathbf{H}_{r(m),u\left(L_{IF,m}\right)}^{\mathrm{T}}\right]^{\mathrm{T}}$. A similar procedure as in Section 5.4.2 is then applied to the product of $\mathbf{J}_m \tilde{\mathbf{V}}_{\bar{\mathcal{U}}_m^{IF}}^{null}$ for the mth RS instead of jointly for all the M RSs to obtain $\tilde{\mathbf{V}}_{u(l),m}^{null}$, $\mathbf{V}_{u(l),m}^{base}$ and $\left(\mathbf{\Pi}_{u(l),m}\right)^{\frac{1}{2}}$. Therefore, the precoder matrix of the mth RS for the lth UE is $\mathbf{W}_{u(l),m} = \tilde{\mathbf{V}}_{\bar{\mathcal{U}}_m^{IF}}^{null} \tilde{\mathbf{V}}_{u(l),m}^{null} \mathbf{V}_{u(l),m}^{base} \left(\mathbf{\Pi}_{u(l),m}\right)^{\frac{1}{2}}$. The overall spectral efficiency of IF relaying is

$$C_{IF} = \min\left\{C_{BC,IDEC}^{select}, C_{R,IF}\right\}. \tag{5.23}$$

5.4.3.2 Maximum Ratio Transmit Relaying

In contrast, each RS in this technique selfishly relays to its associated UE group independent of the other RSs [187]. Each RS performs a maximum ratio transmit precoding on its signals before relaying them to its designated UEs to maximise its

own spectral efficiency and to remove multiuser interference from its own UE group. Since it is not coordinated with the other RSs, the receive signal of its UE group will be interfered with by the transmission of the other RSs. Let L_M be the number of UEs that each RS can support in MT relaying. As the RSs do not need to null interference to other UE groups, all spatial dimensions can be used to transmit to their own UE groups. Each RS designs the precoder matrix of the lth UE so that its signal is relayed in the null spaces of the remaining $L_M - 1$ UEs in its group. Therefore, the total spatial dimensions of any $L_M - 1$ UEs must be less than the available spatial dimensions of the RS. Thus,

$$(L_M - 1)\, N_u < N_r \;\Rightarrow\; L_M < \frac{Nr}{N_u} + 1 \tag{5.24}$$

$$\Rightarrow\; L_M^* = \left\lceil \frac{Nr}{N_u} \right\rceil \tag{5.25}$$

where L_M^* denotes the smallest integer not less than $\frac{Nr}{N_u}$ and satisfies the inequality in (5.24). Considering the actual K_m UEs (defined above) that are available to participate in the transmission, the $L_{MT,m}$ UEs effectively selected by the mth RS is given by the minimum between L_M^* and K_m, that is,

$$L_{MT,m} = \min\left\{L_M^*, K_m\right\}. \tag{5.26}$$

From (5.19) and (5.24), we observe that $L_M^* > L_I^*$ as the RSs in the MT relaying technique do not need to reserve some of their spatial dimensions for interference suppression but by doing so, incur an interference penalty to the other UEs not in its own relay group. From (5.14) and (5.24), we see that $ML_M^* = L_C^*$ but the CMP relaying has a further advantage of being able to transmit without interference to the other UEs. Let the set $\mathcal{U}_m^{MT} = \{u(l)\,|u(l) \in \mathcal{G}_{Relay}, l = 1, \cdots, L_{MT,m}\}$ be the selected $L_{MT,m}$ UEs of the mth RS. The relay-destination link spectral efficiency is thus

$$C_{R,MT} = \sum_{m\in\mathcal{M}} \sum_{u(l)\in\mathcal{U}_m^{MT}} \bar{\tau}\log_2\det\left[\mathbf{I}_{N_u} + \frac{P_r}{L_{MT,m}}\right.$$

$$\times \left(\frac{\mathbf{H}_{r(m),u(l)} \mathbf{W}_{u(l),m} \mathbf{W}_{u(l),m}^{\mathrm{H}} \mathbf{H}_{r(m),u(l)}^{\mathrm{H}}}{\sum\limits_{n \in \mathcal{M}, n \neq m} \mathbf{R}_{u(l),n} + \mathbf{R}_{R}^{u(l)} + N_0 B_{sys} \mathbf{I}_{N_u}} \right) \Bigg] \quad (5.27)$$

where $\mathbf{W}_{u(l),m}$ is the mth RS precoder of the lth UE and $\sum\limits_{n \in \mathcal{M}, n \neq m} \mathbf{R}_{u(l),n}$ is the interference covariance matrix of the other RSs to the lth UE of the mth RS. Likewise, the design of $\mathbf{W}_{u(l)}$ is described in [187] for a MISO system while we extend it here to a MIMO system. The mth RS calculates the precoder matrix by performing the SVD on the concatenated channel matrix $\mathbf{J}_m$ as defined in Section 5.4.3.1 but with $u(l) \in \mathcal{U}_m^{MT}$ instead. Likewise, a similar procedure as in Section 5.4.2 is then applied to $\mathbf{J}_m$ to obtain $\tilde{\mathbf{V}}_{u(l),m}^{null}$, $\mathbf{V}_{u(l),m}^{base}$ and $\left(\mathbf{\Pi}_{u(l),m}\right)^{\frac{1}{2}}$ for the mth RS instead of jointly for all the M RSs. The precoder matrix of the mth RS for the lth UE is thus $\mathbf{W}_{u(l),m} = \tilde{\mathbf{V}}_{u(l),m}^{null} \mathbf{V}_{u(l),m}^{base} \left(\mathbf{\Pi}_{u(l),m}\right)^{\frac{1}{2}}$. The overall spectral efficiency of MT relaying is

$$C_{MT} = \min \left\{ C_{BC,IDEC}^{select}, C_{R,MT} \right\}. \quad (5.28)$$

5.4.3.3 Localised Precoding Relaying

A variant of CMP relaying, referred to as LoP relaying, is also compared. Similar to CMP relaying, the RSs in LoP relaying cooperate to select common UEs for transmission. Unlike CMP relaying, the RSs in LoP relaying then transmit data independently to these UEs. Therefore, LoP relaying has limited RS cooperation and is used to illustrate the intermediate change in performance as one evolves from MT relaying with no RS cooperation to full RS cooperation techniques like the IF and CMP relaying.

System Capacities

So far, we have described the capacities of the various types of relay transmission techniques for the UEs in $\mathcal{G}_{Relay}$ of the RACN. As for the UEs in $\mathcal{G}_{Direct}$, the TDMA transmission technique is used to transmit information to them. Letting $\bar{L} = |\mathcal{G}_{Direct}|$,

the achievable spectral efficiency for the UEs in $\mathcal{G}_{Direct}$ is

$$C_D = \sum_{u(l)\in\mathcal{G}_{Direct}} \frac{t_D}{\bar{L}} \log_2 \det \left[\mathbf{I}_{N_r} + \frac{P_b}{N_b} \left(\frac{\mathbf{H}_{b,u(l)} \mathbf{H}_{b,u(l)}^{\mathrm{H}}}{\mathbf{R}_D^{u(l)} + N_0 B_{sys} \mathbf{I}_{N_r}} \right) \right] \tag{5.29}$$

where the interference covariance matrix $\mathbf{R}_D^{u(l)}$ is defined in (5.8). Therefore, the system spectral efficiency for the RACN is give by

$$C_{relay} = C_D + C_{\Theta,\Delta} \tag{5.30}$$

where $C_{\Theta,\Delta}$ is either (5.18), (5.23) or (5.28) with $\Theta = \{CMP,\, IF,\, MT\}$ while Δ are the user selection methods to be described in Section 5.5.

In contrast, all K UEs of the set $\mathcal{K}$ in the DTCN will be served using the TDMA transmission approach. Its system spectral efficiency is thus

$$C_{direct} = \sum_{u(l)\in\mathcal{K}} \frac{t_D}{K} \log_2 \det \left[\mathbf{I}_{N_r} + \frac{P_b}{N_b} \left(\frac{\mathbf{H}_{b,u(l)} \mathbf{H}_{b,u(l)}^{\mathrm{H}}}{\mathbf{R}_D^{u(l)} + N_0 B_{sys} \mathbf{I}_{N_r}} \right) \right]. \tag{5.31}$$

The DTCN will be used as a baseline comparison to the various relaying techniques of the RACN.

5.4.4 Degrees of Freedom

Let us assume there are L UEs participating in the relay transmission. As defined earlier, let L_m be the total UEs assigned to the mth RS for transmission, where $\sum_{m=1}^{M} L_m = L$. This is applicable to IF and MT relaying where each RS is assigned to a group of UEs. The total degrees of freedom for CMP, IF and MT relaying can be derived from (5.14), (5.19) and (5.24), respectively, while that of LoP relaying is similar to CMP relaying but without M as the RSs transmit independently. Thus, the total degrees of freedom of the various relaying techniques is given as

$$\Phi_{CMP} = L \cdot \min\left\{ MN_r - (L-1)\, N_u, N_u, N_b \right\}, L \leqslant L_C^* \tag{5.32}$$

$$\Phi_{IF} = L \cdot \min\left\{N_r - (L-1)\,N_u, N_u, N_b\right\}, L \leqslant ML_I^* \tag{5.33}$$

$$\Phi_{MT} = \sum_{m=1}^{M} \min\left\{N_r - (L_m - 1)\,N_u, N_u, N_b\right\}, L_m \leqslant L_M^* \tag{5.34}$$

$$\Phi_{LoP} = L \cdot \min\left\{N_r - (L-1)\,N_u, N_u, N_b\right\}, L \leqslant L_M^* \tag{5.35}$$

where L_C^*, L_I^* and L_M^* are defined in (5.14), (5.19) and (5.24), respectively.

5.5 User Selection Methods for Relay Cooperation

5.5.1 Optimum User Selection

In the Optimum User Selection (OUS) method, all possible combinations of L_{CMP} UEs in $\mathcal{G}_{Relay}$ is evaluated and the combination that returns the highest relay-destination link spectral efficiency is selected. The number of combinations is given as

$$Q = \begin{pmatrix} |\mathcal{G}_{Relay}| \\ L_{CMP} \end{pmatrix} = \frac{|\mathcal{G}_{Relay}|!}{L_{CMP}!\,(|\mathcal{G}_{Relay}| - L_{CMP})!}. \tag{5.36}$$

Let set $\mathcal{L} = \{\zeta_q\,|q = 1, \cdots, Q; |\zeta_q| = L_{CMP}\}$ contain all the Q possible permutations of the L_{CMP} UEs, each represented by ζ_q. Assuming global CSI is available at the RSs, the optimum set of UEs is the one that maximises (5.17) and is given as

$$\mathcal{U}_{Opt} = \underset{\zeta_q \in \mathcal{L}}{\arg\max}\, C_{R,CMP}. \tag{5.37}$$

The disadvantage of the OUS method is the cost of exchanging the global CSI and the rapidly increasing cost of computing the Q values of $C_{R,CMP}$ as $|\mathcal{G}_{Relay}|$ increases.

5.5.2 Full Semi-Orthogonal User Selection

The OUS method is prohibitive in terms of computational complexity. Given the global CSI, the Semi-orthogonal User Selection (SUS) method [183] does not need to evaluate all Q permutations. Instead, the UEs are selected sequentially with each

newly added UE being as orthogonal as possible to the selected UEs before it. Thus, computational complexity is reduced albeit some tolerable performance loss. The SUS idea is incorporated into the Full Semi-orthogonal User Selection (FSUS) method with the following execution steps.

1. Each RS shares its CSI with all the other RSs.
2. Each RS invokes the SUS algorithm (Fig. 5.4) using the global CSI in Step 1 as its input. The SUS algorithm is as follows:
   (a) Firstly, the UE with the highest sum eigenvalues of its RS–UE channel **H** is chosen.
   (b) Next, the UEs that are closely orthogonal to the already selected set of UEs are identified among the remaining UEs.
   (c) From these UEs, the one with the highest sum eigenvalues is chosen and included into the set of selected UEs.
   (d) Repeat from Step (b) until L_{CMP} UEs are selected.

As the global CSI is available, the L_{CMP} selected UEs by each RS will be the same. The disadvantage of the FSUS method is again the cost of exchanging the global CSI.

5.5.3 Partial Semi-Orthogonal User Selection

The OUS and FSUS methods suffer from costly exchanges of global CSI among the RSs and thus putting a high toll on the cooperative link. Although it is imperative that the RSs must know the CSI for cooperative relaying, the strain on the cooperative link can be decreased by avoiding premature CSI exchange of all the UEs among the RSs. This is the motivation behind the proposed PSUS method.

The key idea behind the PSUS method is that all RSs will firstly select their own set of UEs based upon their local CSI. Consequently, the selected UEs may differ from one RS to the other. A negotiation phase among the RSs will follow next to decide

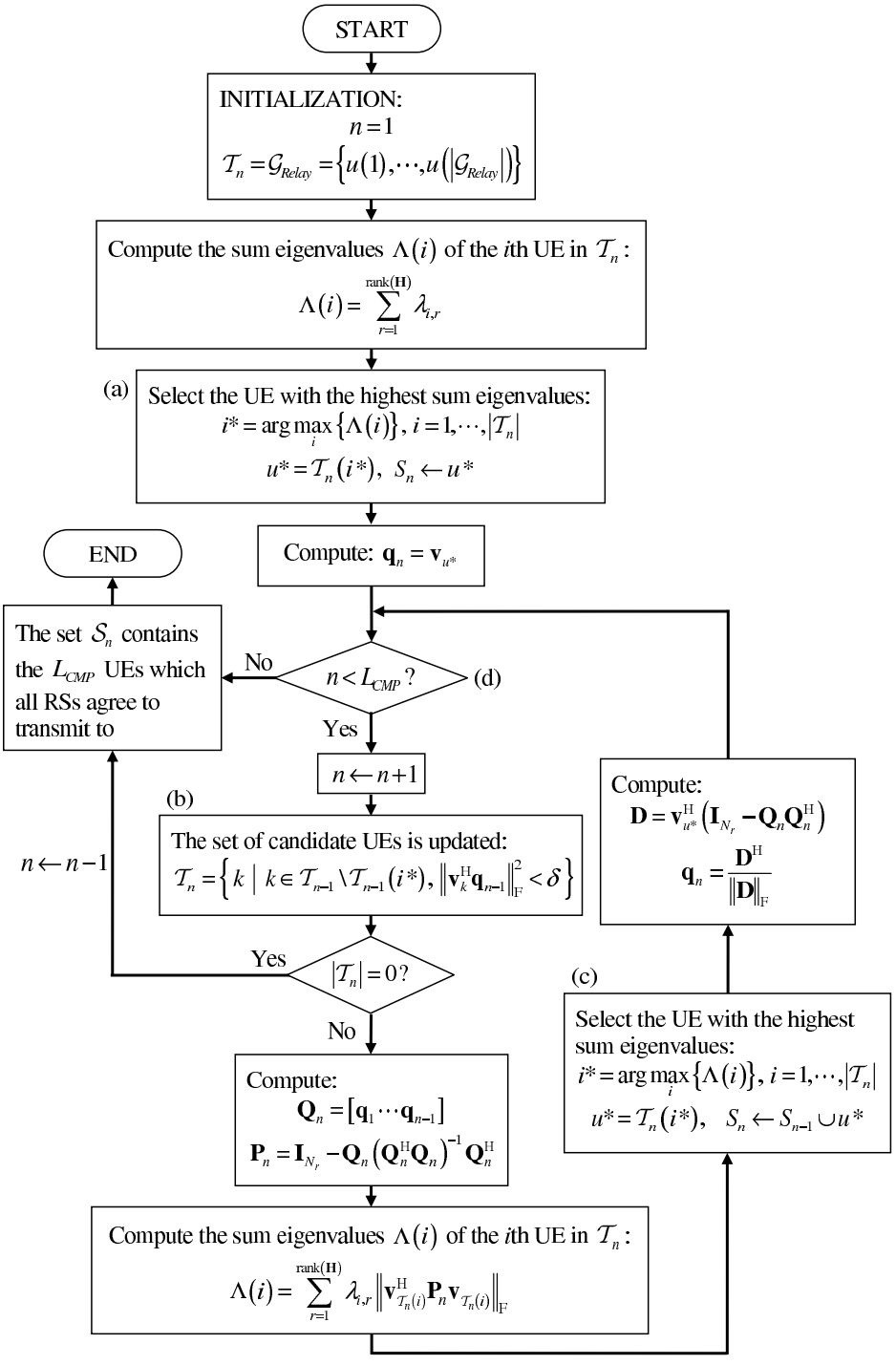

FIGURE 5.4: The SUS algorithm.

on a common set of UEs that is agreed upon by all RSs. Finally, only then will the global CSI of this common set of UEs be exchanged among the RSs. The following details the execution steps of the PSUS method.

1. Each RS independently selects L_{CMP} UEs by invoking the SUS algorithm using

its local CSI as input. Consequently, the initially selected UEs may differ from one RS to the other.

2. The mth RS then shares the user index representing its initially selected set of UEs $\mathcal{T}_m$ and their corresponding channel norms Λ_m.

3. Using the information at Step 2, each RS invokes the Norm-based User Negotiation (NUN) algorithm (Fig. 5.5):

   (a) The UEs in the first entries of each set $\mathcal{T}_m(1)$ are initially selected to include UEs with high channel norms (UEs are arranged in descending channel norm values).

   (b) Subsequent UEs in each set are sequentially compared across all sets. The UE with the highest channel norm is identified.

   (c) Include this UE into the set of selected UEs if it is not already selected in the previous selection round.

   (d) Increment the sequence counter of the selected UE's set.

   (e) Repeat from Step (b) until L_{CMP} UEs are selected.

4. The CSI of only these L_{CMP} UEs which all RSs agree to transmit to are then shared.

The PSUS method reduces the signalling overhead of the cooperative link as it avoids the high cost of communicating the CSI of all the UEs in set $\mathcal{G}_{Relay}$ to all RSs.

5.6 Cooperative Cost

We assume that the cooperative link has a separate bandwidth B_{coop} from the underlying cellular system. Let the transmit time interval be T_{TTI} and the fraction of time for cooperative transmission be $\tau_{coop}\,(0 \leq \tau_{coop} \leq 1)$. At each RS, the cooperative information will initially be sampled and quantised at a resolution of θ bits per sample before broadcasting it through the cooperative link to the other RSs.

5.6.1 Joint RS Decoding Cost

There are two costs associated with the JDEC strategy during the broadcast phase. Firstly, all RSs need to know the CSIs of the other RSs. As we assume that the channel states do not change during one transmission frame, so the CSI needs to

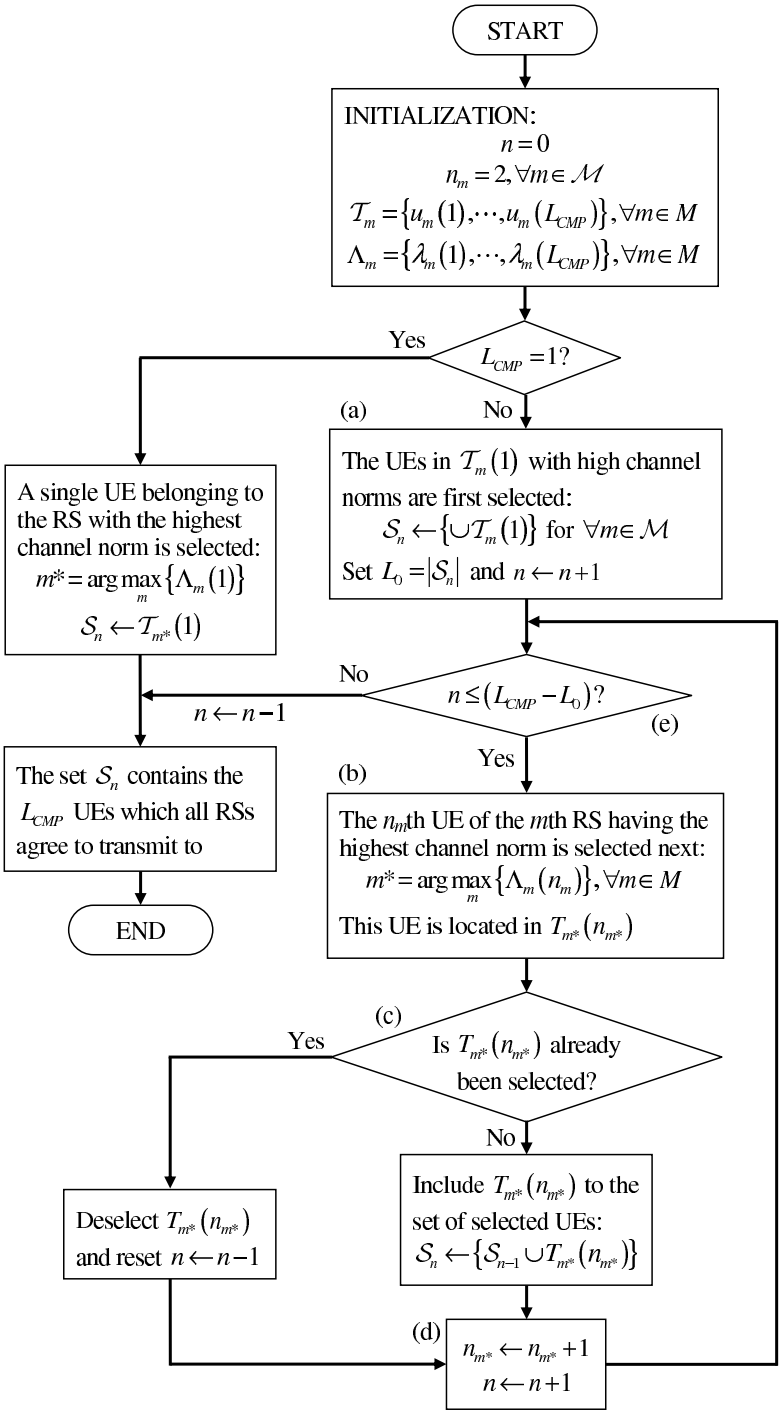

FIGURE 5.5: The NUN algorithm for negotiation of users between RSs.

be exchanged only once. The second and more costly cooperative information to be frequently exchanged among the RSs are the received signals. All the M RSs must know the other $(M-1)$ RSs received signals each time the BS broadcasts them. We now quantify these two costs.

5.6.1.1 RS Received Signal Exchange Cost

For each channel use, the BS transmits a signal vector of length N_b. Due to the broadcast nature of the BS, each RS will receive a version of this transmit signal as a vector of length N_r. Since the elements of the received vector are complex numbers with real and imaginary parts, each vector will consist of $2N_r$ separate values to be sampled and transmitted through the cooperative link. Assume that the BS will transmit at a rate of B_{sys} channel uses per second during the broadcast phase, the minimum bit rate that the cooperative link has to support for RS received vector exchanges is given as

$$R_{JDEC,vec} = 2N_r\theta M B_{sys}. \tag{5.38}$$

Only the CMP relaying technique incurs this cost if it performs JDEC as given in (5.11) but is exempted from it if IDEC is employed as in (5.12).

5.6.1.2 Broadcast Phase CSI Exchange Cost

The total elements of the channel matrix between the BS and each RS is N_rN_b. Since the channel matrix elements are complex, there are $2N_rN_b$ separate values to be sampled and transmitted through the cooperative link. We assume that the information exchange happens in a fraction τ_{coop} of one T_{TTI} duration. Thus, the minimum bit rate that the cooperative link has to support for CSI exchanges during broadcast phase is

$$R_{JDEC,CSI} = \frac{2N_rN_b\theta M}{\tau_{coop}T_{TTI}}. \tag{5.39}$$

Similarly, only the CMP relaying technique incurs this cost if it performs JDEC as given in (5.11) but is exempted from it if IDEC is employed as in (5.12).

5.6.2 User Selection Cost

The CSI exchange which is necessary for the user selection methods occurs once per transmission frame as it is assumed that the channel does not change during that period. Since the user selection methods differ in the extent of the CSI that must be shared, so will the associated costs vary. We will now quantify the cost for the three user selection methods.

5.6.2.1 OUS and FSUS Cooperative Cost

The total elements of the channel matrix between the mth RS and the lth UE is $N_u N_r$. Since each channel matrix consists of complex elements, there will be $2N_u N_r$ separate values to be sampled and transmitted through the cooperative link for each UE of every RS. In the OUS and FSUS methods, each RS must obtain from the other $(M-1)$ RSs the CSI of all K UEs for its selection mechanism. Thus, assuming that the information is exchanged in a fraction τ_{coop} of one T_{TTI} duration, the minimum bit rate that the cooperative link has to support for the OUS and FSUS methods is

$$R_{OUS} = R_{FSUS} = \frac{2N_u N_r K \theta M}{\tau_{coop} T_{TTI}}. \tag{5.40}$$

5.6.2.2 PSUS Cooperative Cost

Each of the two stages in the PSUS method has an associated cost. After independently selecting the L_{CMP} UEs, each RS broadcasts the channel norms of its selected UEs and an index representing the selected UE sequence. This requires $(L_{CMP}+1)$ separate values to be sampled and transmitted through the cooperative link for each RS. Next, each RS is required to share the channel matrix between itself and the reselected L_{CMP} common UEs. As the elements of each channel matrix are complex

numbers, this requires $2N_uN_r$ separate values to be sampled and transmitted through the cooperative link for each reselected UE of every RS. Thus assuming that the information is exchanged in τ_{coop} fraction of one TTI duration, the minimum bit rate that the cooperative link has to support for the PSUS method is

$$R_{PSUS} = \frac{(L_{CMP} + 1 + 2N_uN_rL_{CMP})\,\theta M}{\tau_{coop}T_{TTI}}. \tag{5.41}$$

5.6.2.3 Cooperative Cost Comparison

In order for PSUS to operate at a bit rate that is lower than FSUS, we have

$$R_{PSUS} < R_{FSUS} \tag{5.42}$$

which, after some algebraic manipulation, gives

$$L_{CMP} < \frac{2N_uN_rK - 1}{2N_uN_r + 1} \Rightarrow \hat{L}_{CMP} = \left\lceil \frac{2N_uN_r\,(K-1) - 2}{2N_uN_r + 1} \right\rceil \tag{5.43}$$

where $\hat{L}_{CMP}$ is the largest integer satisfying the inequality in (5.43). Therefore, while the L_{CMP} in (5.16) is necessary due to the dimensional constraint, the $\hat{L}_{CMP}$ in (5.43) provides a constraint in which PSUS would perform better than FSUS.

5.7 Energy Efficiency Optimisation

We begin by modifying the ECR expression in (5.5) to include the power consumption of the RS cooperative link. This is given as

$$\mathrm{ECR}_{sys}^{modified} = \frac{\mathbb{E}\left\{P_{op,total}^{sys} + P_{op,total}^{coop}\right\}}{B_{sys} \cdot \mathbb{E}\left\{C_{sys}\right\}} \tag{5.44}$$

where $P_{op,total}^{coop}$ is the total operational power consumption of the RS cooperation link in order to achieve the necessary bit rate of (5.38)–(5.41) for cooperative information exchange so that the system could achieve the spectral efficiency of C_{sys}. Taking CMP

relaying as an example, we formulate the following problem to minimise (5.44):

$$\begin{aligned} \underset{N_r}{\text{minimise}} \quad & \text{ECR}_{sys,CMP}^{modified} \\ \text{subject to:} \quad & \text{trace}\left(\mathbf{W}_{u(l)}\mathbf{W}_{u(l)}^{\text{H}}\right) \leqslant 1, \;\; l = 1, \cdots, L_{CMP} \\ & P_b, P_r > 0 \\ & \min\left\{MN_r - (L_{CMP}-1)\,N_u, \;\; N_u\right\} > 0. \end{aligned} \tag{5.45}$$

The objective of this constrained optimisation problem is to find the optimum number of RS antennas N_r in order to minimise the ECR while considering the cooperative cost. The first constraint ensures that the RS precoder matrix $\mathbf{W}_{u(l)}$ for user $u\,(l)$ does not violate the power constraint of the RS. The second constraint ensures that the transmit power is always positive. Lastly, the third constraint is the spatial degrees of freedom constraint for cooperative relaying among the M RSs.

5.8 Economic Efficiency

The economic efficiency metric has been defined in (4.36) of Section 4.6. It is modified here to include the cooperative cost of the RS cooperation link. Thus, the modified economic efficiency metric is given as

$$U_{sys}^{modified} = \kappa_r r_{base} \log_2\left(1 + \frac{B_{sys}C_{sys}}{r_{base}}\right) - \kappa_c\left(P_{op,total}^{sys} + P_{op,total}^{coop}\right) \tag{5.46}$$

where r_{base} is the base service data rate which refers to the essential service expected by every mobile user, while κ_r and κ_c are the revenue per bit and energy cost per Ws, respectively. Both revenue and cost are measured in the same m.u., e.g., in pence. The total operational power consumption of the system and RS cooperation link is denoted as $P_{op,total}^{sys}$ and $P_{op,total}^{coop}$, respectively. The definition of $P_{op,total}^{coop}$ is as given in Section 5.7. Furthermore, the spectral efficiency and bandwidth of the system are represented by C_{sys} and B_{sys}, respectively.

5.8.1 Economic Efficiency Optimisation

In this section, we present the formulation for the optimisation of the modified economic efficiency metric in (5.46) which takes into consideration both the SEET and the cooperative cost of the RS cooperation link. Taking CMP relaying as an example, the following problem is formulated to maximise (5.46):

$$\begin{aligned} \underset{N_r}{\text{maximise}} \quad & U_{sys}^{modified} \\ \text{subject to:} \quad & \text{trace}\left(\mathbf{W}_{u(l)}\mathbf{W}_{u(l)}^{\text{H}}\right) \leqslant 1, \;\; l = 1, \cdots, L_{CMP} \\ & P_b, P_r > 0 \\ & \min\left\{MN_r - (L_{CMP}-1)\,N_u, \;\; N_u\right\} > 0. \end{aligned} \tag{5.47}$$

Similar to (5.45), the first constraint ensures that the RS precoder matrix $\mathbf{W}_{u(l)}$ for user $u\,(l)$ does not violate the power constraint of the RS. The second constraint ensures that the transmit power is always positive. Lastly, the third constraint is the spatial degrees of freedom constraint for cooperative relaying among the M RSs.

5.9 Simulation Results and Discussions

We present some numerical results for the downlink transmission of a suburban macrocell scenario. This scenario with a moderately large cell size and medium to heavy traffic load was found to provide the most benefit for relaying techniques. We set $d_{ISD} = 1300$ m while $r_{cell} = d_{ISD}/\sqrt{3}$, $d_{RS} = 0.7r_{cell}$ and $N_{Sec} = 3$. Also, $P_b = 40$ W, $P_r = 2$ W and $P_{c,ref} = 577$ W at $P_{ref} = 40$ W. Furthermore, we set $\alpha_b = \alpha_r = 2.84$ and $B_{sys} = B_{coop} = 10$ MHz. The rest of the simulation parameters are in Table 5.1. The link level performance of the CMP, IF, MT and LoP relaying techniques will be evaluated first. This is followed by the system level performance evaluation of CMP relaying for different RFR patterns. Subsequently, the performance of CMP relaying with various combinations of both the JDEC and IDEC strategies with the OUS, FSUS and PSUS user selection methods will be investigated.

5.9.1 Link Level Performance

The CMP, IF and MT relaying techniques have different capabilities. For example, both CMP and IF relaying are capable of joint RS decoding during the broadcast phase while MT relaying is not as there is no cooperative link among its RSs. Since the focus of this section is to evaluate the effectiveness of relay phase techniques, IDEC is assumed for all relaying techniques during the broadcast phase. Furthermore, in this subsection, the interference covariance matrix representing the external interference surrounding the base sector is set to zero, leaving only the interference from within the base sector. This setup is to clearly measure the effectiveness of the various relaying techniques in mitigating the interference that is expected from within its own (base) sector. Besides that, the optimum OUS user selection method is employed for all the relaying techniques. This is to ascertain that the performance evaluated is solely on account of the relaying mechanisms during the relay phase alone.

In Fig. 5.6, the link level spectral efficiency of the relaying techniques is illustrated both with and without the OUS user selection method while direct transmission is taken as the baseline. When no user selection is employed (Fig. 5.6(a)), the IF relaying performs only slightly better than MT relaying. This is because it has to sacrifice some spatial multiplexing gains for interference free relaying. However, neither performs any better than direct transmission. By contrast, the average spectral efficiency of CMP relaying at 16.5 bits/s/Hz/sector is 5% better than direct transmission although its spectral efficiency at 10% outage probability is lower. Despite having access to more spatial dimensions for data transmission, we observe that LoP relaying performs only marginally better than IF relaying which sacrifices some spatial dimension for interference cancellation. The performance loss is due to the signals arriving incoherently at the destinations, resulting in the loss in signal strength.

When user selection is employed in Fig. 5.6(b), the spectral efficiency of the relaying techniques generally improves due to multiuser diversity. Both MT and IF relaying are now marginally better than direct transmission at higher Cumulative Distribution Function (CDF) values. A clear advantage of IF relaying over MT relaying is now observed. As user selection guarantees that the UEs with the best channel conditions

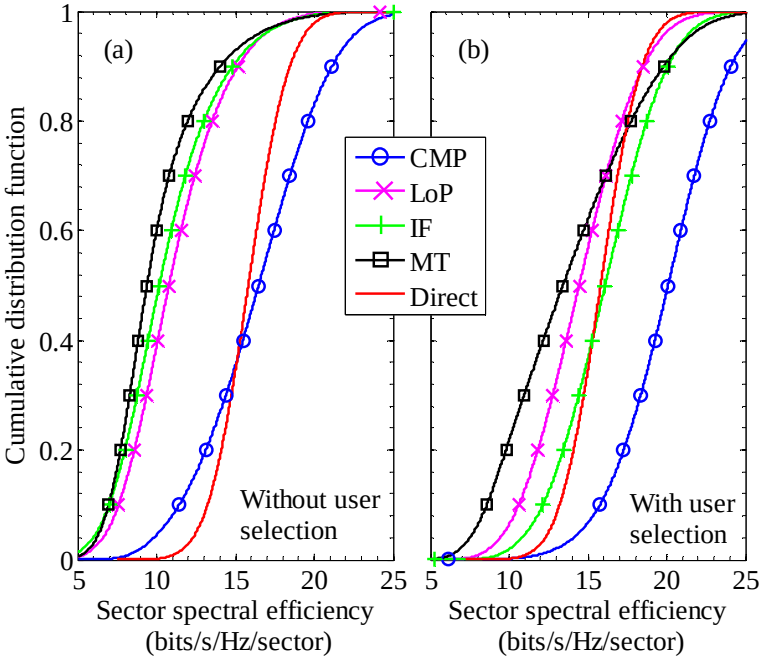

FIGURE 5.6: Link level spectral efficiency of various relaying techniques: (a) without user selection and (b) with the OUS method ($N_b = 8$, $N_r = 4$, $N_u = 2$, $M = 2$, $K = 10$).

are selected for relay transmission, the channel gain from this outweighs the reduction in spatial multiplexing capability incurred in IF relaying. However, the loss due to incoherent transmission in LoP relaying means that it is not able to benefit from user selection even if the best UEs are selected, resulting in its performance now being poorer than IF relaying. Nevertheless, the benefit of joint relaying transmission in CMP relaying ensures that its spectral efficiency significantly outperforms both the direct transmission and other relaying techniques.

Next, the spectral efficiency of CMP and MT relaying techniques with identical degrees of freedom is compared in Fig. 5.7. The maximum number of users is when CMP and MT relaying are serving L_C^* and ML_M^* UEs, respectively. Going from two users to the maximum number of users, the total degrees of freedom of both CMP and MT relaying increases from 4 to 8. As the RSs in CMP relaying cooperatively transmit across all spatial dimensions, its spectral efficiency doubles as Φ_{CMP} doubles. However, as Φ_{MT} doubles, the spectral efficiency of MT relaying increases by a lesser amount. This is due to the presence of interference at each group of UEs as the RSs in MT relaying transmit independently of one another.

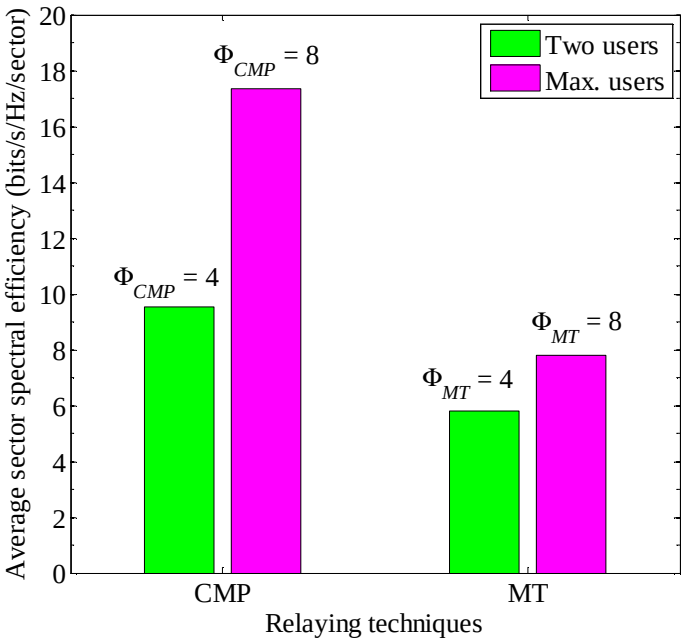

FIGURE 5.7: The spectral efficiency of CMP and MT relaying with two users ($L = 2$) where $\Phi_{CMP} = \Phi_{MT} = 4$ and with the maximum number of users where $\Phi_{CMP} = \Phi_{MT} = 8$ ($N_b = 8, N_r = 4, N_u = 2, M = 2$).

5.9.2 System Level Performance

We further investigate the performance of CMP relaying at the system level for a RACN where we have both direct and relay transmission present. The effect of external interference surrounding the base sector is considered in this subsection. In Fig. 5.8, the impact of different RFR patterns on the 10% outage capacity of CMP relaying is illustrated with the Adaptive Relaying (AR) scheme taken as a comparison. The AR scheme switches between direct and relay transmission, depending on which provides better throughput to the group of UEs currently being served. The MT relaying technique described in Section 5.4.3.2 is employed by the RSs of the AR scheme. At $P_{RS} = 2$ W, CMP relaying outperforms the AR scheme by 4% and 10% for $\eta_r = 1/3$ and $\eta_r = 1$, respectively. As η_r goes from 1/3 to 1, the outage capacity of CMP relaying improves by 22% while the AR scheme achieves a lower improvement of 16%. Therefore, CMP relaying is better at suppressing intra-cell and strong inter-cell interference through its Type I RFR pattern with relay cooperation. The aggressive full bandwidth Type III RFR pattern is also exploited by CMP relaying by mitigating intra-cell interference through relay cooperation. The benefit of CMP

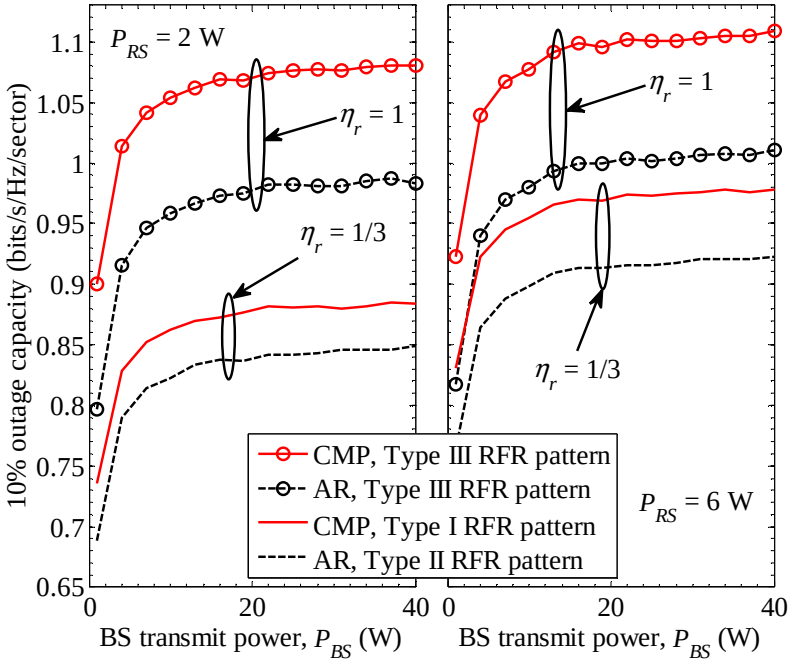

FIGURE 5.8: Outage capacity v.s. P_{BS} of CMP relaying and the AR scheme with their corresponding $\eta_r = 1/3$ (Type I,II) and $\eta_r = 1$ (Type III) RFR patterns at P_{RS} of 2 W and 6 W (figures share common y-axis).

relaying over the AR scheme is observed again at $P_{RS} = 6$ W albeit a 2% reduction in gains due to stronger interference. Increasing P_{RS} from 2 W to 6 W while maintaining the RFR patterns achieves only marginal outage improvement. Thus, adopting a full bandwidth RFR pattern provides higher gains than increasing relay transmit power, especially at low P_{RS}.

Next, the average sector spectral efficiency and ECR of CMP relaying and the AR scheme are shown in Fig. 5.9 at different RFR patterns. For $P_{RS} = 2$ W, the spectral efficiency of the AR scheme saturates at 2.51 bits/s/Hz/sector with an ECR of 9.8 μJ/bit/sector while CMP relaying achieves the same spectral efficiency at 3.6 μJ/bit/sector when $\eta_r = 1/3$. At $\eta_r = 1$, the spectral efficiency of the AR scheme saturates at 2.63 bits/s/Hz/sector with an ECR of 10.8 μJ/bit/sector while CMP relaying requires 2.7 μJ/bit/sector for the same spectral efficiency. Furthermore, at 3.6 μJ/bit/sector the spectral efficiency of CMP relaying improves by 11% as it switches from $\eta_r = 1/3$ to $\eta_r = 1$ while the AR scheme gains only 3%. Thus, while CMP relaying is more energy efficient than the AR scheme at $\eta_r = 1/3$, further spectral and energy efficiency gains are achieved for $\eta_r = 1$. At $P_{RS} = 6$ W, we see the same

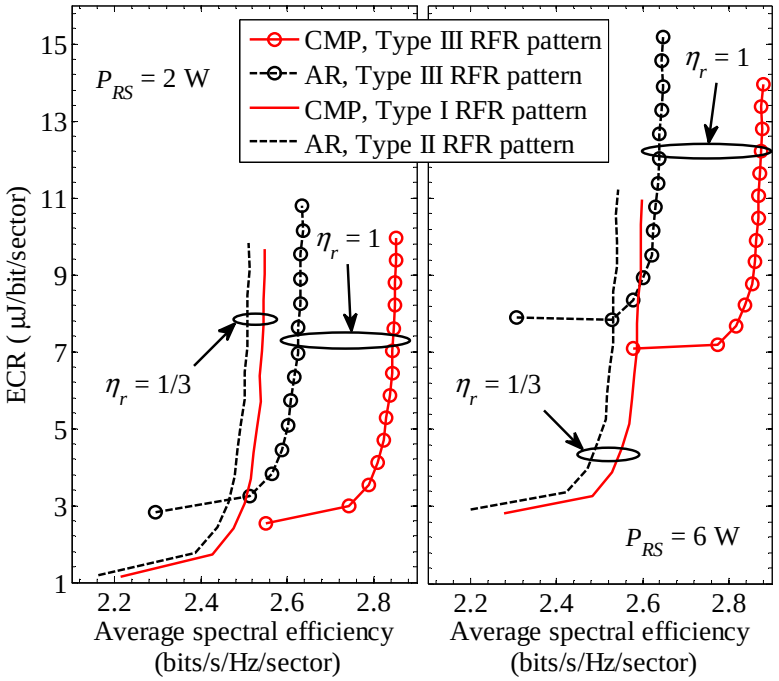

FIGURE 5.9: ECR v.s. average sector spectral efficiency of CMP relaying and the AR scheme with their corresponding $\eta_r = 1/3$ (Type I,II) and $\eta_r = 1$ (Type III) RFR patterns at P_{RS} of 2 W and 6 W (figures share common y-axis).

energy saving trend but at higher energy per bit values. An overall loss in energy efficiency is observed when going from $P_{RS} = 2$ W to $P_{RS} = 6$ W for the same RFR pattern due to the increase in interference from the surrounding RSs as higher energy per bit is necessary at $P_{RS} = 6$ W to achieve the same spectral efficiency as when $P_{RS} = 2$ W for both $\eta_r = 1/3$ and $\eta_r = 1$. The overall results indicate that utilising full bandwidth RFR pattern ($\eta_r = 1$) is more energy efficient at low P_{RS} while partial bandwidth RFR pattern ($\eta_r = 1/3$) is favoured at high P_{RS} though at lower energy efficiency. Therefore, the rest of the CMP relaying simulation results assume $P_{RS} = 2$ W and $\eta_r = 1$ (Type III RFR pattern).

In Fig. 5.10, the influence of β_R on the the ECR performance and percentage of unserved UEs is shown for CMP relaying. At low β_R (low relay confidence), all UEs will be served by direct transmission (0% unserved UEs) regardless of their distances from the BS. This results in poor energy efficiency as evident from the high ECR values. As β_R increases (higher relay confidence), more UEs will be assigned to the relay transmission group, especially those further away from the BS. This improves energy efficiency and thus the ECR values decrease. However, due to having the user

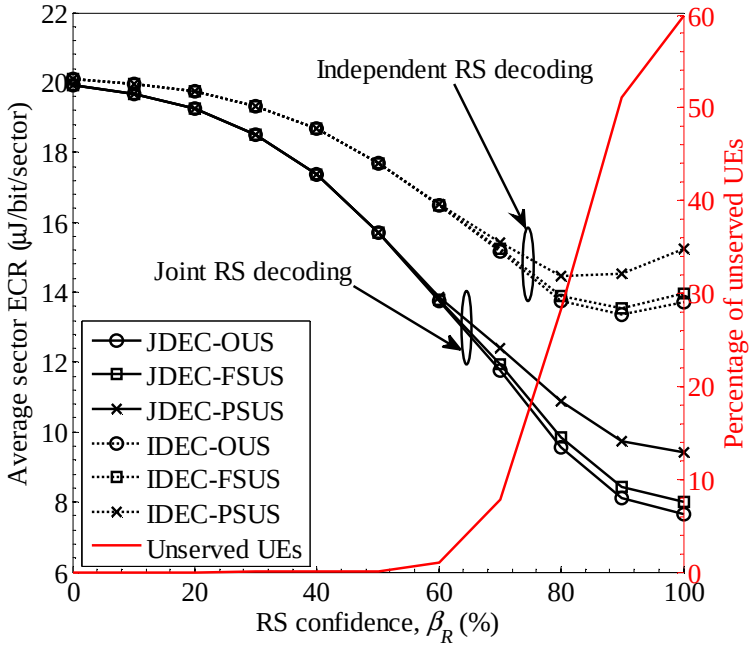

FIGURE 5.10: Average sector ECR and percentage of unserved UEs v.s. relay confidence of CMP relaying in a RACN ($N_b = 8$, $N_r = 4$, $N_u = 2$, $M = 2$, $K = 10$).

selection methods, not all of the assigned UEs are selected for relaying and thus the percentage of unserved UEs begins to increase. At $\beta_R = 1$, all UEs will be assigned to the relay transmission group. From (5.16), at most $L_{CMP} = 4$ UEs will be selected during each cooperative relay transmission, resulting in a maximum of 60% unserved UEs. To achieve user coverage of around 90%, we therefore select $\beta_R = 0.7$ as the value for simulation.

In Fig. 5.11, the spectral efficiency and ECR performance of CMP relaying is evaluated with various BS transmit antennas and different cooperation levels. When JDEC is employed, the broadcast phase is effectively a full spatial multiplexing system with up to $\min(N_b, MN_r)$ parallel data streams available between the BS and RSs. Thus, with $N_r = 4$ and $M = 2$, the CMP relaying spectral efficiency in Fig. 5.11(a) increases as N_b increases up to $MN_r = 8$ antennas. Because P_b and P_r are fixed, a decrease in ECR is registered in Fig. 5.11(b) for the same N_b range. For $N_b > 8$, the gains of CMP relaying with JDEC begin to saturate as the number of data streams remains the same. In IDEC, each RS has only its own antennas for decoding, thus, supporting $\min(N_b, N_r)$ parallel data streams between the BS and each RS. This limits the gains

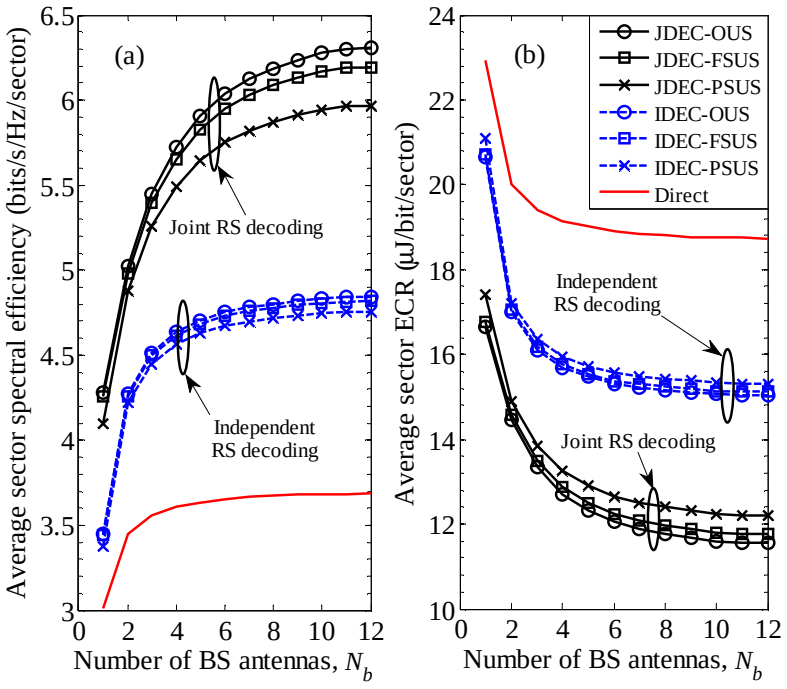

FIGURE 5.11: (a) Spectral efficiency and (b) ECR v.s. the number of BS antennas for CMP relaying in a RACN ($\beta_R = 70\%$, $N_r = 4$, $N_u = 2$, $M = 2$, $K = 10$).

when $N_b > 4$. A performance gap of around 1.3 bit/s/Hz/sector for spectral efficiency and 3.1 μJ/bit/sector for ECR is typically observed between JDEC and IDEC.

The impact of various user selection methods on the CMP relaying system performance is also evident in Fig. 5.11. As expected, OUS performs the best while FSUS performs slightly better than PSUS. The performance gap between OUS and PSUS is more significant when JDEC, rather than IDEC, is considered. This is because the performance of CMP relaying with JDEC is limited by the relay phase. Thus, the type of user selection method will influence the overall system performance more profoundly as it is implemented at the relay phase. This is less significant in CMP relaying with IDEC where the bottleneck is at the broadcast phase.

In Fig. 5.12, the average sector ECR of CMP relaying at different cooperation levels is illustrated as the BS transmit power per sector P_b varies. The ECR generally increases with P_b for all schemes as more power is consumed by the system. At low P_b, it is observed that the DTCN is more energy efficient as it registers lower ECR values. This is because the network interference at low P_b is not too severe. In that situation, direct transmission is able to offer better spectral efficiency than relay transmission

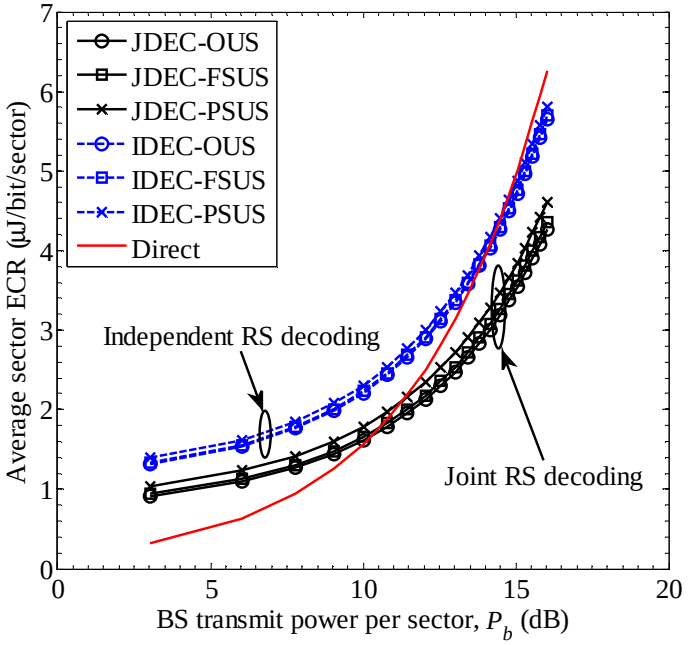

FIGURE 5.12: Average sector ECR v.s. BS transmit power of the CMP relaying technique at different cooperation levels for a RACN ($\beta_R = 70\%$, $N_b = 8$, $N_r = 4$, $N_u = 2$, $M = 2$, $K = 10$).

which incurs multiplexing loss due to its two-hop relaying protocol. This results in a lower energy consumed per bit for the DTCN as compared to the RACN. However, the RACN outperforms the DTCN when P_b is in excess of 10 dB and 13 dB for CMP relaying with JDEC and IDEC, respectively. At higher P_b, the network interference is now increased. The interference mitigation property of CMP relaying employed in the RACN results in better spectral efficiency performance as compared to the DTCN which is interference limited. Thus, at high P_b regime, the RACN requires lower energy per bit than the DTCN during transmission. For the RACN, we observe that CMP relaying with JDEC performs better than with IDEC by a difference of 0.8μJ/bit/sector. However, the superior performance of JDEC requires a prohibitively high cooperative cost.

The cooperative costs of CMP relaying for different cooperative levels are tabulated in Table 5.2. It is established that CMP relaying with JDEC performs better than IDEC both in terms of spectral efficiency and energy efficiency. To realise such gains, the cooperative links between the RSs must be able to at least support a bit rate of 640 Mbits/s to share all the signals received during the broadcast phase. This bit

TABLE 5.2: Cooperative Cost.

Strategies	**Broadcast phase:** Joint RS decoding (JDEC)		**Relay phase:** User selection method		
	Signal sharing	CSI sharing	OUS	FSUS	PSUS
Bit rate (Mbits/s)	640	5.12	12.8	12.8	5.52
RF transmit power (mW)	very high	58.2	164.6	164.6	63.2
Operational power (W)	very high	1.0	2.8	2.8	1.1

rate is an order of magnitude higher than that can be delivered by the underlying RACN system. Besides that, CSI sharing requires a further bit rate of at least 5.12 Mbits/s. Needless to say, the power consumption to operate the cooperative link will be excessively high. Therefore, the performance gain of CMP relaying with JDEC must be traded off against a very large increase in cooperative signalling costs.

From Table 5.2, both the OUS and FSUS methods require a cooperative link with a bit rate of 12.8 Mbits/s. Assuming an $N_r \times N_r$ MIMO cooperative link with a shadow margin of 16.4 dB (corresponding to $\sigma_s = 10$ dB) for 90% link reliability, the RF transmit power and operational power are 164 mW and 2.8 W, respectively. The operational power is calculated using (5.2) as direct transmission is assumed for the cooperative links. As for the PSUS method, the cooperative link has to support a bit rate of just 5.52 Mbits/s and operational power of 1.1 W. Although the PSUS method has slightly lower gains as compared to the OUS and FSUS methods in terms of system performances, this shortcoming is more than compensated by being able to operate at less than half the cooperative cost of the other two methods.

In Fig. 5.13, the ECR of (5.44) is numerically optimised for IDEC-PSUS and IDEC-FSUS relay cooperation schemes while considering the cooperative cost of two different user selection methods. The ECR of (5.5) is also evaluated to illustrate the performance when the cooperative cost is not considered. For both IDEC-PSUS and IDEC-FSUS, the ECR with no cooperative cost decreases monotonically with N_r. Furthermore, for a given N_b, the ECR performance of PSUS without cooperative cost is slightly worse than FSUS.

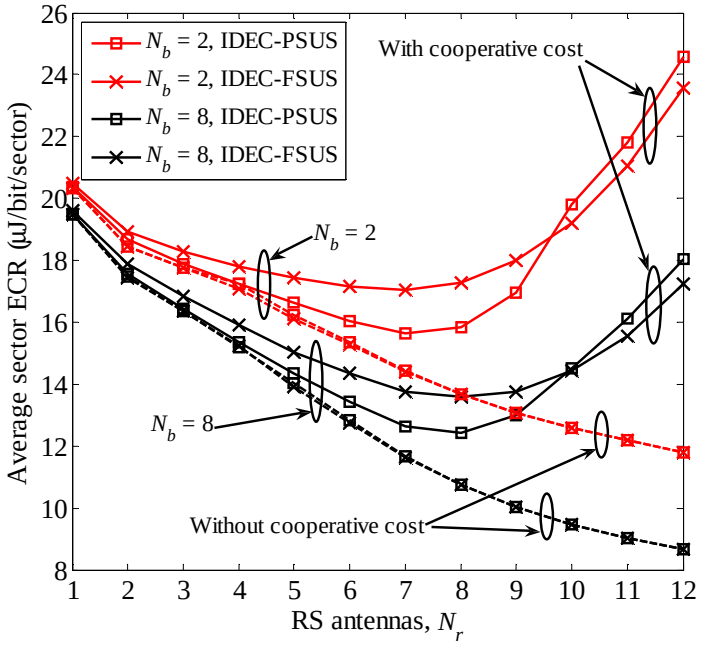

FIGURE 5.13: The average sector ECR v.s. the number of RS antennas of the IDEC-PSUS and IDEC-FSUS relay cooperation schemes for both with and without the cooperative cost for $N_b = 2$ and $N_b = 8$.

When the cooperative cost is considered, the minimum ECR is achieved for both schemes when $N_r = 7$ and $N_r = 8$ for $N_b = 2$ and $N_b = 8$, respectively. It is also observed that PSUS outperforms FSUS by registering lower ECR values when cooperative cost is included. For $N_r > 8$, the operational power consumption at the RS cooperation link becomes excessively large as the required bit rate for the exchange of cooperative information becomes prohibitively high. This increases the ECR values which, in turn, reduces the energy efficiency.

For $N_r \geq 10$, the performance of PSUS begins to degrade as compared to FSUS. This is because at higher N_r values, the number of UEs supported for joint transmission, which is given by (5.16), surpasses the threshold in (5.43), i.e., $L_{CMP} > \hat{L}_{CMP}$ for $N_r \geq 10$. For example, at $N_r = 11$, we have $L_{CMP} = 11$ while $\hat{L}_{CMP} = 9$, resulting in PSUS having a higher ECR value than FSUS.

Finally, the economic efficiency metric of (5.46) is optimised in Fig. 5.14 for IDEC-PSUS and IDEC-FSUS relay cooperation schemes while taking into account the cooperative cost of the RS cooperation link. For $N_r \leq 9$, we see that relay cooperation incorporating PSUS registers higher economic efficiency values than those employing

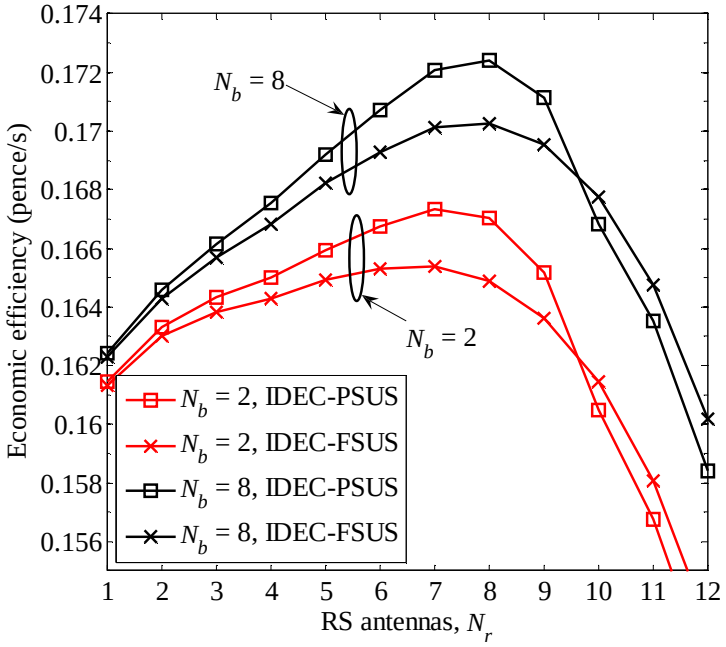

FIGURE 5.14: The economic efficiency v.s. the number of RS antennas of the IDEC-PSUS and IDEC-FSUS relay cooperation schemes, taking into consideration the cooperative cost of the RS cooperation link.

FSUS. As PSUS consumes significantly less power than FSUS for the operation of the RS cooperation link, the OPEX of IDEC-PSUS is reduced, resulting in it having higher profitability than IDEC-FSUS. The maximum economic efficiency is achieved for both schemes when $N_r = 7$ and $N_r = 8$ for $N_b = 2$ and $N_b = 8$, respectively. For $N_r \geq 10$, FSUS begins to demonstrate improved performance over PSUS as the threshold given in (5.43) is, once again, surpassed at higher N_r values.

5.10 Conclusions

A relay cooperation scheme has been proposed for downlink multicell MIMO cellular networks. Different RS decoding strategies (JDEC and IDEC) for the broadcast phase and joint relay transmission with different degrees of CSI sharing for the relay phase have been investigated. It has been demonstrated that compared with direct transmission, relay cooperation can achieve energy reductions of up to 36% with JDEC and up to 19% with IDEC. However, JDEC requires a cooperative link with a bit rate of an order of magnitude greater than that achievable by the relay network. We have

also proposed the PSUS user selection method for relay phase joint transmission which enables the cooperative link to operate at 39% of the cooperative cost incurred by competing methods that require global CSI. This significant cost reduction more than compensates for the 4% to 5% degradation caused by the PSUS method to the system spectral efficiency. When the cooperative cost of the RS cooperation link is taken into consideration, it is demonstrated that the PSUS method is 10% more energy efficient at minimum ECR, and thus more economically profitable, than the FSUS method.

5.10.1 The Applicability of Relay Cooperation for Uplink Transmission

The relay cooperation technique is developed so that the RSs can cooperatively transmit to the destinations during the relay phase. Since the relay phase is essentially the same for downlink or uplink transmission with the destination being the UEs and BS, respectively, the relay cooperation technique can be implemented for both of these transmission scenarios. However, some modifications may be needed during the first hop of the utilised relaying protocol. This first hop is referred to as the broadcast phase for downlink transmission. As for the uplink transmission, it is called the access phase. While only one node (the BS) is communicating with the RSs in the broadcast phase of the downlink transmission, multiple nodes (the UEs) will be communicating with the RSs in the access phase of the uplink transmission. Therefore, different decoding approaches have to be considered in the access phase as compared to the broadcast phase described in Section 5.4.1.1 and Section 5.4.1.2. Typically, the RS decoding for the access phase will be more complex than the broadcast phase if the number of supported UEs is large.

Chapter 6

Conclusions and Future Work

Relaying transmission has been identified as one of the key technologies in future wireless networks to facilitate green communications as the power consumption of a RACN is expected to be reduced. However, relaying may incur multiplexing loss due to its multi-hop nature which, in turn, may lead to a decrease in spectral efficiency. As a result, there exists an inherent spectral-energy efficiency trade-off that must be considered. Furthermore, the deployment of RSs may increase the cellular network interference, especially in the urban and suburban areas where the cell density is high. Therefore, innovative relaying methods to mitigate interference is necessary to improve the spectral-energy efficiency of the RACN. In this concluding chapter, we summarise the key findings of the chapters and suggest several interesting future research directions.

6.1 Summary of Results

Firstly, the BS power consumption of the DTCN in the presence of inter-cell interference is investigated in Chapter 3 with different IC techniques being considered at the receiver. The power consumption model includes the power consumed at both the RF power amplifier and signal processing modules with its energy efficiency measure in ECR. It is shown that the number of transceiver antennas and the receiver

weight optimisation approach influence the ECR of the BS. The BS power consumption is reduced when MMSE based receivers are employed, as opposed to ZF based receivers, for the same targeted SINR at the receiver output. Specifically, the MMSE-SIC receiver facilitates the highest reduction in BS power consumption. Besides that, treating inter-cell interference as background noise has been shown not to be an energy efficient approach as this requires the desired BS to transmit at higher power in order to maintain the targeted SINR. This, in turn, may cause interference level to rise even further if all adjacent BSs opt for the same transmitting strategy. Results also indicate that the impact of the circuit power consumption at the signal processing module may be substantial in some cases. It may erase off the transmission power savings obtained through receive diversity gains and receiver IC techniques if it is too high. Because of this, power consumption at the signal processing module may be more detrimental than the effects of inter-cell interference in causing the increase in BS power consumption.

In Chapter 4, the performance of the RACN has been investigated with the DTCN taken as the baseline. Two types of relaying paradigms, namely, the SFR relaying and IFR relaying, have been considered with each of them employing the adaptive MIMO relaying scheme. The spectral-energy-economic efficiency values of the transmission schemes have been investigated. Both the RF and circuit power consumption values have been considered in the energy efficiency calculation. From the simulation results, it has been established that the RACN with SFR is more energy efficient than the DTCN. The SFR scheme also outperforms the IFR scheme by a considerable margin, suggesting that increasing the received signal reliability by enhancing the strength of the desired signal is more favourable than suppressing the interference found in the received signal. However, an inherent spectral-energy efficiency trade-off has been found to exist in the scheme. Due to this trade-off, it is demonstrated that it may no longer be beneficial to optimise energy efficiency alone. The economic efficiency metric has been proposed as an alternate performance metric to decide the best balance in the spectral-energy efficiency trade-off in order to maximise profitability, a factor which is most important to mobile operators as can be seen in Section 2.3.1. Furthermore, investigation results on the various frequency reuse planning modes of the SFR scheme

have indicated that aggressive bandwidth utilisation is favoured over bandwidth allocation strategies that avoid interference. This suggests that efficient bandwidth utilisation is important towards improving network performance. Nevertheless, methods to mitigate interference must be devised to further enhance the performance of interference-limited networks if full bandwidth utilisation is to be employed.

In Chapter 5, an advanced RACN incorporating relay cooperation concepts has been proposed to reduce interference while employing full bandwidth utilisation. The scheme is named CMP relaying. During the broadcast phase, both the JDEC and IDEC decoding strategies at the RSs have been investigated. During the relay phase, user selection methods with various degrees of CSI sharing for joint relay transmission have been considered. A cooperative link between the RSs that provides a channel to share cooperative information is employed. It has been demonstrated that CMP relaying with JDEC outperforms CMP relaying with IDEC due to the increased multiplexing gains in JDEC by means of sharing antennas in a virtual MIMO setting. However, due to the fact that the RSs in JDEC are also required to share both data and CSI to perform joint decoding, a cooperative link with a bit rate of an order of magnitude greater than that achievable by the relay network is required. Next, the PSUS method has been proposed to be incorporated into CMP relaying. It is a user selection method designed specifically for relay cooperation, requiring only partial sharing of the network CSI. It has been demonstrated that the proposed PSUS method is able to operate at almost half of the cooperative cost incurred by the competing OUS and FSUS methods that require global CSI. This significant cost reduction more than compensates for the slight degradation caused by the PSUS method to the underlying system performance. As a result of the reduced energy requirement, it is shown that relay cooperation incorporating the PSUS method is also more economically profitable than those employing the FSUS method. In a word, the work in this chapter establishes that relay cooperation is beneficial to interference-limited networks employing relaying transmission. However, the cost incurred at the cooperative links should be considered in a practical relay cooperation system.

Overall, the studies in Chapter 3 through Chapter 5 have demonstrated how the BS

power consumption of DTCNs is influenced by certain factors, how relay transmission is able to improve the energy efficiency of DTCNs, how the optimal spectral-energy efficiency trade-off point is obtained to maximise the profitability of RACNs and how to further improve their performance through relay cooperation. The research conducted in this thesis are of great practical significance in assisting the deployment of relaying networks in future green wireless communication systems.

6.2 Future Research Topics

For the investigation on the BS power consumption in DTCNs, inter-cell interference has been considered as background noise as this is customary in current real world implementation. However, it is worth expanding the investigation to include more sophisticated receiver interference cancellation techniques that are interference-aware. In investigating such techniques, the cost in obtaining the necessary information from adjacent cells to facilitate inter-cell interference mitigation should be considered.

For the work in spectral-energy efficiency trade-off, it is demonstrated that communication systems cannot be optimised only for energy efficiency. Instead, a right balance between spectral and energy efficiency could be more beneficial. The economic efficiency metric is presented in this thesis to obtain a suitable balance point that maximises profitability, a key performance indicator for mobile operators. Besides solely depending on the trade-off, this metric can be further developed to take into account the variability of traffic load in the network. While higher spectral efficiency would be desirable during peak hours, switching to operating modes that prioritise energy efficiency during off-peak hours is more favourable. The economic implication may be different in these two operating modes. Thus, the economic efficiency metric which tracks traffic load variability is able to maximise economic profitability by selecting the appropriate balance point as the loading factor changes.

For the work on relay cooperation, this thesis considers interference mitigation in individual sectors of the cell. A possible future research direction would be to extend

the work to enable intra-sector relay cooperation for more extensive interference mitigation in each cell. Here, the nearest RSs from adjacent sectors belonging to the same cell would be transmitting cooperatively. The CSI can be efficiently shared between the RSs by utilising the proposed PSUS method. However, the RSs may not be able to intercept the data transmitted in each other's sector during the broadcast phase. This is due to the weak received signal strength as the BS employs antennas with beams directed only to individual sectors. Thus, data has to be shared between the RSs of different sectors. Sharing of data through the RS cooperative links is not feasible as it is shown in Section 5.9.2 that the cooperative cost involved would be prohibitively high. A possible solution is to distribute the data to the RSs via the common BS. It is anticipated that further reduction in energy consumption may be possible with this research extension.

Furthermore, the work in this thesis assumes that the required CSI is obtained in a timely manner whereby there is negligible delay in the feedback channel. Therefore, the CSI which is fed back to the BS and RSs is assumed to accurately represent the channel condition during subsequent data transmission. In practice, however, there may be delay in the feedback channel causing the received CSI to be outdated. As the outdated CSI is being utilised in the precoders of the BS and RSs, interference may not be perfectly cancelled as the precoding matrix no longer matches the transmission channel. Consequently, the presence of residue interference at the received signals will cause degradation to the system performance. As a future research direction, the effects of outdated CSI on the performance of relay cooperation in RACNs can be investigated. Improved protocols and transmission techniques which are less sensitive towards outdated CSI can then be devised to further robustify the proposed relay cooperation scheme.

References

[1] Guglielmo Marconi. In Wikipedia. Retrieved Mar. 29, 2013, from http://http://en.wikipedia.org/wiki/Guglielmo_Marconi.

[2] A. K. Trehan, "Energy conservation solutions for mobile networks," in *Proc. IEEE INTELEC'12*, Arizona, USA, Sep. 2012, pp. 1–5.

[3] 3GPP, "Evolved Universal Terrestrial Radio Access (E-UTRA); further advancements for E-UTRA physical layer aspects," Tech. Rep. TR36.814 v9.0.0, 3GPP, Valbonne, France.

[4] Intergovernmental Panel on Climate Change, "Climiate change 2007: the physical science basis," WGI AR4 Rep., Feb. 2007. [Online]. Available: http://www.ipcc.ch/pdf/assessment-report/ar4/wg1/ar4_wg1_full_report.pdf.

[5] D. J. C. MacKay, "Sustainable energy - without the hot air," Dec. 2008. [Online]. Available: http://www.withouthotair.com.

[6] The UK Climate Change Act 2008, http://www.legislation.gov.uk/ukpga/2008/27/contents.

[7] International Telecommun. Union, "Monitoring the WSIS targets - a mid-term review," World Telecommun./ICT Dev. Rep., 2010. [Online]. Available: http://www.itu.int/ITU-D/ict/publications/wtdr_10/index.html.

[8] The Economist, "Mobile marvels," Special Rep., Telecoms in Emerging Markets, Sep. 2009. [Online]. Available: http://www.economist.com/node/14483896.

[9] Cisco, "Cisco VNI: global mobile data traffic forecast update (2012 – 2017)," White Paper, Feb. 2013. [Online]. Available: http://www.cisco.com/en/US/netsol/ns827/networking_solutions_white_papers_list.html.

[10] E. Candy, "HSPA transition to LTE – the issues," in *LTE World Summit*, Amsterdam, Netherlands, May 2010.

[11] T. Edlar, "Green base stations – how to minimize CO2 emission in operator networks," in *The Base Station Conference*, Bath, UK, Apr. 2008.

[12] F. Meywerk, "The mobile broadband vision – how to make LTE a success," in *LTE World Summit*, London, UK, Nov. 2008.

[13] OpenBTS, "What stuff costs, part 2: CAPEX," The OpenBTS Chronicles, Jan. 2009. [Online]. Available: http://openbts.blogspot.co.uk/2009/01/what-stuff-costs-part-1-capex.html.

[14] NAO, "The auction of radio spectrum for the third generation of mobile telephones," Radiocommunications Agency Rep., 2001. [Online]. Available: http://http://www.nao.org.uk/wp-content/uploads/2001/10/0102233.pdf.

[15] O. Holland, V. Friderikos, and H. Aghvami. "Green mobile communications," in *Encyclopedia of Wireless and Mobile Communications*, 2nd ed., vol. 1. B. Furht, Ed.: CRC Press, 2011.

[16] S. Chia, "As the internet takes to the air, do mobile revenue go sky high?," in *IEEE WCNC Workshops'08*, LA, USA, Apr. 2008.

[17] J. Thompson, "Green radio for energy efficient wireless communications," Plenary Talk, *WICON'11*, Xi'An, China, Oct. 2011.

[18] PBL Netherlands Environmental, "Trends in global CO_2 emissions," Background Studies Rep., Jul. 2012. [Online]. Available: http://www.pbl.nl/en/publications/2012/trends-in-global-co2-emissions-2012-report.

[19] Gartner, "Gartner estimates ICT industry accounts for 2 percent of global CO2 emissions," Press Release, Apr. 2007. [Online]. Available: http://www.gartner.com/it/page.jsp?id=503867.

[20] IDATE, "Green telecom – calling for a better future," News 453, Jan. 2009. [Online]. Available: http://www.idate.org/en/News/Green-Telecom_553.html.

[21] T. O'Farrell, "Green radio – designing sustainable future wireless networks," in *Next Generation Wireless Green Networks Workshop*, Paris, France, Nov. 2009.

[22] T. O'Farrell, "Green radio for energy efficient communications," in *CommNet Future of Wireless Access Workshop*, Southampton, UK, Nov. 2011.

[23] Groupe Speciale Mobile Association, "Mobile's green manifesto," Rep., Jun. 2012. [Online]. Available: http://www.gsma.com/publicpolicy/wp-content/uploads/2012/06/Green-Manifesto-2012.pdf.

[24] W. Tuttlebee, S. Fletcher, D. Lister, T. O'Farrell, and J. Thompson, "Saving the planet - the rationale, realities and research of green radio," *J. Institute Telecommun. Professionals*, vol. 4, no. 3, pp. 9–20, 2010.

[25] Orange, "Better future," Partner Commun. Corporate Responsibility Rep., 2007. [Online]. Available: http://www.orange.co.il/Documents/investors_relations/pdf_eng.%20report%20pdf.pdf.

[26] Vodafone, "Live the moment," Corporate Responsibility Rep., 2007. [Online]. Available: http://www.eurocharity.gr/files/Vodafone_Review_EN_0708.pdf.

[27] J. Thompson and C. Khirallah, "Overview of Green Radio research outcomes," in *Proc. IEEE ICCC'12*, Beijing, China, Aug. 2012, pp. 69–73.

[28] I. Telatar, "Capacity of multi-antenna Gaussian channels," *European Trans. Telecommun.*, vol. 10, no. 6, pp. 585–595, Dec. 1999.

[29] A. Paulraj, R. Nabar, and D. Gore. "Capacity of ST channels," in *Introduction to Space-Time Wireless Commun.*, 1st ed. Cambridge, UK: Cambridge University Press, 2003, pp. 66–69.

[30] T. O'Farrell, "Book of assumptions," Mobile VCE Rep., D-GR-0011, 2011.

[31] I. Ku, C. -X. Wang, J. S. Thompson, and P. M. Grant, "Transmission energy consumption in MIMO systems under inter-cell interference," in *Proc. WiAd'11*, London, UK, Jun. 2011, pp. 263–267.

[32] I. Ku, C. -X. Wang, J. S. Thompson, and P. M. Grant, "Impact of receiver interference cancellation techniques on the base station power consumption in MIMO systems with inter-cell interference," in *Proc. IEEE PIMRC'11*, Toronto, Canada, Sep. 2011, pp. 1798–1802.

[33] I. Ku, C. -X. Wang, and J. S. Thompson, "Spectral-energy efficiency tradeoff in multicell cellular networks with adaptive relay cooperation," in *Proc. IEEE GLOBECOM'12*, California, USA, Dec. 2012, pp. 4585–4590.

[34] A. J. Fehske, F. Richter, and G. P. Fettweis, "Energy efficiency improvements through micro sites in cellular mobile radio networks," in *Proc. IEEE GLOBECOM'09*, Honolulu, Hawaii, USA, Nov. 2009, pp. 1–5.

[35] O. Arnold, F. Richter, G. Fettweis, and O. Blume, "Power consumption modeling of different base station types in heterogeneous cellular networks," in *Proc. Future Network and Mobile Summit*, Florence, Italy, Jun. 2010, pp. 1–8.

[36] 3GPP, "Application scenarios for LTE-Advanced relay," R1-082975, RAN1 #54, China Mobile, Vodafone, Huawei, Aug. 2008.

[37] J. Sydir and R. Taori, "An evolved cellular system architecture incorporating relay stations," *IEEE Commun. Mag.*, vol. 47, no. 6, pp. 115–121, Jun. 2009.

[38] E. C. van der Meulen, "Three-terminal communication channels," *Adv. Appl. Probab.*, vol. 3, no. 1, pp. 120–154, Spring 1971.

[39] E. Beres and R. Adve, "Optimal relay-subset selection and time-allocation in decode-and-forward cooperative networks," *IEEE Trans. Wireless Commun.*, vol. 9, no. 7, pp. 2145–2155, Jul. 2010.

[40] T. Wu, C. Wang, H. Zhao, Y. Pei, and G. Li, "Joint power and frame allocation for TDD-based cooperative relaying system," in *Proc. IEEE ICCTA'09*, Alexandria, Egypt, Oct. 2009, pp. 101–105.

[41] N. Yang, H. Tian, S. Chen, and P. Zhang, "An adaptive frame resource allocation strategy for TDMA-based cooperative transmission," *IEEE Commun. Lett.*, vol. 11, no. 5, pp. 417–419, May 2007.

[42] B. Niu, and A. M. Haimovich, "Optimal throughput of two-hop relay networks with different relay cooperation," in *Proc. IEEE MILCOM'09*, Boston, USA, Oct. 2009, pp. 1–5.

[43] S. Simoens, O. Muoz-Medina, J. Vidal, and A. Del Coso, "Compress-and-forward cooperative MIMO relaying with full channel state information," *IEEE Trans. Signal Proc.*, vol. 58, no. 2, pp. 781–791, Feb. 2010.

[44] S. Simoens, J. Vidal, and O. Munoz, "Compress-and-forward cooperative relaying in MIMO-OFDM systems," in *Proc. IEEE SPAWC'06*, Cannes, France, Jul. 2006, pp. 1–5.

[45] J. Jiang, J. S. Thompson, H. Sun, and P. M. Grant, "Performance assessment of virtual multiple-input multiple-output systems with compress-and-forward cooperation," *IET Commun.*, vol. 6, no. 11, pp. 1456–1465, Feb. 2012.

[46] S. Karmakar, and M. K. Varanasi, "The diversity-multiplexing tradeoff of the dynamic decode-and-forward protocol on a MIMO half-duplex relay channel," *IEEE Trans. Info. Theory*, vol. 57, no. 10, pp. 6569–6590, Oct. 2011.

[47] D. Gunduz, M. A. Khojastepour, A. Goldsmith, and H. V. Poor, "Multi-hop MIMO relay networks: diversity-multiplexing trade-off analysis," *IEEE Trans. Wireless Commun.*, vol. 9, no. 5, pp. 1738–1747, May 2010.

[48] E. Chiu, V. K. N. Lau, S. Zhang, and B. S. M. Mok, "Precoder design for multi-antenna partial decode-and-forward (PDF) cooperative systems with statistical CSIT and MMSE-SIC receivers," *IEEE Trans. Wireless Commun.*, vol. 11, no. 4, pp. 1343–1349, Apr. 2012.

[49] C. K. Lo, S. Vishwanath, and R. W. Heath, "Relay subset selection in wireless networks using partial decode-and-forward transmission," *IEEE Trans. Veh. Tech.*, vol. 58, no. 2, pp. 692–704, Feb. 2009.

[50] J. Haghighat and W. Hamouda, "Decode-compress-and-forward with selective-cooperation for relay networks," *IEEE Commun. Lett.*, vol. 16, no. 3, pp. 378–381, Mar. 2012.

[51] F. Xue and S. Sandhu, "Cooperation in a half-duplex gaussian diamond relay channel," *IEEE Trans. Info. Theory*, vol. 53, no. 10, pp. 3806–3814, Oct. 2007.

[52] S. -H. Lee and S. -Y. Chung, "When is compress-and-forward optimal?," in *Proc. IEEE ITA'10*, San Diego, USA, Feb. 2010, pp. 1–3.

[53] W. Jaafar, W. Ajib, and D. Haccoun, "Adaptive transmission in cooperative wireless communications," in *Proc. IEEE IFIP'09*, Paris, France, Dec. 2009, pp. 1–5.

[54] B. Rankov and A. Wittneben, "Spectral efficient protocols for half-duplex fading relay channels," *IEEE J. Sel. Areas Commun.*, vol. 25, no. 2, pp. 379–389, Feb. 2007.

[55] Z. Chen, H. Liu, and W. Wang, "A novel decoding-and-forward scheme with joint modulation for two-way relay channel," *IEEE Commun. Lett.*, vol. 14, no. 12, pp. 1149–1151, Dec. 2010.

[56] S. S. Ikki and S. Aissa, "Performance analysis of two-way amplify-and-forward relaying in the presence of co-channel interferences," *IEEE Trans. Commun.*, vol. 60, no. 4, pp. 933–939, Apr. 2012.

[57] X. Ji, B. Zheng, Y. Cai, and L. Zou, "On the study of half-duplex asymmetric two-way relay transmission using an amplify-and-forward relay," *IEEE Trans. Veh. Tech.*, vol. 61, no. 4, pp. 1649–1664, May 2012.

[58] W. Li, J. Li, and P. Fan, "Network coding for two-way relaying networks over Rayleigh fading channels," *IEEE Trans. Veh. Tech.*, vol. 59, no. 9, pp. 4476–4488, Nov. 2010.

[59] T. Koike-Akino, P. Popovski, and V. Tarokh, "Optimized constellations for two-way wireless relaying with physical network coding," *IEEE J. Sel. Areas*, vol. 27, no. 5, pp. 773–787, Jun. 2009.

[60] S. Bagheri, F. Verde, D. Darsena, and A. Scaglione, "Randomized decode-and-forward strategies for two-way relay networks," *IEEE Trans. Wireless Commun.*, vol. 10, no. 12, pp. 4214–4225, Dec. 2011.

[61] D. Gunduz, A. Goldsmith, and H. V. Poor, "MIMO two-way relay channel: diversity-multiplexing tradeoff analysis," in *Proc. ACSSC'08*, Pacific Grove, CA, USA, Oct. 2008, pp. 1474–1478.

[62] C. Schnurr, S. Stanczak, and T. J. Oechtering, "Achievable rates for the restricted half-duplex two-way relay channel under a partial-decode-and-forward protocol," in *Proc. IEEE ITW'08*, Porto, Portugal, May 2008, pp. 134–138.

[63] Q. F. Zhou, Y. Li, F. C. M. Lau, and B. Vucetic, "Decode-and-forward two-way relaying with network coding and opportunistic relay selection," *IEEE Trans. Commun.*, vol. 58, no. 11, pp. 3070–3076, Nov. 2010.

[64] Y. Fan, C. Wang, J. Thompson, and H. V. Poor, "Recovering multiplexing loss through successive relaying using repetition coding," *IEEE Trans. Wireless Commun.*, vol. 6, no. 12, pp. 4484–4493, Dec. 2007.

[65] H. Wicaksana, S. H. Ting, C. K. Ho, W. H. Chin, and Y. L. Guan, "AF two-path half duplex relaying with inter-relay self interference cancellation: diversity analysis and its improvement," *IEEE Trans. Wireless Commun.*, vol. 8, no. 9, pp. 4720–4729, Sep. 2009.

[66] W. H. Chin, C. K. Ho, and S. H. Ting, "Beamforming and interference cancellation for half duplex relaying," in *Proc. IEEE VTC-Spring'09*, Barcelona, Spain, Apr. 2009, pp. 1–5.

[67] R. Zhang, "On achievable rates of two-path successive relaying," *IEEE Trans. Commun.*, vol. 57, no. 10, pp. 2914–2917, Oct. 2009.

[68] Q. Lin, X. Wang, Y. Wang, and J. Liao, "Performance evaluation of frequency planning in a novel cellular architecture based on sector relay," in *Proc. IEEE VTC-Spring'10*, Taipei, Taiwan, May 2010, pp. 1–5.

[69] O. Oyman, "Opportunistic scheduling and spectrum reuse in relay-based cellular networks," *IEEE Trans. Wireless Commun.*, vol. 9, no. 3, pp. 1074–1085, Mar. 2010.

[70] Z. Zhao, X. Fang, Y. Zhu, and Y. Long, "Two frequency reuse schemes in OFDMA-TDD based two-hop relay networks," in *Proc. IEEE WCNC'10*, Sydney, Australia, Apr. 2010, pp. 1–6.

[71] T. Balercia, T. Kuerner, and M. Mueck, "(m,n)-relaying as an alternative to base station cooperation for cellular OFDMA networks," in *Proc. IEEE ICC'11*, Kyoto, Japan, Jun. 2011, pp. 1–5.

[72] S. Kim, W. Choi, Y. Choi, J. Lee, and Y. Han, "Interference reduction of cellular relay networks in multiple-cell environment by spectrum agility," in *Proc. IEEE PIMRC'08*, Cannes, France, Sep. 2008, pp. 1–5.

[73] A. Agustin and J. Vidal, "Amplify-and-forward cooperation under interference-limited spatial reuse of the relay slot," *IEEE Trans. Wireless Commun.*, vol. 7, no. 5, pp. 1952–1962, May 2008.

[74] S. Mohajer, S. N. Diggavi, C. Fragouli, and D. Tse, "Transmission techniques for relay-interference networks," in *Proc. ALLERTON'08*, Illinois, USA, Sep. 2008, pp. 467–474.

[75] C. Abgrall, E. C. Strinati, and J. -C. Belfiore, "Inter-cell interference mitigation allocation for half-duplex relays based cooperation," in *Proc. IEEE WD'09*, Paris, France, Dec. 2009, pp. 1–6.

[76] W. Chen, K. B. Letaief, and Z. Cao, "Network interference cancellation," *IEEE Trans. Wireless Commun.*, vol. 8, no. 12, pp. 5982–5995, Dec. 2009.

[77] O. Simeone, O. Somekh, Y. Bar-Ness, H. V. Poor, and S. Shamai, "Capacity of linear two-hop mesh networks with rate splitting, decode-and-forward relaying and cooperation," in *Proc. ALLERTON'07*, Monticello, Illinois, USA, Sep. 2007.

[78] A. Adinoyi and H. Yanikomeroglu, "Cooperative relaying in multi-antenna fixed relay networks," *IEEE Trans. Wireless Commun.*, vol. 6, no. 2, pp. 533–544, Feb. 2007.

[79] R. Dabora, I. Maric, and A. Goldsmith, "Relay strategies for interference-forwarding," in *Proc. IEEE ITW'08*, Porto, Portugal, May 2008, pp. 46–50.

[80] I. Maric, R. Dabora, and A. Goldsmith, "On the capacity of the interference channel with a relay," in *Proc. IEEE ISIT'08*, Toronto, Canada, Jul. 2008, pp. 554–558.

[81] I. Maric, R. Dabora, and A. Goldsmith, "Generalized relaying in the presence of interference," in *Proc. ACSSC'08*, Pacific Grove, CA, USA, Oct. 2008, pp. 1579–1582.

[82] Y. Ohwatari, N. Miki, T. Asai, T. Abe, and H. Taoka, "Performance of advanced receiver employing interference rejection combining to suppress inter-cell interference in LTE-Advanced downlink," in *Proc. IEEE VTC-Fall'11*, San Francisco, USA, Sep. 2011, pp. 1–7.

[83] G. J. Foschini and M. J. Gans, "On limits of wireless communications in a fading environment when using multiple antennas," *Wireless Personal Commun.*, vol. 6, no. 3, pp. 311–335, Mar. 1998.

[84] P. W. Wolniansky, G. Foschini, G. D. Golden, and R. A. Valenzuela, "V-BLAST: An architecture for realizing very high data rates over the rich-scattering wireless channel," in *Proc. IEEE ISSSE'98*, Pisa, Italy, Sep. 1998, pp. 295–300.

[85] H. Lee, B. Lee, and I. Lee, "Iterative detection and decoding with an improved V-BLAST for MIMO-OFDM systems," *IEEE J. Sel. Areas Commun.*, vol. 24, no. 3, pp. 504–513, Mar. 2006.

[86] X. Li, H. Huang, G. Foschini, and R. Valenzuela, "Effects of iterative detection and decoding on the performance of BLAST," in *Proc. IEEE GLOBECOM'00*, San Francisco, CA, USA, Nov. 2000, pp. 1061–1066.

[87] C. N. Manchon, L. Deneire, P. Mogensen, and T. B. Sorensen, "On the design of a MIMO-SIC receiver for LTE downlink," in *Proc. IEEE VTC-Fall'08*, Calgary, Canada, Sep. 2008, pp. 1–5.

[88] C. S. Park and K. B. Lee, "Transmit power allocation for successive interference cancellation in multicode MIMO systems," *IEEE Trans. Commun.*, vol. 56, no. 12, pp. 2200–2213, Dec. 2008.

[89] L. -C. Wang and C. -J. Yeh, "Adaptive joint subchannel and power allocation for multi-user MIMO-OFDM systems," in *Proc. IEEE PIMRC'08*, Cannes, France, Sep. 2008, pp. 1–5.

[90] C. Kotchasarn, "Robust joint transceiver power allocation for multi-user downlink MIMO transmissions," in *Proc. IEEE ICACT'10*, Gangwon-Do, Korea, Feb. 2010, pp. 1708–1712.

[91] F. She, W. Chen, H. Luo, T. Huang, and X. Wang, "Joint power allocation and scheduling of multi-antenna OFDM system in broadcast channel," in *Proc. IEEE ICC'09*, Dresden, Germany, Jun. 2009, pp. 1–5.

[92] L. Dong, A. P. Petropulu, and H. V. Poor, "Weighted cross-layer cooperative beamforming for wireless networks," *IEEE Trans. Sig. Processing*, vol. 57, no. 8, pp. 3240–3252, Aug. 2009.

[93] J. Choi, "Opportunistic beamforming with single beamforming matrix for virtual antenna arrays," *IEEE Trans. Veh. Tech.*, vol. 60, no. 3, pp. 872–881, Mar. 2011.

[94] R. de Francisco and D. T. M. Slock, "An optimized unitary beamforming technique for MIMO broadcast channels," *IEEE Trans. Wireless Commun.*, vol. 9, no. 3, pp. 990–1000, Mar. 2010.

[95] H. -H. Lee and Y. -C. Ko, "Non-iterative symbol-wise beamforming for MIMO-OFDM systems," *IEEE Trans. Wireless Commun.*, vol. 11, no. 10, pp. 3788–3798, Oct. 2012.

[96] E. Vagenas, G. S. Paschos, and S. A. Kotsopoulos, "Beamforming capacity optimization for MISO systems with both mean and covariance feedback," *IEEE Trans. Wireless Commun.*, vol. 10, no. 9, pp. 2994–3001, Sep. 2011.

[97] P. Tejera, W. Utschick, J. Nossek, and G. Bauch, "Rate balancing in multiuser MIMO OFDM systems," *IEEE Trans. Commun.*, vol. 57, no. 5, pp. 1370–1380, May 2009.

[98] N. Prasad and X. Wang, "Outage minimization and rate allocation for the multiuser Gaussian interference channels with successive group decoding," *IEEE Trans. Info. Theory*, vol. 55, no. 12, pp. 5540–5557, Dec. 2009.

[99] X. Wang and X. -D. Zhang, "Linear transmission for rate optimization in MIMO broadcast channels," *IEEE Trans. Wireless Commun.*, vol. 9, no. 10, pp. 3247–3257, Oct. 2010.

[100] V. Kostina and S. Loyka, "Optimum power and rate allocation for coded V-BLAST: average optimization," *IEEE Trans. Commun.*, vol. 59, no. 3, pp. 877–887, Mar. 2011.

[101] V. Kostina and S. Loyka, "Optimum power and rate allocation for coded V-BLAST: instantaneous optimization," *IEEE Trans. Commun.*, vol. 59, no. 10, pp. 2841–2850, Oct. 2011.

[102] S. Sanayei and A. Nosratinia, "Antenna selection in MIMO systems," *IEEE Commun. Mag.*, vol. 42, no. 10, pp. 68–73, Oct. 2004.

[103] S. Y. Park and D. J. Love, "Capacity limits of multiple antenna multicasting using antenna subset selection," *IEEE Trans. Sig. Proc.*, vol. 56, no. 6, pp. 2524–2534, Jun. 2008.

[104] M. Sandell and J. Coon, "Performance of combined bulk and per-tone antenna selection precoding in coded OFDM systems," *IEEE Trans. Commun.*, vol. 60, no. 3, pp. 655–660, Mar. 2012.

[105] C. -T. Lin and W. -R. Wu, "QRD-based antenna selection for ML detection of spatial multiplexing MIMO systems: algorithms and applications," *IEEE Trans. Veh. Tech.*, vol. 60, no. 7, pp. 3178–3191, Sep. 2011.

[106] H. Kim, C. B. Chae, G. Veciana, and R. W. Heath, "A cross-layer approach to energy efficiency for adaptive MIMO systems exploiting spare capacity," *IEEE Trans. Wireless Commun.*, vol. 8, no. 8, pp. 4264–4275, Aug. 2009.

[107] S. Yatawatta, A. P. Petropulu, and C. J. Graff, "Energy efficient channel estimation in MIMO systems," in *Proc. IEEE ICASSP'05*, Philadelphia, PA, USA, Mar. 2005, pp. IV-317–IV-320.

[108] X. Ge, J. Hu, C. -X. Wang, J. Zhang, and X. Yang, "Energy efficiency analysis of MISO-OFDM communication systems considering power and capacity constraints," *Mob. Netw. Appl.*, vol. 17, no. 1, pp. 29–35, Feb. 2012.

[109] C. Khirallah, D. Vukobratovic, and J. S. Thompson, "Performance evaluation and energy efficiency of random network coding in LTE-Advanced," in *Proc. IEEE ICC'12*, Ottawa, Canada, Jun. 2012.

[110] S. Cui, A. J. Goldsmith, and A. Bahai, "Energy-constrained modulation optimization," *IEEE Trans. Wireless Commun.*, vol. 4, no. 5, pp.2349–2360, Sep. 2005.

[111] R. J. Baxley and G. T. Zhou, "Power savings analysis of peak-to-average power ratio reduction in OFDM," *IEEE Trans. Consumer Elec.*, vol. 50, no. 3, pp. 792–798, Aug. 2004.

[112] M. C. Gursoy, D. Qiao, and S. Velipasalar, "Analysis of energy efficiency in fading channels under QoS constraints," *IEEE Trans. Wireless Commun.*, vol. 8, no. 8, pp. 4252–4263, Aug. 2009.

[113] S. Z. Asif, "Interference cancellation technique for CDMA2000 handsets," in *Proc. IEEE VTC-Fall'05*, Dallas, USA, Sep. 2005, pp. 737–740.

[114] L. Wang and N. R. Shanbhag, "Low-power filtering via adaptive error-cancellation," *IEEE Trans. Sig. Proc.*, vol. 51, no. 2, pp. 575–583, Feb. 2003.

[115] J. Wang and B. Daneshrad, "A comparative study of MIMO detection algorithms for wideband spatial multiplexing systems," in *Proc. IEEE WCNC'05*, New Orleans, LA, USA, Mar. 2005, pp. 408–413.

[116] S. Chen and T. Zhang, "Low power soft-output signal detector design for wireless MIMO communication systems," in *Proc. IEEE ISLPED'07*, Oregon, USA, Aug. 2007, pp. 232–237.

[117] W. Luo and A. Ephremides, "Energy efficiency of multiuser detection," in *Proc. IEEE WCNC'99*, New Orleans, USA, Sep. 1999, pp. 854–858.

[118] C. Han, T. Harrold, S. Armour, I. Krikidis, S. Videv, P. M. Grant, H. Haas, J. S. Thompson, I. Ku, C. -X. Wang, T. A. Le, M. R. Nakhai, J. Zhang, and L. Hanzo, "Green radio: Radio techniques to enable energy efficient wireless networks," *IEEE Commun. Mag.*, vol. 49, no. 6, pp. 46–54, Jun. 2011.

[119] T. M. Cover and A. El Gamal, "Capacity theorems for the relay channel," *IEEE Trans. Info. Theory*, vol. IT-25, no. 5, pp. 572–584, Sep. 1979.

[120] A. Sendonaris, E. Erkip, and B. Aazhang, "User cooperation diversity-Part I: System description," *IEEE Trans. Info. Theory*, vol. 51, no. 11, pp. 1927–1938, Nov. 2003.

[121] J. N. Laneman, D. N. C. Tse, and G. W. Wornell, "Cooperative diversity in wireless networks: Efficient protocols and outage behaviour," *IEEE Trans. Info. Theory*, vol. 50, no. 12, pp. 3062–3080, Dec. 2004.

[122] A. Host-Madsen and J. Zhang, "Capacity bounds and power allocation for wireless relay channels," *IEEE Trans. Info. Theory*, vol. 51, no. 6, pp. 2020–2040, Jun. 2005.

[123] J. Hu and N. C. Beaulieui, "Performance analysis of decode-and-forward relaying with selection combining," *IEEE Commun. Letters*, vol. 11, no. 6, pp. 489–491, Jun. 2007.

[124] S. Berger, M. Kuhn, A. Wittneben, T. Unger, and A. Klein, "Recent advances in amplify-and-forward two-hop relaying," *IEEE Commun. Mag.*, vol. 47, no. 7, pp. 50–56, Jul. 2009.

[125] T. T. Kim, G. Caire, and M. Skoglund, "Decode-and-forward relaying with quantized channel state feedback: an outage exponent analysis," *IEEE Trans. Info. Theory*, vol. 54, no. 10, pp. 4548–4564, Oct. 2008.

[126] Y. Yang and S. Aissa, "Information-guided transmission in decode-and-forward relaying systems: spatial exploitation and throughput enhancement," *IEEE Trans. Wireless Commun.*, vol. 10, no. 7, pp. 2341–2351, Jul. 2011.

[127] Z. Yi and I. -M. Kim, "Diversity order analysis of the decode-and-forward cooperative networks with relay selection," *IEEE Trans. Wireless Commun.*, vol. 7, no. 5, pp. 1792–1799, May 2008.

[128] T. Wang, A. Cano, G. B. Giannakis, and J. N. Laneman, "High-performance cooperative demodulation with decode-and-forward relays," *IEEE Trans. Commun.*, vol. 55, no. 7, pp. 1427–1438, Jul. 2007.

[129] C. -B. Chae, T. Tang, R. W. Heath, and S. Cho, "MIMO relaying with linear processing for multiuser transmission in fixed relay networks," *IEEE Trans. Sig. Proc.*, vol. 56, no. 2, pp. 727–738, Feb. 2008.

[130] H. A. Suraweera, H. K. Garg, and A. Nallanathan, "Performance analysis of two hop amplify-and-forward systems with interference at the relay," *IEEE Commun. Lett.*, vol. 14, no. 8, pp. 692–694, Aug. 2010.

[131] Y. Zhao, R. Adve, and T. J. Lim, "Improving amplify-and-forward relay networks: optimal power allocation versus selection," *IEEE Trans. Wireless Commun.*, vol. 6, no. 8, pp. 3114–3123, Aug. 2007.

[132] S. Yang and J. -C. Belfiore, "Towards the optimal amplify-and-forward cooperative diversity scheme," *IEEE Trans. Info. Theory*, vol. 53, no. 9, pp. 3114–3126, Sep. 2007.

[133] G. Zeitler, G. Bauch, and J. Widmer, "Quantize-and-forward schemes for the orthogonal multiple-access relay channel," *IEEE Trans. Commun.*, vol. 60, no. 4, pp. 1148–1158, Apr. 2012.

[134] A. Chakrabarti, A. Sabharwal, and B. Aazhang, "Practical quantizer design for half-duplex estimate-and-forward relaying," *IEEE Trans. Commun.*, vol. 59, no. 1, pp. 74–83, Jan. 2011.

[135] M. Yuksel and E. Erkip, "Multiple-antenna cooperative wireless systems: a diversity–multiplexing tradeoff perspective," *IEEE Trans. Info. Theory*, vol. 53, no. 10, pp. 3371–3393, Oct. 2007.

[136] M. Uppal, Z. Liu, V. Stankovic, and Z. Xiong, "Compress-forward coding with BPSK modulation for the half-duplex Gaussian relay channel," *IEEE Trans. Sig. Proc.*, vol. 57, no. 11, pp. 4467–4481, Nov. 2009.

[137] O. Sahin and E. Erkip, "Achievable rates for the Gaussian interference relay channel," in *Proc. IEEE GLOBECOM'07*, Washington D. C., USA, Nov. 2007, pp. 1627–1631.

[138] T. Han and K. Kobayashi, "A new achievable rate region for the interference channel," *IEEE Trans. Info. Theory*, vol. 27, no. 1 pp. 49–60, Jan. 1981.

[139] Y. Cao and B. Chen, "Capacity bounds for two-hop interference networks," in *Proc. ALLERTON'09*, Urbana-Champaign, Illinois, USA, Sep. 2009, pp. 272–279.

[140] P. S. C. Thejaswi, A. Bennatan, J. Zhang, R. Calderbank, and D. Cochran, "Rate-achievability strategies for two-hop interference flows," in *Proc. ALLERTON'08*, Urbana-Champaign, Illinois, USA, Sep. 2008, pp. 1432–1439.

[141] S. Ganesan, Z. Ding, T. Ratnarajah, and M. Sellathurai, "Distributed STBC for single carrier relay-assisted transmissions over frequency-selective channels," in *Proc. IEEE ISIT'08*, Toronto, Canada, Jul. 2008, pp. 827–831.

[142] S. Ganesan, W. Liu, and M. Sellathurai, "Limited feedback precoding for distributed space-time coding in wireless relay networks," in *Proc. WCSP'09*, Nanjing, China, Nov. 2009, pp. 1–5.

[143] C. Zhong, T. Ratnarajah, S. Jin, M. Sellathurai, and C. Cowan, "Performance analysis of optimal beamforming in MIMO dual-hop amplify-and-forward systems," in *Proc. IEEE ICASSP'11*, Prague, Czech Republic, May 2011, pp. 2820–2823.

[144] T. Ratnarajah, M. Sellathurai, and Z. Ding, "On the performance of cooperative communication via best relay path," in *Proc. IEEE PIMRC'07*, Athens, Greece, Sep. 2007, pp. 1–5.

[145] I. Maric, R. Dabora, and A. J. Goldsmith, "Relaying in the presence of interference: achievable rates, interference forwarding, and outer bounds," *IEEE Trans. Info. Theory*, vol. 58, no. 7, pp. 4342–4354, Jul. 2012.

[146] K. Nishimori, K. Riichi, Y. Takatori, A. Ohta, and S. Kubota, "Cooperative interference cancellation for multiuser transmission," in *Proc. IEEE EuCAP'07*, Edinburgh, UK, Nov. 2007, pp. 1–6.

[147] O. Sahin, O. Simeone, and E. Erkip, "Interference channel aided by an infrastructure relay," in *Proc. IEEE ISIT'09*, Seoul, Korea, Jun. 2009, pp. 2023–2027.

[148] W. -J. Huang, Y. -W. P. Hong, and C. -C. J. Kuo, "Lifetime maximization for amplify-and-forward cooperative networks," *IEEE Trans. Wireless Commun.*, vol. 7, no. 5, pp. 1800–1805, May 2008.

[149] R. Madan, N. B. Mehta, A. F. Molisch, and J. Zhang, "Energy-efficient cooperative relaying over fading channels with simple relay selection," *IEEE Trans. Wireless Commun.*, vol. 7, no. 8, pp. 3013–3025, Aug. 2008.

[150] C. -X. Wang, X. Hong, X. Ge, X. Cheng, G. Zhang, and J. S. Thompson, "Cooperative MIMO channel models: A survey," *IEEE Commun. Mag.*, vol. 48, no. 2, pp. 80–87, Feb. 2010.

[151] T. Himsoon, W. P. Siriwongpairat, Z. Han, and K. J. R. Liu, "Lifetime maximization via cooperative nodes and relay deployment in wireless networks," *IEEE J. Sel. Areas Commun.*, vol. 25, no. 2, pp. 306–317, Feb. 2007.

[152] Y. -W. Hong and A. Scaglione, "Energy-efficient broadcasting with cooperative transmissions on wireless sensor networks," *IEEE Trans. Wireless Commun.*, vol. 5, no. 10, pp. 2844–2855, Oct. 2006.

[153] Y. -W. Hong, W. -J. Huang, F. -H. Chiu, and C. -C. J. Kuo, "Cooperative communications in resource-constrained wireless networks," *IEEE Sig. Proc. Mag.*, vol. 24, no. 3, pp. 47–57, May 2007.

[154] A. E. Gamal, M. Mohseni, and S. Zahedi, "Bounds on capacity and minimum energy-per-bit for AWGN relay channels," *IEEE Trans. Info. Theory*, vol. 52, no. 4, pp. 1545–1561, Apr. 2006.

[155] O. Oyman and M. Z. Win, "Power-bandwidth tradeoff in multiuser relay channels with opportunistic scheduling," in *Proc. ALLERTON'08*, Urbana-Champaign, Illinois, USA, Sep. 2008, pp. 72–78.

[156] O. Oyman and A. J. Paulraj, "Power-bandwidth tradeoff in dense multi-antenna relay networks," *IEEE Trans. Wireless Commun.*, vol. 6, no. 6, pp. 2282–2293, Jun. 2007.

[157] J. Akhtman and L. Hanzo, "Power versus bandwidth efficiency in wireless communications: The economic perspective," in *Proc. IEEE VTC-Fall'09*, Anchorage, Alaska, USA, Sep. 2009, pp. 1–5.

[158] W. Guo and T. O'Farrell, "Capacity-energy-cost tradeoff in small cell networks," in *Proc. IEEE VTC-Spring'12*, Yokohama, Japan, May 2012, pp. 1–5.

[159] Ericsson, "Sustainable energy use in mobile communications," White Paper, Aug. 2007. [Online]. Available: www.ericsson.com/technology/whitepapers/sustainable_energy.pdf.

[160] Business Enterprise & Regulatory Reform, "Quarterly energy prices," Mar. 2008. [Online]. Available: http://www.berr.gov.uk/files/file45393.pdf.

[161] S. Videv, J. S. Thompson, H. Haas, and P. M. Grant, "Resource allocation for energy efficient cellular systems," *EURASIP J. Wireless Commun. and Networking*, vol. 181, pp. 1–15, May 2012.

[162] R. Wang, J. S. Thompson, H. Haas, and P. M. Grant, "Sleep mode design for green base stations," *IET Commun.*, vol. 5, no. 18, pp. 2606–2616, Dec. 2011.

[163] X. Tao, X. Xu, and Q. Cui, "An overview of cooperative communications," *IEEE Commun. Mag.*, vol. 50, no. 6, pp. 65–71, Jun. 2012.

[164] P. Wang, H. Wang, L. Ping, and X. Lin, "On the capacity of MIMO cellular systems with base station cooperation," *IEEE Trans. Wireless Commun.*, vol. 10, no. 11, pp. 3720–3731, Nov. 2011.

[165] M. Katz and S. Shamai, "Cooperative schemes for a source and an occasional nearby relay in wireless networks," *IEEE Trans. Info. Theory*, vol. 55, no. 11, pp. 5138–5160, Nov. 2009.

[166] I. Krikidis, J. Thompson, S. McLaughlin, and N. Goertz, "Optimization issues for cooperative amplify-and-forward systems over block-fading channels," *IEEE Trans. Veh. Tech.*, vol. 57, no. 5, pp. 2868–2884, Sep. 2008.

[167] C. T. K. Ng and A. Goldsmith, "The impact of CSI and power allocation on relay channel capacity and cooperation strategies," *IEEE Trans. Wireless Commun.*, vol. 7, no. 12, pp. 5380–5389, Dec. 2008.

[168] H. Ganapathy, J. G. Andrews, and C. Caramanis, "Inter-cell relay cooperation in heterogeneous cellular uplink systems," in *Proc. ACSSC'08*, California, USA, Oct. 2008, pp. 1443–1447.

[169] Y. Kim, T. Kim, S. Kim, and Y. Han, "Adaptive cooperation strategy for multiple relays in 4G wireless systems," in *Proc. IEEE WCNC'09*, Budapest, Hungary, Apr. 2009, pp. 1–5.

[170] A. W. Eckford, J. P. K. Chu, and R. S. Adve, "Low complexity and fractional coded cooperation for wireless networks," *IEEE Trans. Wireless Commun.*, vol. 7, no. 5, pp. 1917–1929, May 2008.

[171] M. A. Torabi, and J. F. Frigon, "A decomposition approach to MIMO interference relay networks," in *Proc. IEEE GLOBECOM'08*, New Orleans, USA, Dec. 2008, pp. 1–6.

[172] S. -H. Park, K. -H. Park, Y. -C. Ko, and M. -S. Alouini, "Alternate transmission relaying based on interference alignment in 3-relay half-duplex MIMO systems," *IEEE J. Sel. Areas Commun.*, vol. 30, no. 8, pp. 1383–1389, Sep. 2012.

[173] V. R. Cadambe and S. A. Jafar, "Degrees of freedom of wireless networks with relays, feedback, cooperation, and full duplex operation," *IEEE Trans. Info. Theory*, vol. 55, no. 5, pp. 2334–2344, May 2009.

[174] V. R. Cadambe and S. A. Jafar, "Interference alignment and the degrees of freedom of wireless X networks," *IEEE Trans. Info. Theory*, vol. 55, no. 9, pp. 3893–3908, Sep. 2009.

[175] B. Nourani, S. A. Motahari, and A. K. Khandani, "Relay-aided interference alignment for the quasi-static interference channel," in *Proc. IEEE ISIT'10*, Texas, USA, Jun. 2010, pp. 405–409.

[176] Y. Fan and J. Thompson, "MIMO configurations for relay channels: theory and practice," *IEEE Trans. Wireless Commun.*, vol. 6, no. 5, pp. 1774–1786, May 2007.

[177] A. F. Dana and B. Hassibi, "On the power efficiency of sensory and ad hoc wireless networks," *IEEE Trans. Info. Theory*, vol. 52, no. 7, pp. 2890–2914, Jul. 2006.

[178] V. I. Morgenshtern and H. Bolcskei, "Crystallization in large wireless networks," *IEEE Trans. Info. Theory*, vol. 53, no. 10, pp. 3319–3349, Oct. 2007.

[179] M. P. Stef, Z. A. Polgar, and V. Bota, "Network-coded cooperation protocol for multiple source - multiple relay topologies in cellular networks," in *Proc. Future Network and Mobile Summit*, Florence, Italy, Jun. 2010, pp. 1–9.

[180] W. Zeng, C. Xiao, Y. Wang, and J. Lu, "Opportunistic cooperation for multi-antenna multi-relay networks," *IEEE Trans. Wireless Commun.*, vol. 9, no. 10, pp. 3189–3199, Oct. 2010.

[181] J. Zhang, and K. B. Letaief, "Interference management with relay cooperation in two-hop interference channels," *IEEE Wireless Commun. Letter*, vol. 1, no. 3, pp. 165–168, Jun. 2012.

[182] X. Lao, L. Cuthbert, T. Zhang, and L. Xiao, "Energy efficiency and optimal resource allocation in cooperative wireless relay networks," in *Proc. IEEE VTC-Spring'11*, Budapest, Hungary, May 2011, pp. 1–6.

[183] T. Yoo, and A. Goldsmith, "On the optimality of multiantenna broadcast scheduling using zero-forcing beamforming," *IEEE J. Sel. Areas in Commun.*, vol. 24, no. 3, pp. 528–541, Mar. 2006.

[184] M. A. Maddah-Ali, M. A. Sadrabadi, and A. K. Khandani, "Broadcast in MIMO systems based on a generalized QR decomposition: signaling and performance analysis," *IEEE Trans. Info. Theory*, vol. 54, no. 3, pp. 1124–1138, Mar. 2008.

[185] S. Liang and M. R. McKay, "Eigen-based transceivers for the MIMO broadcast channel with semi-orthogonal user selection," *IEEE Trans. Sig. Proc.*, vol. 58, no. 10, pp. 5246–5261, Oct. 2010.

[186] M. Minelli, M. Coupechoux, J. -M. Kelif, Maode Ma, and P. Godlewski, "Relays-enhanced LTE-Advanced networks performance studies," in *Proc. IEEE SARNOF'11*, Princeton, USA, May 2011, pp. 1–5.

[187] J. Zhou and J. Thompson, "Linear precoding for the downlink of multiple input single output coexisting wireless systems," *IET Commun.*, vol. 2, no. 6, pp. 742–752, Mar. 2008.